MARTIN MARIETTA ENERGY SYSTEMS LIBRARIES

3 4456 0315360 0

ORNL/TM-11465

ornl

OAK RIDGE NATIONAL LABORATORY

MARTIN MARIETTA

Fabrication and Mechanical Properties of Fe_3AL-Based Iron Aluminides

V. K. Sikka
C. G. McKamey
C. R. Howell
R. H. Baldwin

OAK RIDGE NATIONAL LABORATORY
CENTRAL RESEARCH LIBRARY
CIRCULATION SECTION
4500N ROOM 175
LIBRARY LOAN COPY
DO NOT TRANSFER TO ANOTHER PERSON
If you wish someone else to see this report, send in name with report and the library will arrange a loan.

Fossil Energy Program

OPERATED BY
MARTIN MARIETTA ENERGY SYSTEMS, INC.
FOR THE UNITED STATES
DEPARTMENT OF ENERGY

This report has been reproduced directly from the best available copy.

Available to DOE and DOE contractors from the Office of Scientific and Technical Information, P.O. Box 62, Oak Ridge, TN 37831; prices available from (615) 576-8401, FTS 626-8401.

Available to the public from the National Technical Information Service, U.S. Department of Commerce, 5285 Port Royal Rd., Springfield, VA 22161.
NTIS price codes—Printed Copy: A05 Microfiche A01

This report was prepared as an account of work sponsored by an agency of the United States Government. Neither the United States Government nor any agency thereof, nor any of their employees, makes any warranty, express or implied, or assumes any legal liability or responsibility for the accuracy, completeness, or usefulness of any information, apparatus, product, or process disclosed, or represents that its use would not infringe privately owned rights. Reference herein to any specific commercial product, process, or service by trade name, trademark, manufacturer, or otherwise, does not necessarily constitute or imply its endorsement, recommendation, or favoring by the United States Government or any agency thereof. The views and opinions of authors expressed herein do not necessarily state or reflect those of the United States Government or any agency thereof.

ORNL/TM-11465

Metals and Ceramics Division

FABRICATION AND MECHANICAL PROPERTIES OF Fe_3Al-BASED IRON ALUMINIDES

V. K. Sikka, C. G. McKamey,
C. R. Howell, and R. H. Baldwin

Date Published: March 1990

Prepared for the
U.S. DOE Fossil Energy AR&TD Materials Program
AA 15 10 10 0

Prepared by the
OAK RIDGE NATIONAL LABORATORY
Oak Ridge, Tennessee 37831-6285
operated by
MARTIN MARIETTA ENERGY SYSTEMS, INC.
for the
U.S. DEPARTMENT OF ENERGY
under contract DE-AC05-84OR21400

MARTIN MARIETTA ENERGY SYSTEMS LIBRARIES

3 4456 0315360 0

CONTENTS

LIST OF TABLES v
LIST OF FIGURES vii
ABSTRACT 1
1. INTRODUCTION 2
2. BACKGROUND 2
3. METAL PREPARATION PROCEDURES 2
4. IMPROVEMENTS IN STRENGTH AND DUCTILITY AT ORNL 4
5. TEMPERATURE AND STRAIN RATE EFFECTS ON TENSILE PROPERTIES 8
6. SCALEUP AND FABRICATION OF LARGE HEATS 14
6.1 SCALEUP AT ORNL 14
6.2 FABRICATION OF ORNL INGOTS 15
6.3 SCALEUP AT COMMERICAL VENDORS 15
6.4 MELTING OF HEATS AT ORNL USING COMMERCIAL MELT STOCK 19
6.5 POWDER PREPARATION BY A COMMERCIAL VENDOR AND ITS CONSOLIDATION AND PROCESSING AT ORNL 19
7. MECHANICAL PROPERTIES OF SCALED-UP HEATS 21
7.1 TENSILE PROPERTIES 25
7.2 CREEP PROPERTIES 38
8. MICROSTRUCTURAL ANALYSIS 43
8.1 OPTICAL MICROSTRUCTURE 43
8.2 SCANNING ELECTRON MICROGRAPHS 52
8.3 X-RAY DIFFRACTION 57
9. DISCUSSION 57
10. APPLICATIONS 67
11. FUTURE WORK 67
12. SUMMARY AND CONCLUSIONS 67
13. REFERENCES 69
14. ACKNOWLEDGMENTS 69

LIST OF TABLES

Table 1. Literature on chronological progress in the improvement of room-temperature ductility of Fe_3Al-based iron aluminides 3

Table 2. Chemical analysis of the experimental heats used for ductility improvement studies 6

Table 3. Target and check analyses of 70- and 230-kg (150- and 500-lb) heats of iron aluminides melted by air-induction melting at Combustion Engineering 16

Table 4. Recovery of various elements during air-induction melting of 7-kg (15-lb) iron-aluminide heats at ORNL 20

Table 5. Chemical analysis of nitrogen-gas-atomized powder of iron-aluminide alloy FAS from Ametek 21

Table 6. Tensile properties of iron aluminide {FA-123 [70-kg (150-lb) heat, Heat X3906]} air-induction melted at Combustion Engineering and processed at ORNL 41

Table 7. Creep data for 7-kg (15-lb) air-induction-melted heat of alloy FAS (Heat 13345) (all tests were conducted in air) 42

Table 8. X-ray diffraction results of high-ductility specimens of iron-aluminide (Heat 13008) FAL 60

Table 9. Effect of environments on tensile properties of iron-aluminide alloy (FAL) 62

Table 10. Effect of quenching and heat treatment on mechanical properties of an experimental iron-aluminide alloy (FA-124) 63

Table 11. Tensile properties of iron aluminide {FA-129MnSi [500 g (1 lb), Heat 13232]} arc melted at ORNL and drop cast into a 25 × 12 × 125 mm (1 × 1/2 × 5 in.) water-cooled copper mold 65

Table 12. Tensile properties of iron aluminide [FAL (Heat 13259)] air-induction melted at ORNL from commercial melting stock provided by The Timken Company 66

LIST OF FIGURES

Fig. 1 Photograph showing the 500-g (1-lb) drop casting, the sheet produced from drop casting, the air-induction-melted ingots, and the extruded tubing fabricated from iron-aluminide alloys. The bar and rod produced by extruding and swaging processes are also shown 5

Fig. 2 Effect of annealing temperature on room-temperature tensile elongation of iron-aluminide FAL (Heat 13008). Data on heat treatment A are included for comparison. Annealing treatments were of 1-h duration followed by oil quenching. All tensile tests were at a strain rate of 0.2/min 6

Fig. 3 Effect of annealing temperature on room-temperature yield strength of iron-aluminide FAL (Heat 13008). Data on heat treatment A are included for comparison. Annealing treatments were of 1-h duration followed by oil quenching. All tensile tests were at a rate of 0.2/min 7

Fig. 4 Effect of annealing temperature on room-temperature ultimate tensile strength of iron-aluminide FAL (Heat 13008). Data on heat treatment A are included for comparison. Annealing treatments were of 1-h duration followed by oil quenching. All tensile tests were at a strain rate of 0.2/min 7

Fig. 5 Comparison of room-temperatue elongation observed for four different compositions of iron aluminide using the newly developed heat treatment B. FAS-28A and FAS-28B represent the same composition but slightly different processing steps. Annealing treatments were of 1-h duration followed by oil quenching. All tensile tests were at a strain rate of 0.2/min 9

Fig. 6 Room-temperature total elongation ratio for heat treatments B and A as a function of total elongation for treatment A for 19 different compositions for Fe_3Al-based iron aluminides 9

Fig. 7 Room-temperature yield-strength ratio for heat treatments B and A as a function of yield strength for treatment A for 19 different compositions of Fe_3Al-based iron aluminides 10

Fig. 8 Ultimate tensile-strength ratio for heat treatments B and A as a function of ultimate tensile strength for treatment A for 19 different compositions for Fe_3Al-based iron aluminide 10

Fig. 9 Effect of annealing temperature on room-temperature total elongation of iron-aluminide alloy FA-129 11

Fig. 10 Effect of annealing time at maximum ductility temperature on room-temperature total elongation of iron-aluminide alloy FA-129 11

Fig. 11 Effect of ordering-treatment temperature on room-temperature total elongation of iron-aluminide alloy FA-129. Specimens were given the maximum ductility treatment prior to the ordering treatment. All tensile tests were at a strain rate of 0.2/min 12

Fig. 12 Yield strength (0.2% offset) as a function of test temperature for iron-aluminide alloy FAL (Heat 13008). Specimens were given a 700°C/1 h/OQ stress-relief treatment followed by a 700°C/1 h/OQ annealing treatment. All tests were in air at a strain rate of 0.2/min 12

Fig. 13 Ultimate tensile strength as a function of test temperature for iron-aluminide alloy FAL (Heat 13008). Specimens were given a 700°C/1 h/OQ stress-relief treatment followed by a 700°C/1 h/OQ annealing treatment. All tests were in air at a strain rate of 0.2 min 13

Fig. 14 Total elongation as a function of test temperature for iron-aluminide alloy FAL (Heat 13008). Specimens were given a 700°C/1 h/OQ stress-relief treatment followed by a 700°C/1 h/OQ annealing treatment. All tests were in air at a strain rate of 0.2/min 13

Fig. 15 Total elongation at room temperature as a function of strain rate for iron-aluminide alloy FAL (Heat 13008). Specimens were tested in two heat treatments 14

Fig. 16 Photograph of iron-aluminide ingots of 70 to 230 kg (150 to 500 lb) melted by air-induction melting at Combustion Engineering 18

Fig. 17 Photograph of billet, extruded bars, and rolled sheet prepared at ORNL from ingots of iron-aluminide alloys received from Combustion Engineering 18

Fig. 18 Optical micrographs of two sample regions of nitrogen-gas-atomized powder of iron aluminide (FAS) from Ametek 22

Fig. 19 Optical micrographs of two sample regions of nitrogen-gas-atomized powder of iron aluminide (FAS) from Ametek. The specimen was etched 23

Fig. 20 Optical microstructure of as-extruded bar of iron-aluminide (FAS) powder prepared by nitrogen-gas atomization at Ametek. The powder was placed in a mild steel can and extruded to a ratio of 9:1 area reduction at 1000°C. The microstructures are from (*a*) edge, (*b*) one-half radius, and (*c*) center of the extruded bar 24

Fig. 21 Effect of cooling sequence and annealing temperature on room-temperature total elongation of iron-aluminide alloy FAL (Heat 13008). All of the specimens were stress relieved for 1 h at 700°C prior to annealing at different temperatures 26

Fig. 22 Effect of cooling sequence and annealing temperature on room-temperature yield strength (0.2% offset) of iron-aluminide alloy FAL (Heat 13008). All of the specimens were stress relieved for 1 h at 700°C prior to annealing at different temperatures 26

Fig. 23 Effect of cooling sequence and annealing temperature on room-temperature ultimate tensile strength of iron-aluminide alloy FAL (Heat 13008). All specimens were stress relieved for 1 h at 700°C prior to annealing at different temperatures 27

Fig. 24 Comparison of room-temperature total elongation of iron-aluminide alloy FAS (Heat 13017) for specimens cooled in air vs oil from various annealing temperatures. All of the sheets were stress relieved at 700°C for 1 h followed by oil cooling prior to punching the specimens 27

Fig. 25 Comparison of room-temperature yield strength (0.2% offset) of alloy FAS (Heat 13017) for specimens cooled in air vs oil from various annealing temperatures. All of the sheets were stress relieved at 700°C for 1 h followed by oil cooling prior to punching the specimens 28

Fig. 26 Comparison of room-temperature ultimate tensile strength of alloy FAS (Heat 13017) for specimens cooled in air vs oil from various annealing temperatures. All of the sheets were stress relieved at 700°C for 1 h followed by oil cooling prior to punching the specimens 28

Fig. 27 Effect of stress-relief treatment on room-temperature elongation of alloy FAL (Heat 13008) for various annealing temperatures 30

Fig. 28 Effect of stress-relief treatment on room-temperature yield strength (0.2% offset) of alloy FAL (Heat 13008) for various annealing temperatures 30

Fig. 29 Effect of stress-relief treatment on room-temperature ultimate tensile strength of alloy FAL (Heat 13008) for various annealing temperatures 31

Fig. 30 Comparison of room-temperature elongation of iron-aluminide alloy FAL [7-kg (15-lb) Heat 13008] melted at ORNL with 70-kg (150-lb) Heat X3908 melted at Combustion Engineering 31

Fig. 31 Comparison of room-temperature yield strength of iron-aluminide alloy FAL [7-kg (15-lb) Heat 13008] melted at ORNL with 70-kg (150-lb) Heat X3908 melted at Combustion Engineering 32

Fig. 32 Comparison of room-temperature ultimate tensile strength of iron-aluminide alloy FAL [7-kg (15-lb) Heat 13008] melted at ORNL with 70-kg (150-lb) Heat X3908 melted at Combustion Engineering 32

Fig. 33 Comparison of room-temperature total elongation as a function of annealing temperature for ingots X3904 and X3905 from air-induction-melted 70-kg (150-lb) heat of FA-129 at Combustion Engineering. All of the sheets were stress relieved at 700°C for 1 h followed by oil quenching prior to punching the specimens 33

Fig. 34 Comparison of room-temperature yield strength (0.2% offset) as a function of annealing temperature for ingots X3904 and X3905 from air-induction-melted 70-kg (150-lb) heat of FA-129 at Combustion Engineering. All of the sheets were stress relieved at 700°C for 1 h followed by oil quenching prior to punching the specimens 33

Fig. 35 Comparison of ultimate tensile strength as a function of annealing temperature for ingots X3904 and X3905 from air-induction-melted 70-kg (150-lb) heat of FA-129 at Combustion Engineering. All of the sheets were stress relieved at 700°C for 1 h followed by oil quenching prior to punching the specimens 34

Fig. 36 Comparison of total elongation as a function of test temperature for ingots X3904 and X3905 from air-induction-melted 70-kg (150-lb) heat of FA-129 at Combustion Engineering 34

Fig. 37 Comparison of yield strength (0.2% offset) as a function of test temperature for ingots X3904 and X3905 from air-induction-melted 70-kg (150-lb) heat of FA-129 at Combustion Engineering 35

Fig. 38 Comparison of ultimate tensile strength as a function of test temperature for ingots X3904 and X3905 from air-induction-melted 70-kg (150-lb) heat of FA-129 at Combustion Engineering 35

Fig. 39 Total elongation as a function of test temperature for ingot X3905 from air-induction-melted 70-kg (150-lb) heat of FA-129 at Combustion Engineering. Data are compared for four different annealing temperatures 36

Fig. 40 Reduction of area as a function of test temperature for ingot X3905 from air-induction-melted 70-kg (150-lb) heat of FA-129 at Combustion Engineering. Data are compared for four different annealing temperatures 36

Fig. 41 Yield strength (0.2% offset) as a function of test temperature for ingot X3905 from air-induction-melted 70-kg (150-lb) heat of FA-129 at Combustion Engineering. Data are compared for four different annealing temperatures 37

Fig. 42 Ultimate tensile strength as a function of test temperature for ingot X3905 from air-induction-melted 70-kg (150-lb) heat of FA-129 at Combustion Engineering. Data are compared for four different annealing temperatures 37

Fig. 43 Comparison of room-temperature total elongation of air-induction-melted ingots (X3904 and X3905) from Combustion Engineering with vacuum-induction ingot 35 melted at The Timken Company for alloy FA-129 39

Fig. 44 Comparison of room-temperature yield strength (0.2% offset) of air-induction-melted ingots (X3904 and X3905) from Combustion Engineering with vacuum-induction ingot 35 melted at The Timken Company for alloy FA-129 39

Fig. 45 Comparison of room-temperature ultimate tensile strength of air-induction-melted ingots (X3904 and X3905) from Combustion Engineering with vacuum-induction ingot 35 melted at The Timken Company for alloy FA-129 40

Fig. 46 Larson-Miller plot showing comparison of creep rupture strength of various iron aluminides to the average value curve for type 304 stainless steel 43

Fig. 47 Creep total elongation as a function of the Larson-Miller parameter for iron-aluminide alloy FAS (Heat 13345) 44

Fig. 48 Optical microstructure of a 76-mm-diam (3-in.) as-cast ingot of iron aluminide (FAL). The ingot was made using commercial melt stock for iron and aluminum. (*a*) Ingot edge, (*b*) one-half radius, and (*c*) center 45

Fig. 49 Optical microstructure of as-extruded bar of iron aluminide [FA-117 (Heat 12864)]. The 76-mm-diam (3-in.) air-melted ingot was extruded at 1100°C to an area reduction ratio of 9:1. (*a*) Near edge, (*b*) one-half radius, and (*c*) bar center 46

Fig. 50 Optical microstructure of iron-aluminide specimen [FAL (Heat 13008)] with a stress relief of 700°C for 1 h followed by oil quenching. No annealing treatment was given to this specimen 48

Fig. 51 Optical microstructure of iron-aluminide specimens [FAL (Heat 13008)] with a stress relief of 700°C for 1 h and subsequent annealing treatment for 1 h at (*a*) 700°C, (*b*) 750°C, (*c*) 800°C, and (*d*) 900°C. Both stress-relief and annealing treatments were followed by oil quenching 49

Fig. 52 Optical microstructure of iron-aluminide specimens [FAL (Heat 13008)] with a stress relief of 700°C for 1 h and a subsequent annealing treatment for 1 h at (*a*) 700°C, (*b*) 750°C, (*c*) 800°C, and (*d*) 850°C. The stress-relief treatment was followed by oil quenching, and the annealing treatment was followed by air cooling 50

Fig. 53 Optical microstructure of iron-aluminide specimens [FAL (Heat 13008)] with a stress relief of 700°C for 1 h and a subsequent annealing treatment for 1 h at (*a*) 700°C (*b*) 750°C, (*c*) 800°C, and (*d*) 850°C. Both stress-relief and annealing treatments were followed by air cooling 51

Fig. 54 Optical microstructure of iron aluminide (FA-129) for various annealing treatments of 1 h followed by oil quenching. Specimens were stress relieved for 1 h at 700°C followed by oil quenching, which preceded the annealing treatment. Heat X3904 was melted in air at Combustion Engineering. (*a*) 750°C, (*b*) 800°C, (*c*) 850°C, and (*d*) 900°C 53

Fig. 55 Optical microstructure of iron aluminide (FA-129) for various annealing treatments of 1 h followed by oil quenching. Specimens were stress relieved for 1 h at 700°C followed by oil quenching, which preceded the annealing treatment. Heat X3904 was melted in air at Combustion Engineering. (*a*) 750°C, (*b*) 800°C, (*c*) 850°C, and (*d*) 900°C 54

Fig. 56 Optical microstructure comparison of vacuum-melted and air-induction-melted iron aluminide (FA-129). Both sheets were 76-mm (0.030-in.) thick, stress relieved at 700°C for 1 h followed by oil quenching prior to die punching the tensile specimen. The specimens were given a final annealing treatment for 1 h at 700°C amd oil quenched. (*a*) through (*c*) Air-induction melted, and (*d*) through (*f*) vacuum melted 55

Fig. 57 Comparison of scanning electron micrographs of air-induction-melted ingot (X3904) and vacuum-induction-melted iron aluminide [FA-129 (Heat 35)]. In both cases a 76-mm-thick (0.030-in.) sheet was stress relieved at 700°C for 1 h followed by oil quenching prior to die punching the tensile specimens. The specimens were given a final annealing treatment for 1 h at 700°C followed by oil quenching. (*a*) through (*c*) Air melted, and (*d*) through (*f*) vacuum melted 56

Fig. 58 Qualitative elemental analyses of matrices and precipitates in air-melted ingot material (X3904) and vacuum-melted material (Heat 35). (*a*) and (*c*) Matrices and (*b*) and (*d*) precipitates 58

Fig. 59 Fracture surfaces of room-temperature tensile-tested specimens of iron-aluminide alloy [FAL (Heat 13008)]. (*a*) Stress relieved and annealed for 1 h at 700°C, and both were followed by air cooling; (*b*) stress relieved and annealed for 1 h at 750°C and 700°C, respectively, and both were followed by oil quenching; and (*c*) stress relieved and annealed for1 h at 750°C, and both were followed by oil quenching 59

Fig. 60 Fracture surfaces at a higher magnification of room-temperature tensile-tested specimens of iron-aluminide alloy [FAL (Heat 13008)]. (*a*) Stress relieved and annealed for 1 h at 700°C, and both were followed by air cooling; (*b*) stress relieved and annealed for 1 h at 750°C and 700°C, respectively, and both were followed by oil quenching; and (*c*) stress relieved and annealed for 1 h at 750°C, and both were followed by oil quenching 60

FABRICATION AND MECHANICAL PROPERTIES OF Fe_3Al-BASED IRON ALUMINIDES*

V. K. Sikka, C. G. McKamey, C. R. Howell, and R. H. Baldwin

ABSTRACT

Iron aluminides based on Fe_3Al are ordered intermetallic alloys that offer good oxidation resistance, excellent sulfidation resistance, and lower material cost than many stainless steels. These materials also conserve strategic elements such as chromium and have a lower density than stainless steels. However, limited ductility at ambient temperature and a sharp drop in strength have been major deterrents to their acceptance for structural applications. This report presents results on iron aluminides with room-temperature elongations of 15 to 20%. Ductility values were improved by a combination of thermomechanical processing and heat-treatment control. This method of ductility improvement has been demonstrated for a range of compositions. Melting, casting, and processing of 7-kg (15-lb) heats produced at the Oak Ridge National Laboratory (ORNL) and 70-kg (150-lb) commercial heats are described. Vacuum melting and other refining processes such as electroslag remelting are recommended for commercial heats.

The Fe_3Al-based iron aluminides are hot workable by forging or extruding at temperatures in the range of 850 to 1100°C. Rolling at 800°C is recommended with a final 50% reduction at 650°C. Tensile and creep properties of 7- and 70-kg (15- and 150-lb) heats are presented. The presence of impurities such as manganese and silicon played an important role in reducing the ductility of commercially melted heats.

The data presented in this report suggest that the Fe_3Al-based compositions tested are sensitive to environmental effects. The environment of concern is moisture in air which reacts with aluminum and iron to form large amounts of hydrogen on the metal surface. The hydrogen produced is adsorbed and absorbed in the specimens during testing and results in low room-temperature ductilities. Results showed that the use of highly elongated grains with essentially no transverse boundaries appeared to be one way of reducing the hydrogen diffusion and thereby increasing ductility. A special treatment serves as an additional improvement in ductility.

---

*Research sponsored by the U.S. Department of Energy, Fossil Energy AR&TD Materials Program under contract DE-AC05-84OR21400 with Martin Marietta Energy Systems, Inc.

1. INTRODUCTION

Iron aluminides based on Fe_3Al are ordered intermetallic alloys that offer good oxidation resistance, excellent sulfidation resistance, and lower material cost than many stainless steels. These materials conserve strategic elements such as chromium. They have a lower density than stainless steels and, therefore, offer a better strength-to-weight ratio. However, limited ductility at ambient temperature and a sharp drop in strength above 600°C have been major deterrents to their acceptance for structural applications. Previous publications have described the initial development[1-3] and sulfidation-oxidation properties[4] of iron aluminides. The purpose of this report is to present the most recent information on ductility improvement, effects of composition modifications, effects of temperature and strain rate on mechanical properties, scaleup and fabrication of selected compositions, mechanical properties of scaled-up heats, environmental effects, potential applications, and future plans.

2. BACKGROUND

Research on iron aluminides began in 1934. A critical review of the key work on mechanical properties as published in both open literature and limited distribution reports has been prepared by Hook et al.[5] Because ductility is the key to the successful development of iron aluminides, maximum ductility values reported by various investigators[5] are presented in Table 1. Over a period of 50 years the ductility had only been increased from 0 to 9%. In the work described here, ductility values of 15 to 20% have been observed for Fe_3Al-based alloys developed at ORNL.

3. METAL PREPARATION PROCEDURES

Heats of 500 g (1 lb) were arc melted in water-cooled copper crucibles in a chamber backfilled with argon. Buttons were melted six times for homogeneity. The buttons were then drop cast through a copper crucible with a bottom hole into a split copper mold to cast 25 × 12 × 125 mm (1 × 0.5 × 5 in.) ingots. The ingots were cut into halves for subsequent processing. Cutting was performed either using a band saw without a coolant or a high-speed cutoff wheel using a water soluble oil (Buehler No. 10-3330-032). Both cutting procedures produced surfaces free of any cracks. The pieces were then hot forged 50% at

Table 1. Literature on chronological progress in the improvement of room-temperature ductility of Fe_3Al-based iron aluminides

Date	Reference	Maximum ductility (%)
1934	Sykes & Brampfylde (Metro.-Vickers Elect. Co., Ltd.)	None
1950s	Nachman & Buehler (Naval Ordnance Labs.)	1 to 2
1957	Kayser (Ford Motor Company)	~ 1
1957	Justusson, Zackay, & Morgan (Ford Motor Company)	2 to 5
1963	Davies & Stoloff (Ford Motor Company)	None
1964	Stoloff & Davies (Ford Motor Company)	None
1967	Leamy (Iowa State University)	2 to 5
1969	Leamy & Kayser (Iowa State University)	Compression
1975	Marcinkowski, Taylor, & Kayser (Iowa State University)	3
1982	Ehlers & Mendiratta (Materials Lab., Wright-Patterson AFB)	Compression
1982	Chattergee, Mendiratta, Ehlers, & Lipsitt (Materials Lab., Wright-Patterson AFB)	Compression
1982-84	Mendiratta, Mah, & Ehlers (Materials Lab., Wright-Patterson AFB)	8
1984	Inouye (ORNL)	None
1984	Horton, Liu, & Koch (ORNL)	~ 1
1986	Hook, Johnson, & Erfort (Armco)	6 to 9

procedures produced surfaces free of any cracks. The pieces were then hot forged 50% at 1000°C, hot rolled 50% at 800°C, and warm rolled 70% at 650°C to a finish thickness of 0.75 mm (0.030 in.). All operations were conducted with bare metal. The sheet produced, Fig. 1, usually had a brownish luster. The 500-g (1-lb) and larger drop-cast ingots (to be discussed later) are also shown in Fig. 1. Sheets were sheared into pieces approximately 100 mm (4 in.) in length for preparation of the specimens. Each sheet was stress relieved by heating in air for 1 h at a given temperature followed by cooling either in air or mineral oil. The stress-relieved sheets were die punched into tensile specimens of 13-mm (0.5-in.) gage lengths with pin holes added in the grip sections for applying the load. Each specimen was (typically) given an annealing treatment by heating in air for 1 h at a given temperature followed by cooling either in air or mineral oil. The oil-cooled specimens were cleaned by repeated wiping with a dry rag, and the prepared specimens were measured and tensile tested in air at various strain rates and test temperatures. The most common strain rate used was 0.2/min. Specimens tested were measured to calculate the plastic elongation and reduction of area values.

4. IMPROVEMENTS IN STRENGTH AND DUCTILITY AT ORNL

Results of chemical analyses of the experimental heats used for ductility improvement are listed in Table 2. Room-temperature (RT) tensile ductilities of an alloy identified as FAL (Heat 13008) are shown for various annealing temperatures and are compared in Fig. 2 with the values observed for a standard heat treatment used for the same alloy in previous work (represented by the black bar).[3] Note that the 700°C stress-relief treatment was the same for all specimens; the only variation was the annealing treatment. Both treatments were for 1-h duration; the standard treatment used earlier[3] consisted of heating in air for 1 h at 850°C plus 5 to 7 d at 500°C followed by cooling in air. This heat treatment is referred to as treatment A; the new heat treatment produces the highest ductility and is referred to as treatment B. Figure 2 shows that for the first time the RT tensile ductility of Fe_3Al-based iron aluminide can be increased to approximately 20%. This value is dependent on the annealing temperature and is a maximum for an annealing temperature of 700°C (Fig. 2). Higher annealing temperatures resulted in somewhat lower ductility. However, the ductility values were higher than the standard treatment in all cases. Furthermore, the ductilities were between 15 and 20% over an annealing temperature range of 50°C. Figures 3 and 4 show the values of yield and tensile strengths observed for treatment B and compares them with those observed for treatment A. Note that the new

YP6549

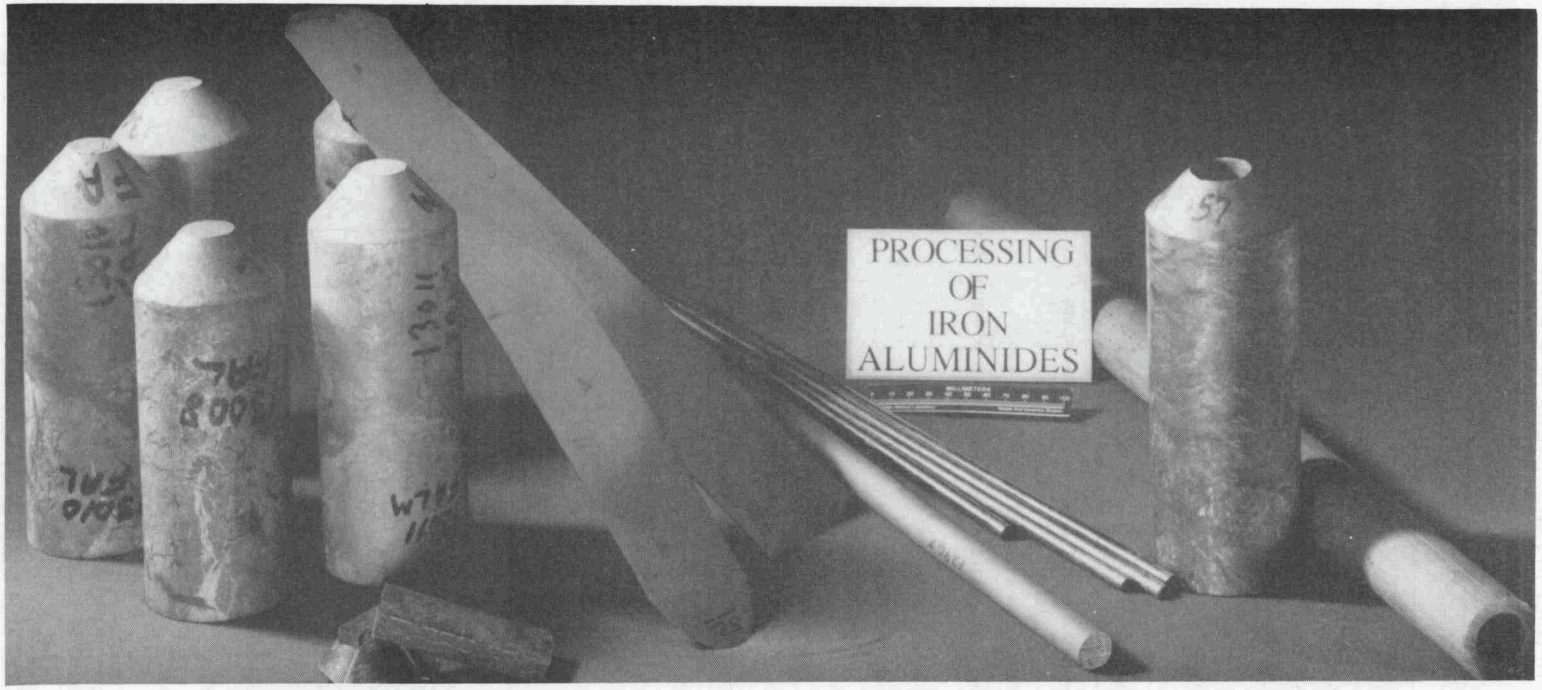

Fig. 1. Photograph showing the 500-g (1-lb) drop casting, the sheet produced from drop casting, the air-induction-melted ingots, and the extruded tubing fabricated from iron-aluminide alloys. The bar and rod produced by extruding and swaging processes are also shown.

Table 2. Chemical analysis of the experimental heats used for ductility improvement studies

Element	Alloy designation (wt %)			
	FAL[a]	FALM[b]	FA-129[c]	FAS[d]
Al	15.88	15.88	15.9	15.93
Cr	5.46	5.46	5.5	2.19
Zr	0.19			
Nb		0.20	1.0	
B	0.01			0.011
C		0.04	0.05	
Fe	Bal.[e]	Bal.[e]	Bal.[e]	Bal.[e]

[a]Alloy for low-temperature (≤600°C) use with maximum room-temperature ductility.

[b]Modification of FAL for low-temperature use.

[c]Alloy for high-temperature (≥600°C) use with somewhat lower room-temperature ductility.

[d]Alloy for use in sulfur-containing environments.

[e]Balance (100 minus total of all other elements).

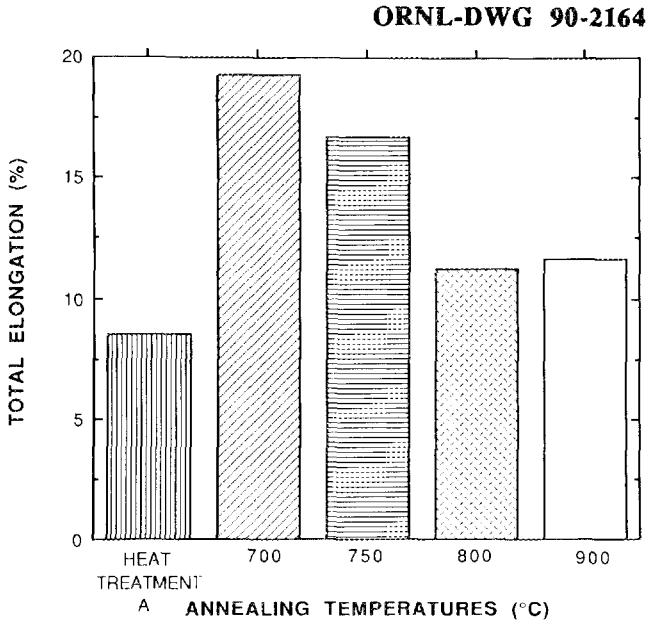

Fig. 2. Effect of annealing temperature on room-temperature tensile elongation of iron-aluminide FAL (Heat 13008). Data on heat treatment A are included for comparison. Annealing treatments were of 1-h duration followed by oil quenching. All tensile tests were at a strain rate of 0.2/min.

ORNL-DWG 90-2165

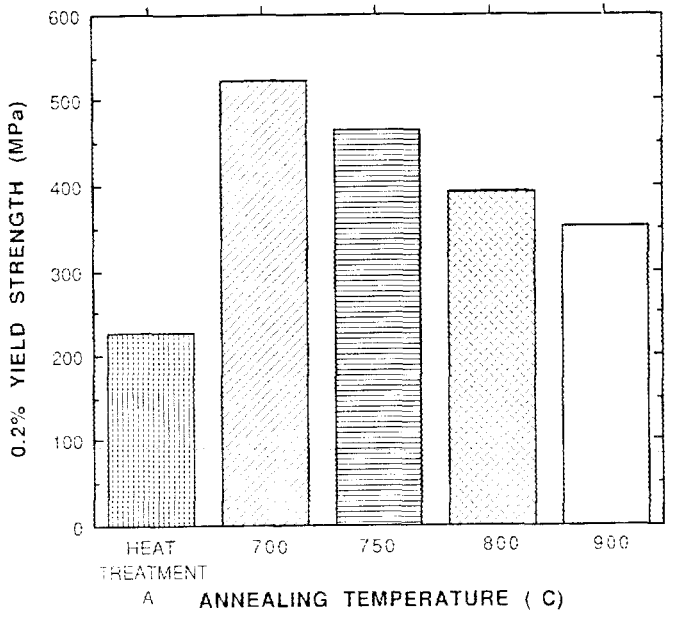

Fig. 3. Effect of annealing temperature on room-temperature yield strength of iron-aluminide FAL (Heat 13008). Data on heat treatment A are included for comparison. Annealing treatments were of 1-h duration followed by oil quenching. All tensile tests were at a rate of 0.2/min.

ORNL-DWG 90-2166

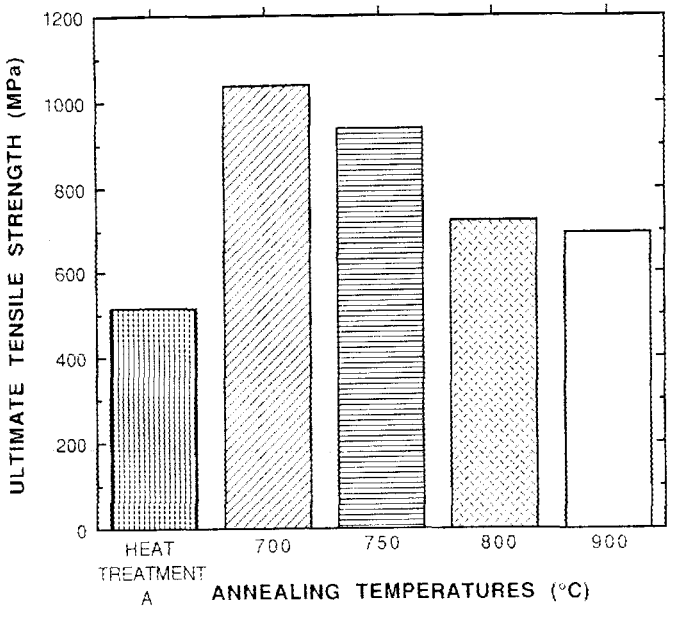

Fig. 4. Effect of annealing temperature on room-temperature ultimate tensile strength of iron-aluminide FAL (Heat 13008). Data on heat treatment A are included for comparison. Annealing treatments were of 1-h duration followed by oil quenching. All tensile tests were at a strain rate of 0.2/min.

annealing treatment significantly enhanced both ductility and strength properties. The heat treatment was then extended to all of the compositions listed in Table 2. Figure 5 shows that treatment B produced over 15% ductility for all of the compositions. At this stage of research, treatment B was extended to 19 developmental compositions. In Fig. 6, the ratio of total elongation for both heat treatments B and A was plotted as a function of total elongation for heat treatment A for 19 different compositions of Fe_3Al-based iron aluminides. This figure shows that heat treatment B nearly doubled the total elongation of all the compositions. Corresponding increases in yield and ultimate tensile strengths for treatment B over A are shown in Figs. 7 and 8.

Once it was established that treatment B produced a factor of 2 higher ductilities than treatment A, additional work was conducted to determine the ranges that could be tolerated for this treatment. The first variable examined was the annealing temperature. It was varied systematically for alloy FA-129 from 650 to 900°C for a fixed time of 1 h and followed by cooling in oil. The RT elongation data from this study are plotted in Fig. 9 and show that the ductility of FA-129 is maximized with an annealing temperature of 750°C. The peak ductility temperature is expected to be different for different alloy compositions; this is explained in Sect. 9. Effects of holding time at 750°C for alloy FA-129 (Fig. 10) show that annealing time is not as important for ductility as is annealing temperature.

Heat treatment A used a 5- to 7-d treatment at 500°C to stabilize the DO_3 ordered structure. A similar ordering treatment was used for specimens of FA-129 following the maximum ductility treatment of 750°C for 1 h. The results of this study showed only minor effects of ordering treatment (Fig. 11).

5. TEMPERATURE AND STRAIN RATE EFFECTS ON TENSILE PROPERTIES

The iron-aluminide alloy FAL (Heat 13008) that showed the highest RT ductility was also tested as a function of test temperature up to 800°C. The results of these tests are plotted in Figs. 12 -14. Yield and ultimate tensile strengths of this alloy hold up very well up to 500°C and drop sharply at higher temperatures. Tensile ductility of this alloy increases with temperature and reaches superplastic values of over 100% at 800°C.

The FAL alloy was also tested as a function of various strain rates at room temperature and is shown in Fig. 15, which indicates that RT ductility of FAL increased as strain rate increased. This effect is contrary to many common materials and is explained in Sect. 9.

ORNL-DWG 90-2167

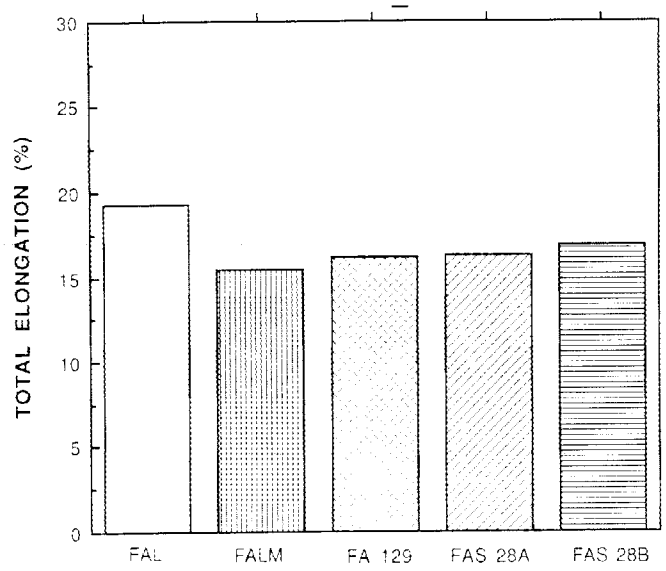

Fig. 5. Comparison of room-temperature elongation observed for four different compositions of iron aluminide using the newly developed heat treatment B. FAS-28A and FAS-28B represent the same composition but slightly different processing steps. Annealing treatments were of 1-h duration followed by oil quenching. All tensile tests were at a strain rate of 0.2/min.

ORNL-DWG 90-2168

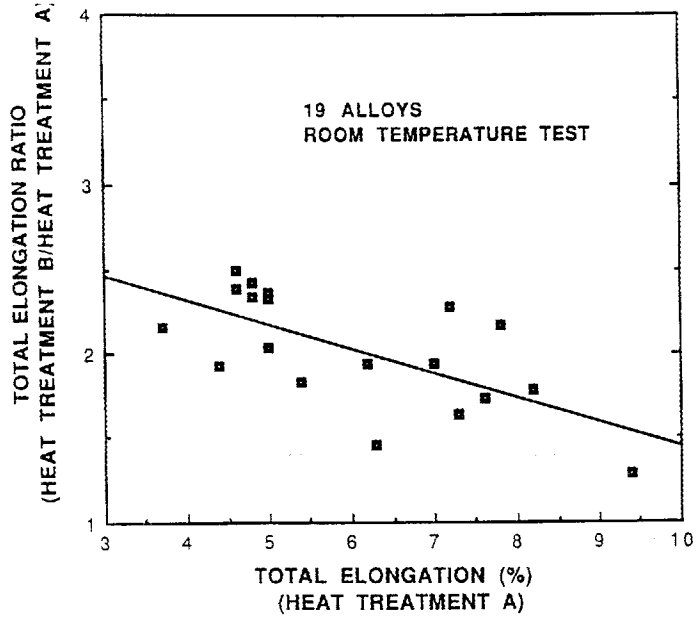

Fig. 6. Room-temperature total elongation ratio for heat treatments B and A as a function of total elongation for treatment A for 19 different compositions for Fe_3Al-based iron aluminides.

ORNL-DWG 90-2169

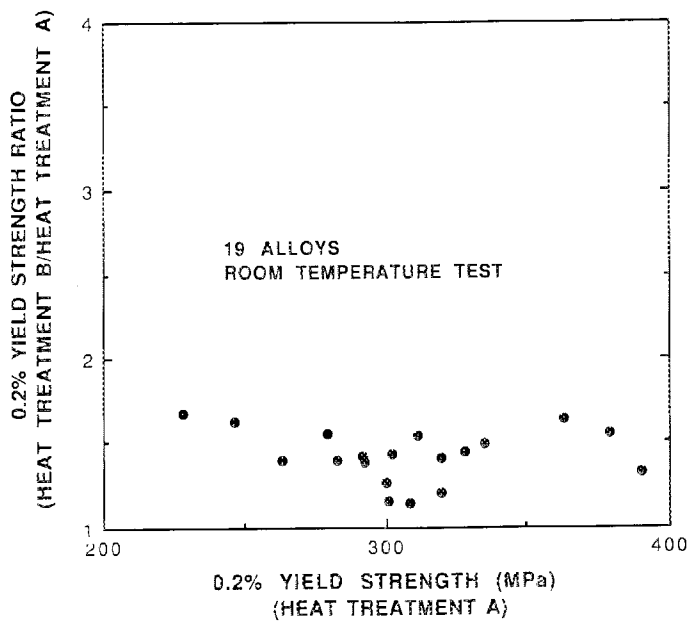

Fig. 7. Room-temperature yield-strength ratio for heat treatments B and A as a function of yield strength for treatment A for 19 different compositions of Fe_3Al-based iron aluminides.

ORNL-DWG 90-2170

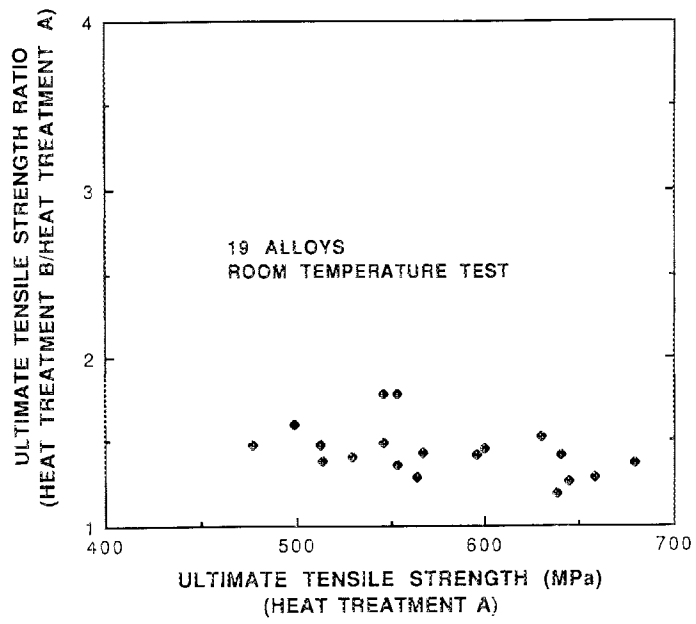

Fig. 8. Ultimate tensile-strength ratio for heat treatments B and A as a function of ultimate tensile strength for treatment A for 19 different compositions for Fe_3Al-based iron aluminide.

ORNL-DWG 90-2171

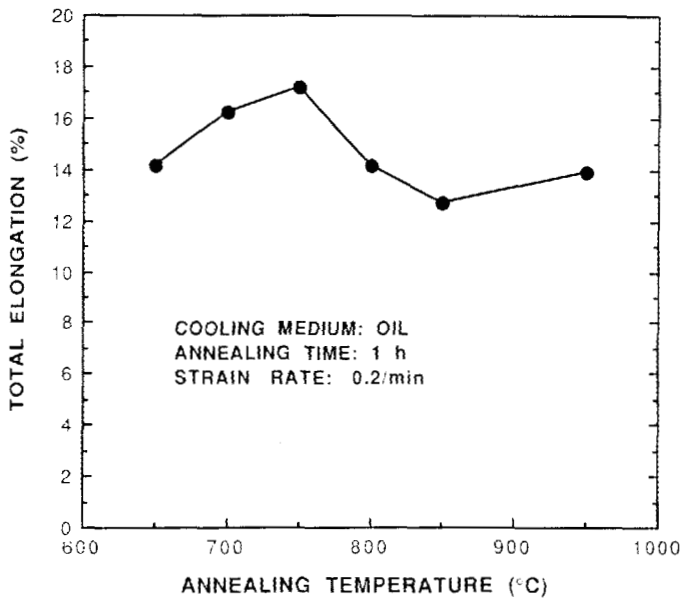

Fig. 9. Effect of annealing temperature on room-temperature total elongation of iron-aluminide alloy FA-129.

ORNL-DWG 90-2172

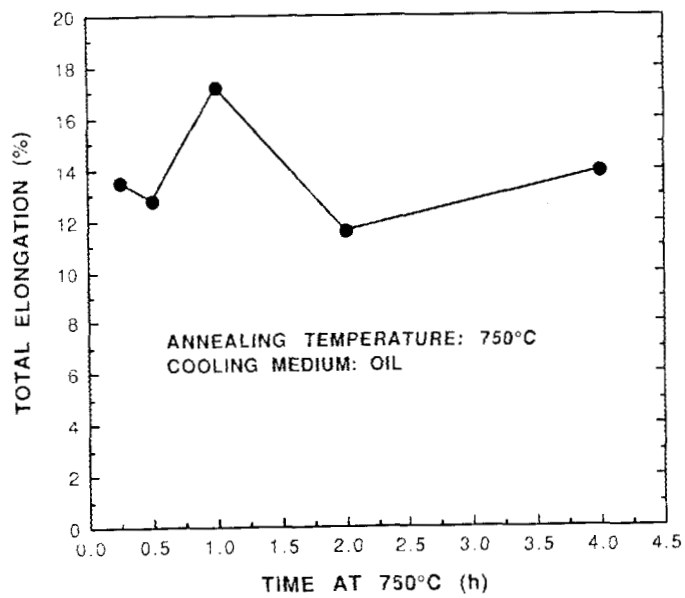

Fig. 10. Effect of annealing time at maximum ductility temperature on room-temperature total elongation of iron-aluminide alloy FA-129.

ORNL-DWG 90-2173

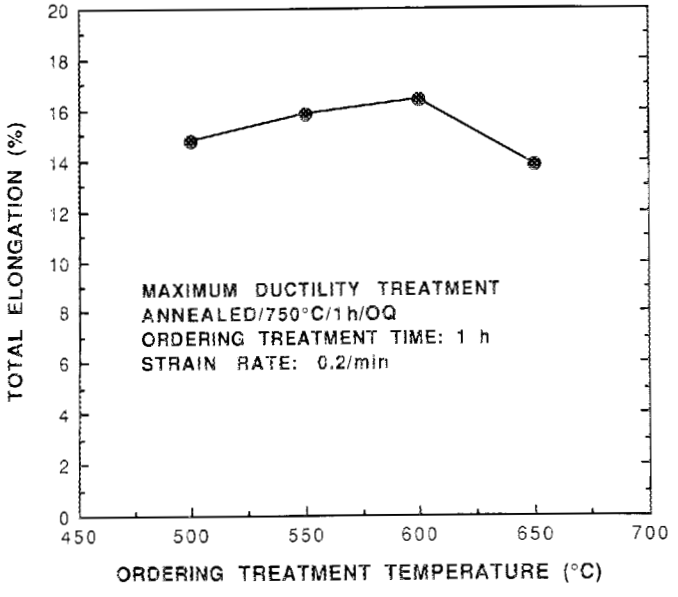

Fig. 11. Effect of ordering-treatment temperature on room-temperature total elongation of iron-aluminide alloy FA-129. Specimens were given the maximum ductility treatment prior to the ordering treatment. All tensile tests were at a strain rate of 0.2/min.

ORNL-DWG 90-2174

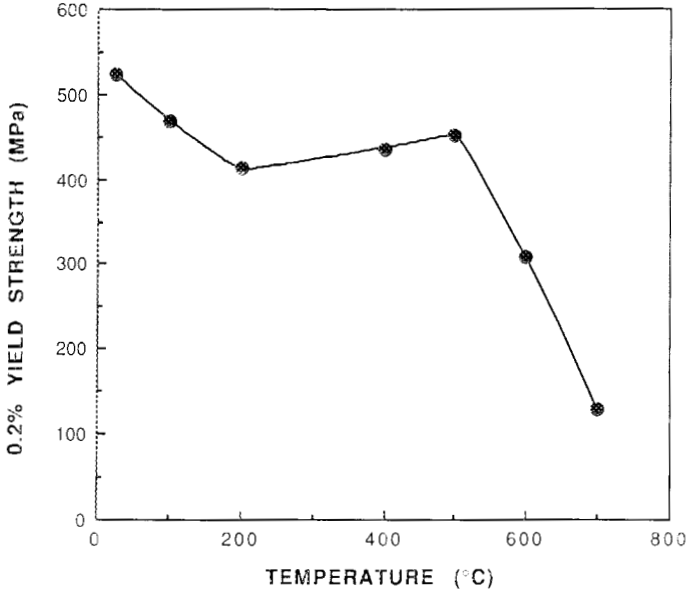

Fig. 12. Yield strength (0.2% offset) as a function of test temperature for iron-aluminide alloy FAL (Heat 13008). Specimens were given a 700°C/1 h/OQ stress-relief treatment followed by a 700°C/1 h/OQ annealing treatment. All tests were in air at a strain rate of 0.2/min.

ORNL-DWG 90-2175

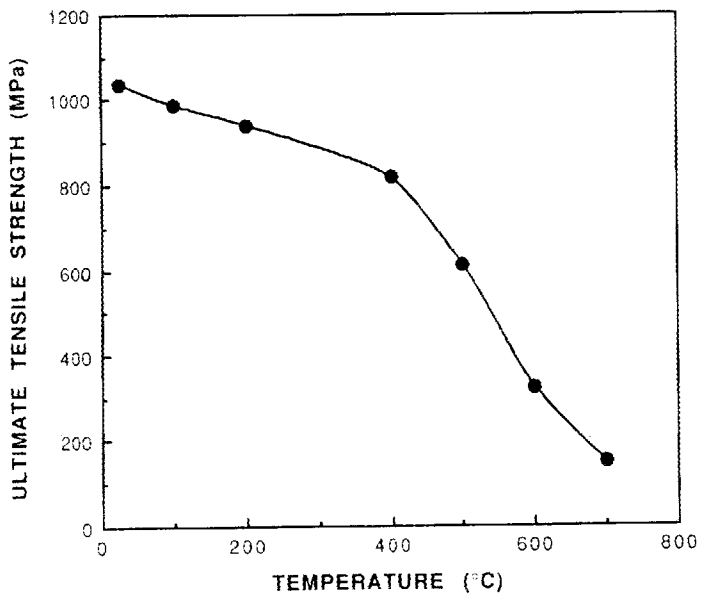

Fig. 13. Ultimate tensile strength as a function of test temperature for iron-aluminide alloy FAL (Heat 13008). Specimens were given a 700°C/1 h/OQ stress-relief treatment followed by a 700°C/1 h/OQ annealing treatment. All tests were in air at a strain rate of 0.2/min.

ORNL-DWG 90-2176

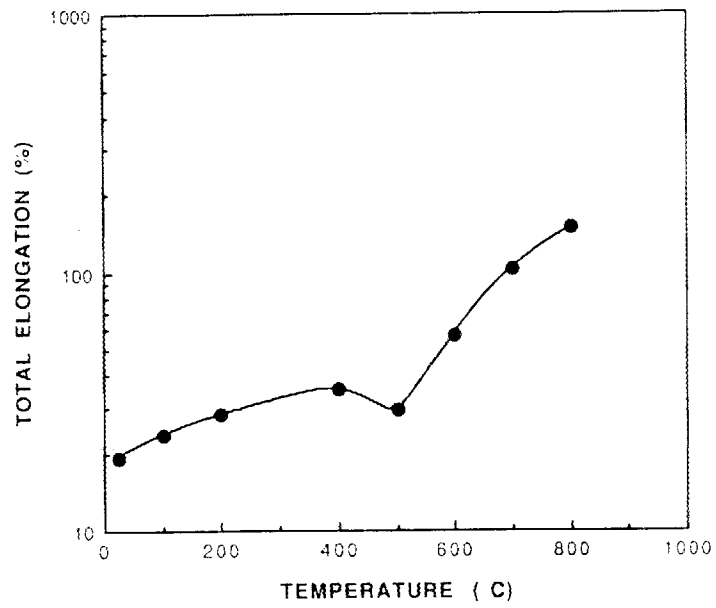

Fig. 14. Total elongation as a function of test temperature for iron-aluminide alloy FAL (Heat 13008). Specimens were given a 700°C/1 h/OQ stress-relief treatment followed by a 700°C/1 h/OQ annealing treatment. All tests were in air at a strain rate of 0.2/min.

ORNL-DWG 90-2177

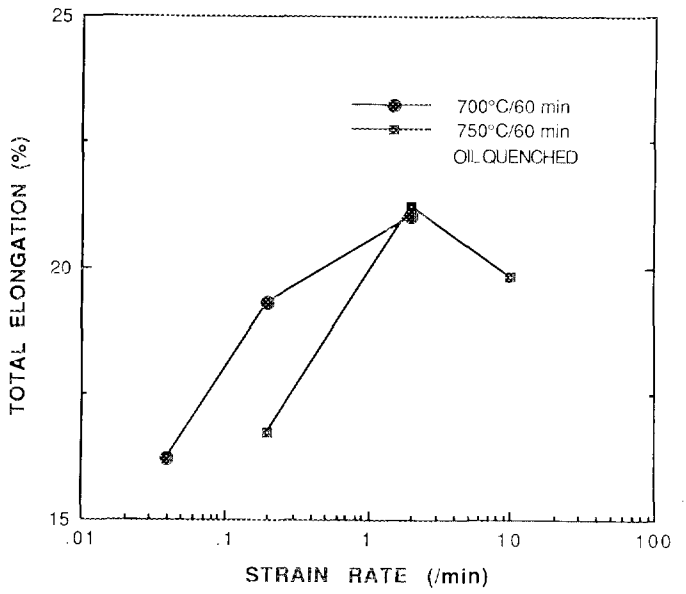

Fig. 15. Total elongation at room temperature as a function of strain rate for iron-aluminide alloy FAL (Heat 13008). Specimens were tested in two heat treatments

6. SCALEUP AND FABRICATION OF LARGE HEATS

After obtaining the relatively high ductilities for several of the Fe_3Al-based alloys, it was decided to scale these compositions from 500-g (1-lb) arc-melt heats to 7-kg (15-lb) heats at ORNL and to larger heats at a commercial vendor. A description of each of the scaleups follows.

6.1 SCALEUP AT ORNL

The scaleup at ORNL consisted of melting 7-kg (15-lb) heats using air-induction melting; $ZrO_2$was used as the crucible material. The melt stock consisted of electrolytic iron that was hydrogen-gas fired at 1000°C and stored in desiccators. The aluminum was pure ingot stock that was forged and rolled to plate and then chopped into melt stock. The aluminum chips were cleaned (using an HCl solution), washed, dried, and stored in a desiccator until ready for melting. When appropriate, elemental additions such as Nb, Mo,

Zr, B, Cr, and C were made using high-purity stock. The melt was normally held at 1650°C for 2 to 5 min and top-poured into graphite molds to make 72-mm-diam (2.85-in.) ingots with an extrusion nose on one end. The graphite mold was preheated to 500°C, and a 100-mm-diam (4-in.) hot-top was used to minimize solidification shrinkage. No shrinkage in the ingot was found, even very close to the hot-top. Typical ingots produced by this method are shown in Fig. 1. Note the surfaces were smooth and essentially no oxidation was observed. One heat of iron aluminide was also cast into a slab, and no unusual problems were encountered. A graphite mold with a core rod of graphite was used to produce hollow ingots by casting. The graphite rod was drilled from the solid ingot, and the resulting hollow ingot is shown in Fig. 1.

6.2 FABRICATION OF ORNL INGOTS

The two primary methods used for fabrication of ORNL ingots were extrusion and forging. The extrusions were conducted on bare ingots, without any surface machining. Extrusion temperatures ranged from 850 to 1100°C, and the reduction ratios varied from 9:1 to 16:1. The extrusion constants for Fe_3Al-based iron aluminides were 219, 125, and 119 MPa (35, 20, and 19 tsi) for temperatures of 850, 1000, and 1100°C, respectively. Extrusions of round-to-round and tube blanks were of excellent quality (Fig. 1).

Forgings were done at temperatures in the range of 850 to 1100°C and were successfully completed on cold platens. The reduction per forging pass was up to 50% without reheating. All ORNL forgings were conducted on a very slow speed 500-ton press. The forging was normally conducted at or below the extrusion temperature, and was generally stopped at a flat thickness of 6 mm (0.25 in.). These 6-mm-thick (0.25-in.) flat sheets were normally hot rolled at 800°C to a 2.5-mm (0.10-in.) thickness. The sheet was then typically hot rolled at 650°C to a finished thickness of 0.76 mm (0.03 in.). All of the rolling was conducted without a cover gas. The 0.76-mm-thick (0.03-in.) sheet was used for tensile and creep property evaluation.

6.3 SCALEUP AT COMMERCIAL VENDORS

The first scaleup of iron aluminides by a commercial vendor was conducted at Combustion Engineering, Chattanooga, Tennessee. The analyses of three iron-aluminide heats are presented in Table 3. The initial plan was to melt all 230-kg (500-lb) heats by air-induction melting and cast them into 150-mm-diam (6-in.) ingots. However, the first cast ingot showed bulging of the hot-top rather than conventional shrinking. Once the hot-top

Table 3. Target and check analyses of 70- and 230-kg (150- and 500-lb) heats of iron aluminides melted by air-induction melting at Combustion Engineering

Element	Heat 1 (wt %)				Heat 2 (wt %)			Heat 3 (wt %)		
	Target	X3902[a]	X3903	X3908	Target	X3904	X3905	Target	X3906	X3907
Al	15.9	16.39	15.9	15.7	15.9	16.0	15.84	15.9	15.84	14.96
Cr	5.5	5.58	5.54	5.38	5.5	5.60	5.44	5.5	5.20	5.40
Zr	0.15	0.18	0.18	0.15				0.15	0.17	0.16
Nb				1.0	1.1	1.01	1.00	1.04	1.05	
Mo								1.00	1.07	1.06
C		0.047	0.063	0.049	0.05	0.047	0.051		0.052	0.05
B	0.01	0.013	0.015	0.013				0.04	0.038	0.035
S		0.007	0.011	0.010		0.012	0.013		0.012	0.010
N		0.0008	0.0006	0.0005		0.0006	0.0005		0.0005	0.0005
O_2		0.0025	0.0025	0.0018		0.0017	0.0017		0.0017	0.0016
Fe	Bal.[b]	Bal.[b]	Bal.[b]	Bal.[b]	Bal.[b]	Bal.[b]	Bal.[b]	Bal.[b]	Bal.[b]	Bal.[b]

[a]A 230-kg (500-lb) heat prepared using unbaked melt stock; all other numbers represent individual ingots from the 70-kg (150-lb) heats prepared using baked iron and aluminide stock.

[b]Balance (100 minus total of all other elements).

was cut, the ingot also showed large voids. At this point, the vendor suggested that the ingots were trapping gas. After a discussion between the staff at ORNL and the vendor, it was suggested that the gas was possibly hydrogen and was resulting from the thermodynamically favored reaction of aluminum with water vapor in the air; for example,

$$2Al + 3H_2O \rightarrow Al_2O_3 + 6H.$$

The free energy for this reaction is -896.6 kJ/mol. Such a process could produce copious amounts of hydrogen. Once the hydrogen-gas entrapment was suspected, it was decided that the iron and aluminum for the melt stock should be baked to remove any moisture. This practice was tried in the induction furnace with an argon cover gas for 70-kg (150-lb) heats, and the problem was significantly reduced. At this stage the vendor supplied one 230-kg (500-lb) heat and one each of the 70-kg (150-lb) heats for all of the compositions. Figure 16 is a photograph showing all of the ingots received by ORNL. All of the ingots were cast in sand molds and, thus, had rough surfaces.

The 100-mm-diam (4-in.) ingots from each heat were cut into pieces 150 mm (6 in.) long. Noses were machined from each piece, and the billets were successfully extruded at 1000°C to round bar and rectangular bar. The rectangular bar was hot forged and hot rolled to 0.76-mm (0.030-in.) thick, using the same procedure as for the ORNL ingots. The billet, extruded products, and finished sheets from the Combustion Engineering ingots are shown in Fig. 17. Mechanical properties of material from these heats are presented in Sect. 7.

The next scaleup was performed by The Timken Company, Canton, Ohio. The first trial involved air-induction melting a 230-kg (500-lb) heat. The entire heat was cast into a 200-mm^2 (8-$in.^2$) ingot. The ingot was found to be riddled with holes, similar to those observed for the 230-kg (500-lb) heat melted by Combustion Engineering. At this point, it was decided to melt these alloys by vacuum-induction melting. One 45-kg (100-lb) heat of FA-129 was vacuum-induction melted and cast into 100-mm-diam (4-in.) tapered molds. These ingots were of excellent quality and did not show any visible porosity. In vacuum melting, the elimination of porosity related to hydrogen was probably caused by a combination of two factors: (1) no moisture came in contact with the melt, and (2) any trapped gas that might have been produced by the reaction shown in the equation was pumped out as the melting proceeded. Thus, from experience at both Combustion Engineering and The Timken Company, it is recommended that Fe_3Al-based iron aluminides be melted by vacuum-induction melting and, if desired, further refined by vacuum-arc remelting or by electroslag remelting.

YP7104

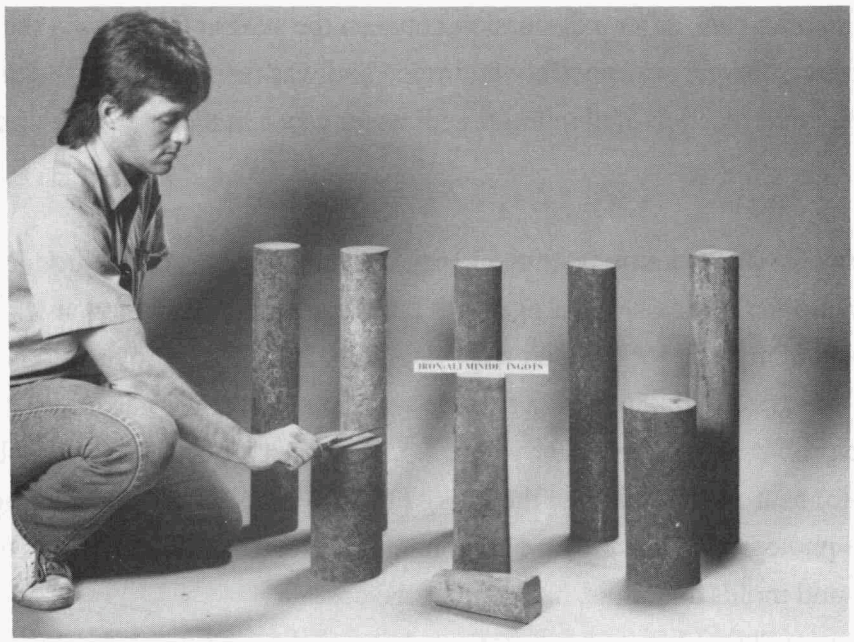

Fig. 16. Photograph of iron-aluminide ingots of 70 to 230 kg (150 to 500 lb) melted by air-induction melting at Combustion Engineering.

YP9578

Fig. 17. Photograph of billet, extruded bars, and rolled sheet prepared at ORNL from ingots of iron-aluminide alloys received from Combustion Engineering.

The chemical analyses of the Combustion Engineering heats (Table 3) showed that the major alloying element target concentrations could be met very well by air-induction melting. The nitrogen and oxygen contents were extremely low. Carbon of 0.05 wt % was present in all of the heats. The carbon in the alloys came from the melt stock, and because air-induction melting permitted no opportunity for removing carbon, the only way to reduce it was to use carbon-free melt stock. In commercial melting, processes such as argon-oxygen deoxidation (AOD) can be used to control the carbon level. The results for recovery of various elements using pure melt stock and air-induction melting at ORNL are shown in Table 4 for 7-kg (15-lb) heats. The recovery of most elements was excellent.

6.4 MELTING OF HEATS AT ORNL USING COMMERCIAL MELT STOCK

A scaleup to 7-kg (15-lb) heats was also conducted at ORNL using commercial melt stock. The melt stock consisted of scrap iron, aluminum shot, ferrochromium, and ferroboron. This melt stock contained impurity elements such as Mn, Si, C, and Mg. A 72-mm-diam (2.85-in.) ingot made from this melt stock had the same surface appearance as an ingot made from the pure elemental melt stock. The ingot was cut, forged, and rolled into a sheet 0.76-mm (0.030-in.) thick. The forging and rolling temperatures required for this ingot were at least 100°C higher than those required for the ingots made from elemental melt stock. The mechanical properties evaluation of this material are discussed in Sect. 7. Because of its importance in commercial practice, it is recommended that chemical analysis of this ingot be done and that the elements carried over from the melt stock be identified. It is further recommended that the effect of detrimental elements be determined by preparation of drop castings with varying amounts of those elements.

6.5 POWDER PREPARATION BY A COMMERCIAL VENDOR AND ITS CONSOLIDATION AND PROCESSING AT ORNL

For most applications, iron aluminides are expected to be produced economically by conventional melting, casting, and processing techniques. However, for applications such as hot-gas cleanup filters and spray coatings for improved oxidation-sulfidation resistance, powders will be required. To meet such potential needs, one heat of sulfidation-resistant composition (FAS) was nitrogen-gas atomized at Ametek Specialty Metal Products Division, Eighty Four, Pennsylvania, a commercial vendor. The melt was prepared by air-induction melting with an inert gas cover. No problems were encountered in the melting or atomization processes. The vendor's chemical analysis of the powder is compared with

Table 4. Recovery of various elements during air-induction melting of 7-kg (15-lb) iron-aluminide heats at ORNL

Element	Alloy 1		Alloy 2		Alloy 3		Alloy 4	
	Target (wt %)	Recovery (%)	Target (wt %)	Recovery (%)	Target (wt %)	Recovery (%)	Target (wt %)	Recovery (%)
C					0.04	250.00[a]		
Cr	2.157	98.75	5.46	91.03	5.46	95.24	2.194	95.72
Mo	0.995	100.00						
Cb	1.542	100.00			0.21	100.00		
Al	15.672	96.86	15.88	96.73	15.88	97.54	15.932	96.67
B	0.011	81.82	0.01	80.00		0.011	27.27	
Zr	0.189	100.00	0.19	100.00				
Fe	Bal.[b]		Bal.[b]		Bal.[b]		Bal.[b]	

[a]Recovery of greater than 100% indicates pickup of carbon from external sources. For example, a graphite rod was used for stirring the liquid metal and a small fraction of the graphite was probably dissolved in the metal.

[b]Balance (100 minus total of all other elements).

the target chemistry in Table 5 and shows close agreement. Optical micrographs of the powder are shown in Figs. 18 and 19. The powder particles were mostly spherical and showed very fine intraparticle structure, indicative of extremely fast cooling rates (> 10^3°C/s). Some powder particles also showed holes from solidification shrinkage.

A 76-mm-diam (3-in.) mild steel can was filled with powder from Ametek. The can was evacuated, sealed, heated for 1.5 h at 1000°C, and extruded through a 25-mm (1-in.) die to obtain an area-reduction ratio of 9:1. Optical microstructure of the as-extruded bar (Fig. 20) showed full consolidation from the surface to the center of the bar. The grain size was very fine (20 mm) and uniform across the bar.

The steel can was removed by dissolving in a 10% HNO_3 solution. Two 76-mm-long (3-in.) sections of the bar were forged 50% at 1000°C, rolled 50% at 850°C, and finish rolled 50% at 650°C to a sheet 0.76-mm (0.030-in.) thick. The sheet was then used for mechanical property evaluations. No problems were encountered in the processing steps.

Table 5. Chemical analysis of nitrogen-gas-atomized powder of iron-aluminide alloy FAS from Ametek

Element	Target (wt %)	Vendor analysis (wt %)
Al	15.93	15.9
Cr	2.19	2.2
B	0.011	0.01
Fe	Bal.[a]	Bal.[a]
S		0.007
N		0.003
O_2		0.013

[a]Balance (100 minus total of all other elements).

7. MECHANICAL PROPERTIES OF SCALED-UP HEATS

The scaled-up heats produced at ORNL, Combustion Engineering, and The Timken Company were primarily tested for tensile properties and heat-treatment effects on tensile and creep properties.

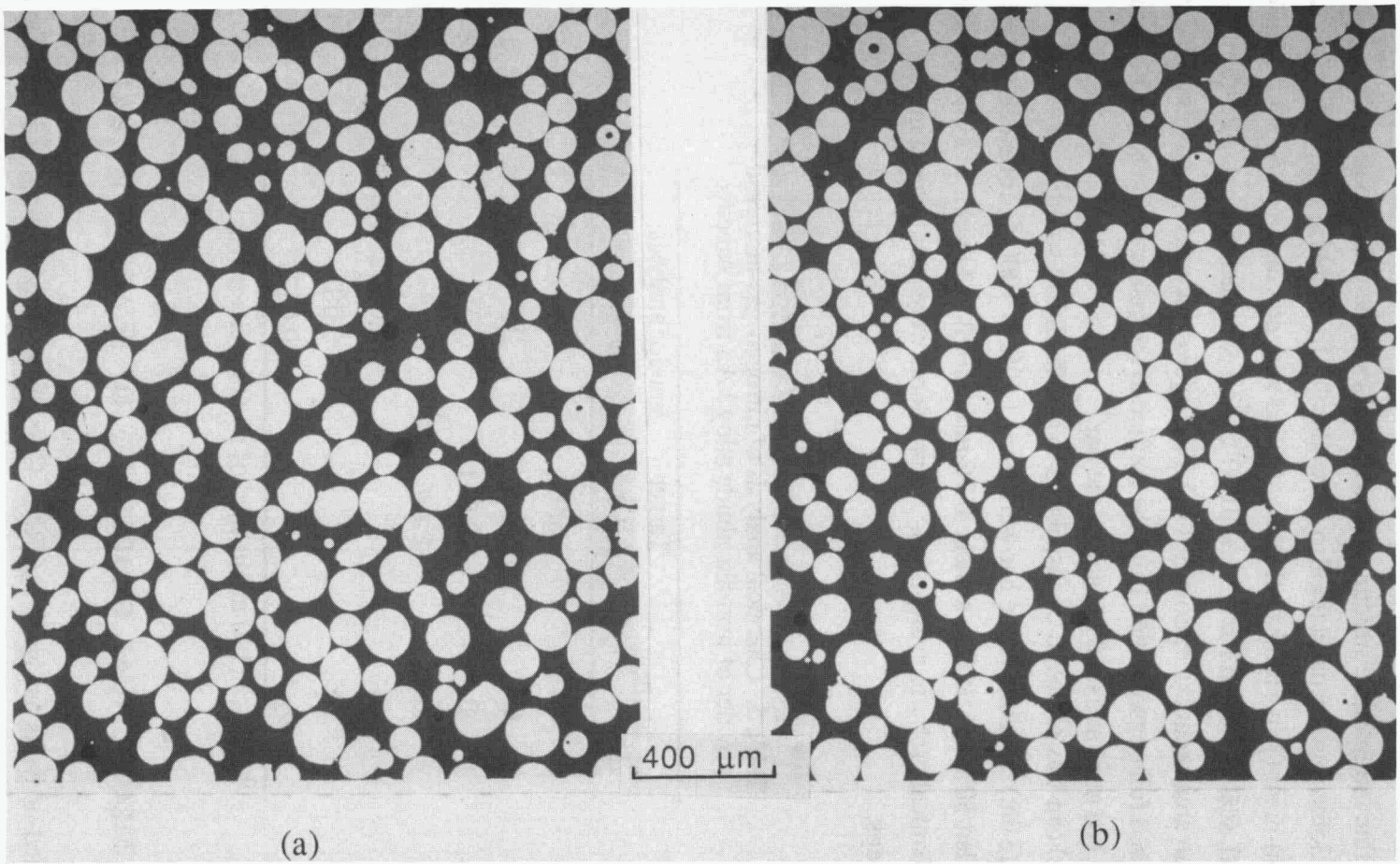

Fig. 18. Optical micrographs of two sample regions of nitrogen-gas-atomized powder of iron aluminide (FAS) from Ametek.

YP9705

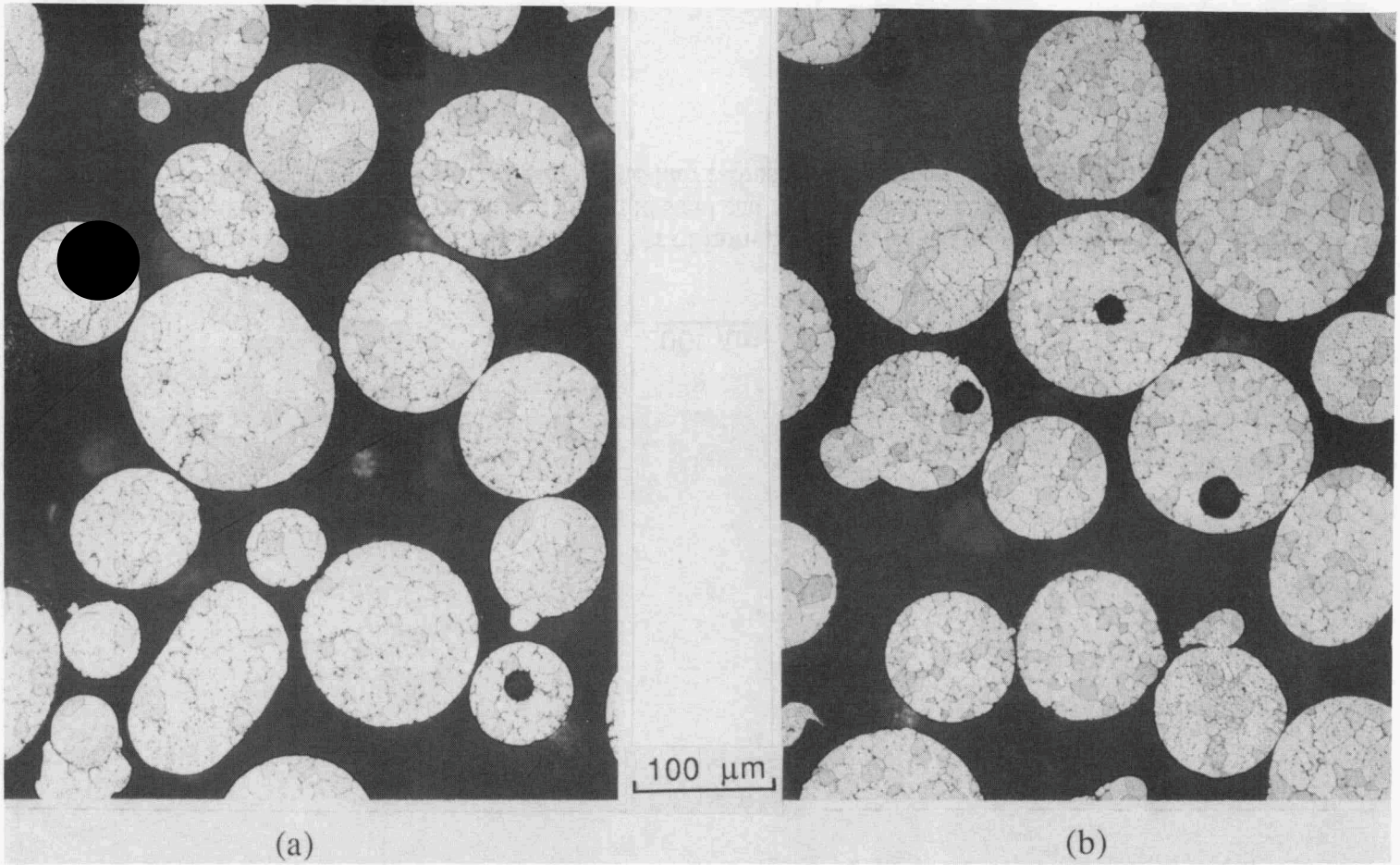

Fig. 19. Optical micrographs of two sample regions of nitrogen-gas-atomized powder of iron aluminide (FAS) from Ametek. The specimen was etched.

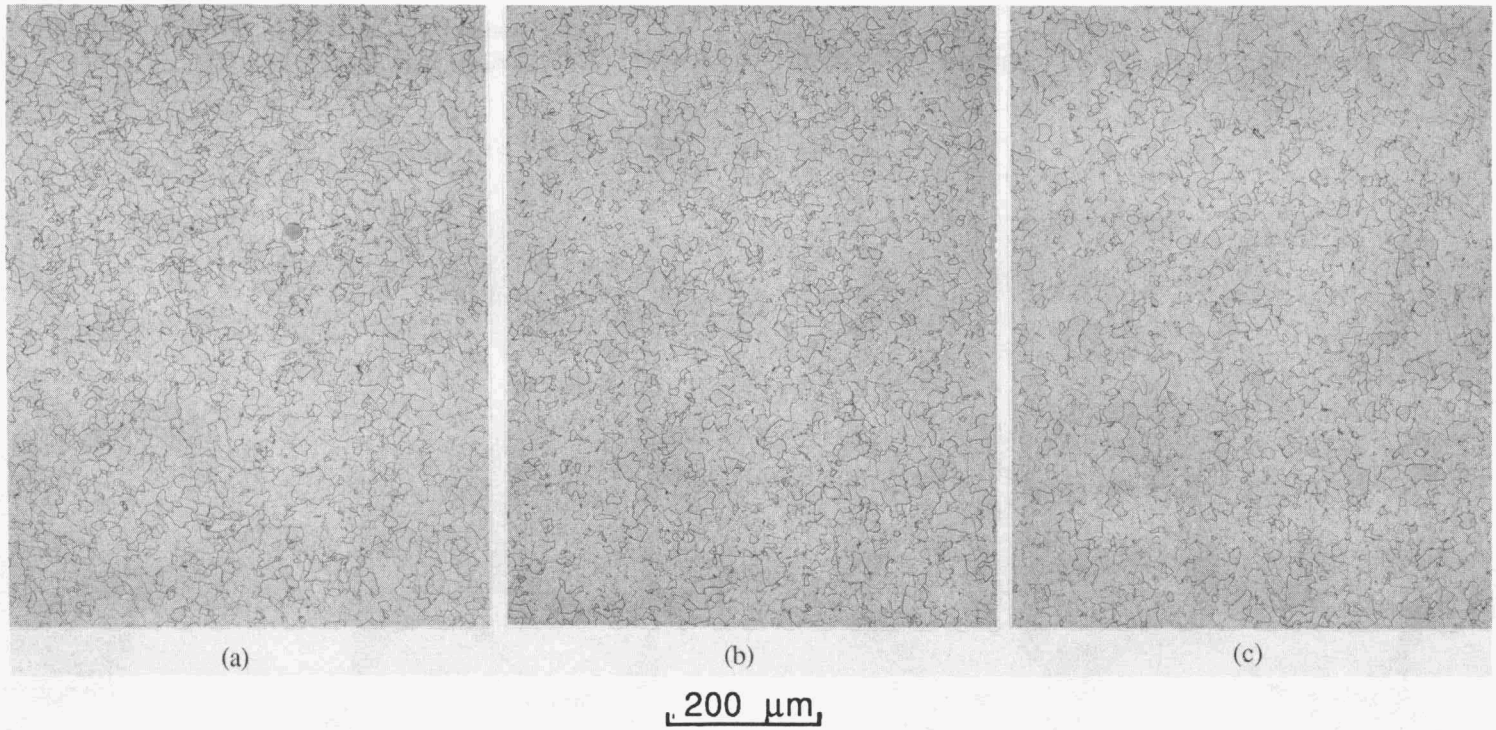

Fig. 20. Optical microstructure of as-extruded bar of iron-aluminide (FAS) powder prepared by nitrogen-gas atomization at Ametek. The powder was placed in a mild steel can and extruded to a ratio of 9:1 area reduction at 1000°C. The microstructures are from (*a*) edge, (*b*) one-half radius, and (*c*) center of the extruded bar.

7.1 TENSILE PROPERTIES

Most of the testing on ORNL scaled-up heats concentrated on determination of the appropriate heat treatments for maximizing RT ductility. Alloy FAL (Heat 13008), for which the RT ductility value of 20% had been achieved, was tested for effects of test temperature and strain rate. These data for alloy FAL are presented in Figs. 2-5 and 12-15.

The effects of cooling sequence and cooling medium on the RT tensile properties of stress-relieved and annealed FAL (Heat 13008) are presented in Figs. 21-23. The stress-relief temperature was 700°C for 1 h, and the annealing temperature was varied from 700 to 900°C. Oil quenching after both stress relief and annealing gave the highest ductility for all annealing temperatures. The final step of cooling in air gave lower ductility values for all annealing temperatures regardless of the stress-relieving step. Figure 21 includes the commonly observed values of the binary composition (approximately 4% for Fe_3Al) and for a composition-modified Fe_3Al (9%), both in the heat treatment A condition. Compared to those values, the heat treatments used in this study gave improved elongation values of 15 to 20%. The results in Fig. 21 also imply that improved ductility is obtained by control of both heat-treatment temperature and cooling medium. When both are used together, the ductility values are maximized. The yield-strength values of FAL (Fig. 22) are not affected by the cooling rate sequence. The tensile-strength values (Fig. 23) followed the ductility trend because they are interrelated.

The effect of a cooling medium on tensile properties was also investigated for the FAS (Heat 13017) alloy containing 2% Cr. In this study, the sheets were stress relieved at 700°C for 1 h followed by oil quenching. The punched tensile specimens were annealed at various temperatures, and one specimen each was cooled in air and oil, respectively. The RT tensile data on these specimens are plotted in Figs. 24-26. These figures show the results similar to those observed for alloy FAL in Figs. 21-23. The total elongation and ultimate tensile strength were consistently higher for oil-quenched specimens than for air-quenched specimens. The yield strength was not significantly affected.

The effect of stress-relief treatment on the sheet prior to punching tensile specimens was also investigated for alloy FAL (Heat 13008). The stress-relief temperatures used were 700 and 750°C for 1 h followed by oil quenching. Punched specimens were tested after various heat treatments followed by oil quenching. Total elongation, yield strength, and ultimate tensile strength at RT for the two different stress-relief conditions are

ORNL-DWG 90-2178

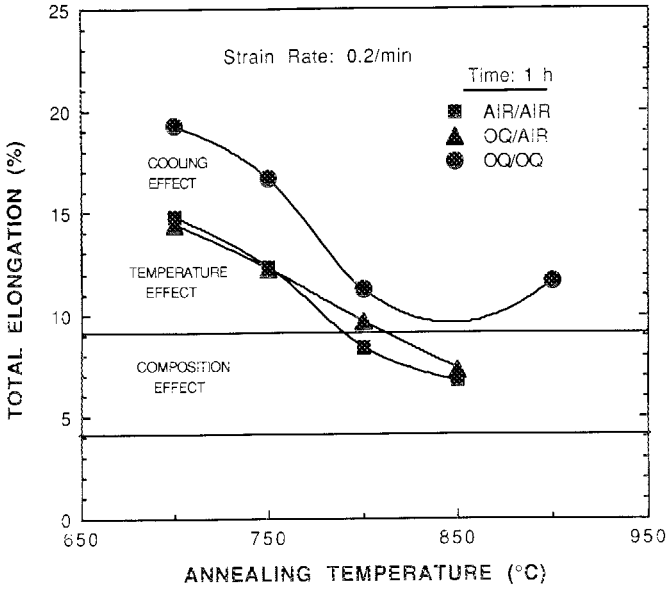

Fig. 21. Effect of cooling sequence and annealing temperature on room-temperature total elongation of iron-aluminide alloy FAL (Heat 13008). All of the specimens were stress relieved for 1 h at 700°C prior to annealing at different temperatures.

ORNL-DWG 90-2179

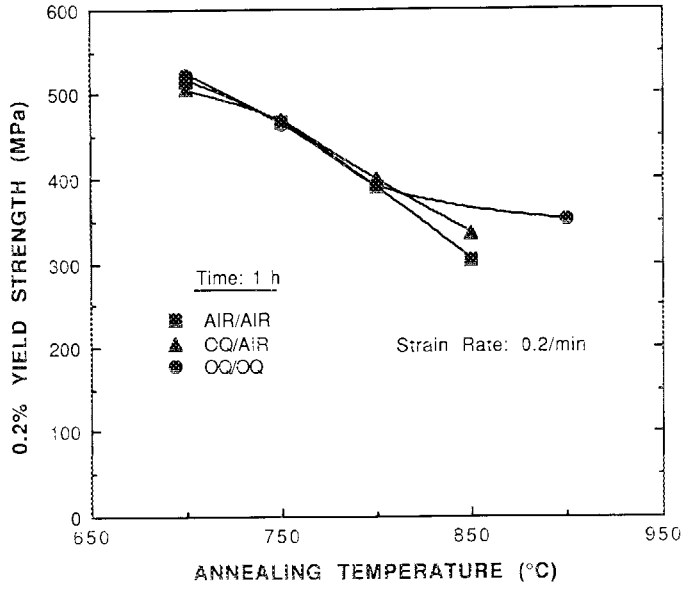

Fig. 22. Effect of cooling sequence and annealing temperature on room-temperature yield strength (0.2% offset) of iron-aluminide alloy FAL (Heat 13008). All of the specimens were stress relieved for 1 h at 700°C prior to annealing at different temperatures.

ORNL-DWG 90-2180

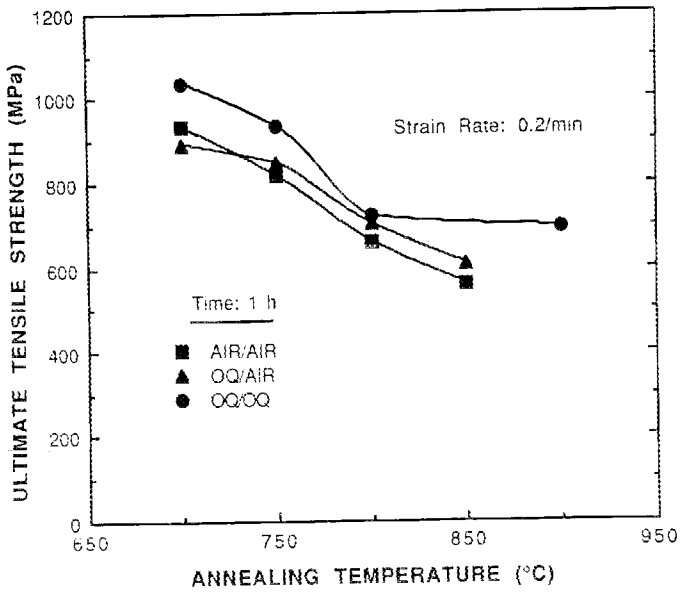

Fig. 23. Effect of cooling sequence and annealing temperatureon room-temperature ultimate tensile strength of iron-aluminide alloy FAL (Heat 13008). All specimens were stress relieved for 1 h at 700°C prior to annealing at differen temperatures.

ORNL-DWG 90-2181

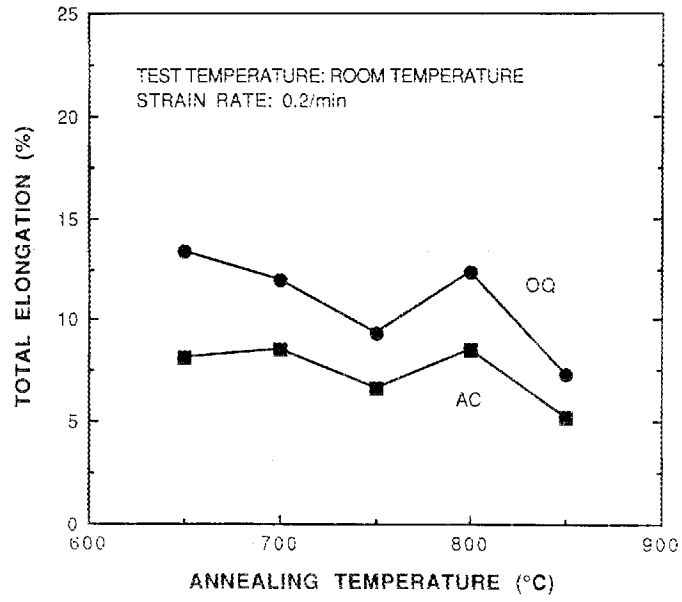

Fig. 24. Comparison of room-temperature total elongation of iron-aluminide alloy FAS (Heat 13017) for specimens cooled in air vs oil from various annealing temperatures. All of the sheets were stress relieved at 700°C for 1 h followed by oil cooling prior to punching the specimens.

ORNL-DWG 90-2182

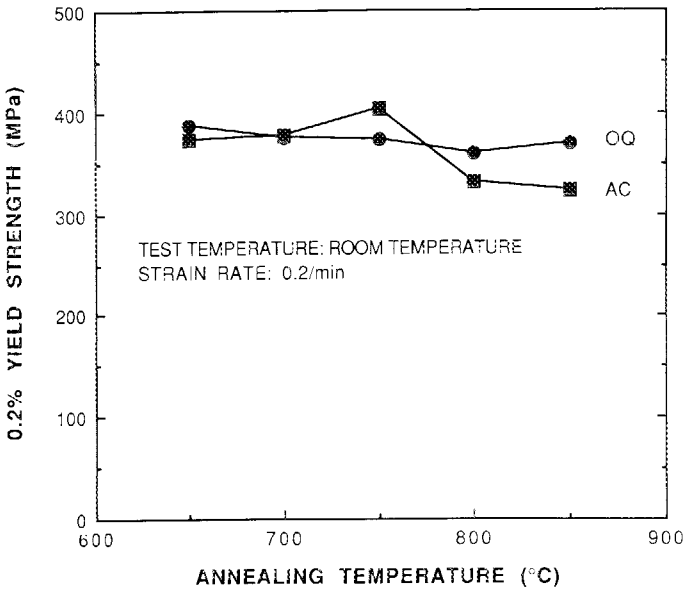

Fig. 25. Comparison of room-temperature yield strength (0.2% offset) of alloy FAS (Heat 13017) for specimens cooled in air vs oil from various annealing temperatures. All of the sheets were stress relieved at 700°C for 1 h followed by oil cooling prior to punching the specimens.

ORNL-DWG 90-2183

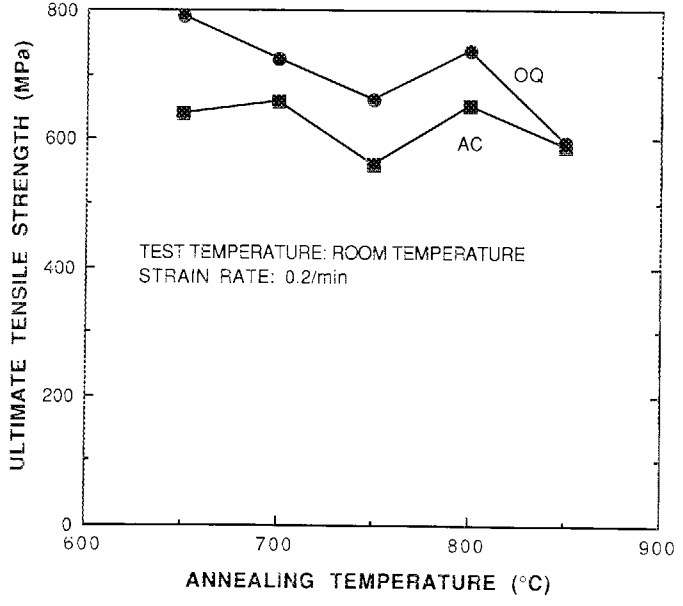

Fig. 26. Comparison of room-temperature ultimate tensile strength of alloy FAS (Heat 13017) for specimens cooled in air vs oil from various annealing temperatures. All of the sheets were stress relieved at 700°C for 1 h followed by oil cooling prior to punching the specimens.

compared in Figs. 27-29. The total elongation values for the 750°C stress-relief temperature remained high over a wider range of annealing temperatures than the stress-relief temperature of 700°C, suggesting that the 750°C treatment should be favored over 700°C. The lower yield-strength value observed for an annealing temperature of 700°C and a stress-relief temperature of 750°C is expected because the annealing temperature is lower than the stress-relief temperature. Higher ultimate tensile-strength values were observed over a wider annealing temperature range for a stress-relief temperature of 750°C. This observation is consistent with the total elongation data in Fig. 27.

The 100-mm-diam (4-in.) ingot from a 70-kg (150-lb) heat of alloy FAL (X3908) from Combustion Engineering was tensile tested at RT. The results of this heat are compared with Heat 13008 of the same composition in Figs. 30-32. These figures show that the total elongation and strength values of the commercial heat are generally significantly lower than experimental heats.

The 100-mm-diam (4-in.) and rectangular ingots from 70-kg (150-lb) heats of alloy FA-129 (X3904 and X3905) from Combustion Engineering were tensile tested at RT and as a function of test temperature. The RT tensile data for air-induction-melted ingots (X3904 and X3905) are compared in Figs. 33-35. Both ingots showed similar values of all properties except for an annealing temperature of 700°C. Note, however, that the ductility and strength value for commercial heats were lower than those observed for laboratory heats. Furthermore, the commercial ingots tended to show more scatter from specimen to specimen than small laboratory heats.

The annealing treatment [700°C/1 h/OQ/800°C/1 h/OQ (OQ = oil quenched)] that produced the highest RT elongation was used to test specimens from both ingots (X3904 and X3905) as a function of temperature. These results were plotted, and they show that the properties of two ingots from a 70-kg (150-lb) air-induction-melted heat were essentially identical (Figs. 36-38). Some small differences may be caused by slight differences in processing history. For example, ingot X3904 was forged and rolled whereas ingot X3905 was hot extruded, forged, and rolled.

Specimens from alloy FA-129, ingot X3905, were also tested at various temperatures for four different annealing treatments. The results of this study show minimal variations in the properties for annealing temperatures in the range of 700 to 850°C (Figs. 39-42). The RT yield strength showed the most variation, which is consistent with annealing temperature, namely, higher yield strength for lowest annealing temperature and lowest yield strength for the highest annealing temperature. Total elongation values ranged from 10 to 12% at RT and 80 to 120% at 800°C. The ultimate tensile strength of ingots X3904

ORNL-DWG 90-2184

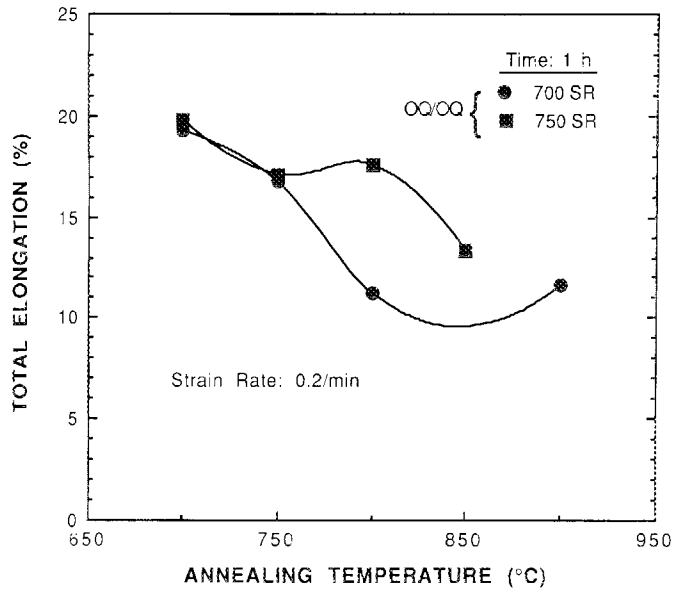

Fig. 27. Effect of stress-relief treatment on room-temperature elongation of alloy FAL (Heat 13008) for various annealing temperatures.

ORNL-DWG 90-2185

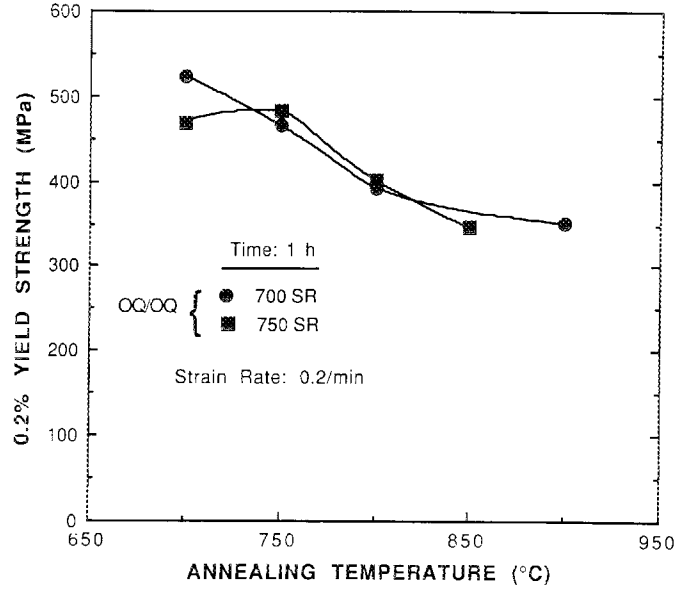

Fig. 28. Effect of stress-relief treatment on room-temperature yield strength (0.2% offset) of alloy FAL (Heat 13008) for various annealing temperatures.

ORNL-DWG 90-2186

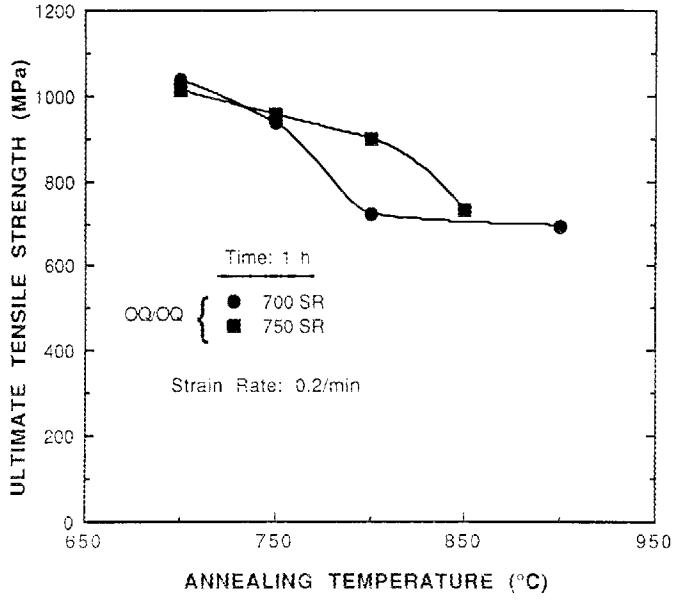

Fig. 29. Effect of stress-relief treatment on room-temperature ultimate tensile strength of alloy FAL (Heat 13008) for various annealing temperatures.

ORNL-DWG 90-2187

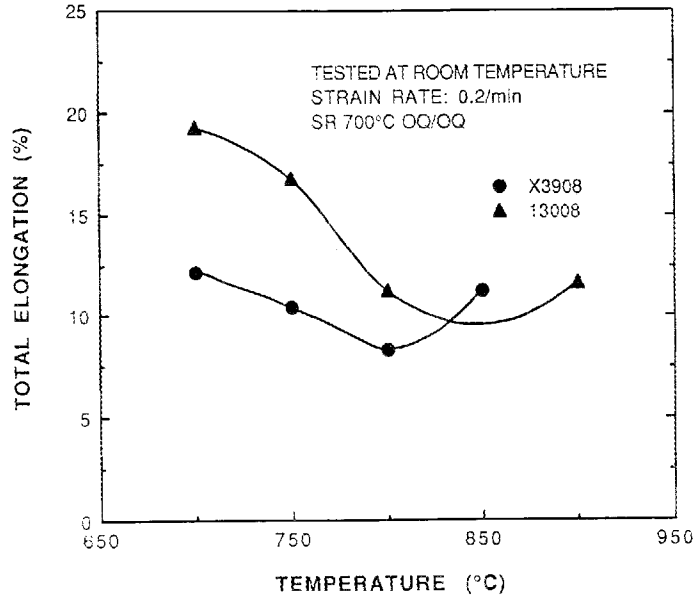

Fig. 30. Comparison of room-temperature elongation of iron-aluminide alloy FAL [7-kg (15-lb) Heat 13008] melted at ORNL with 70-kg (150-lb) Heat X3908 melted at Combustion Engineering.

ORNL-DWG 90-2188

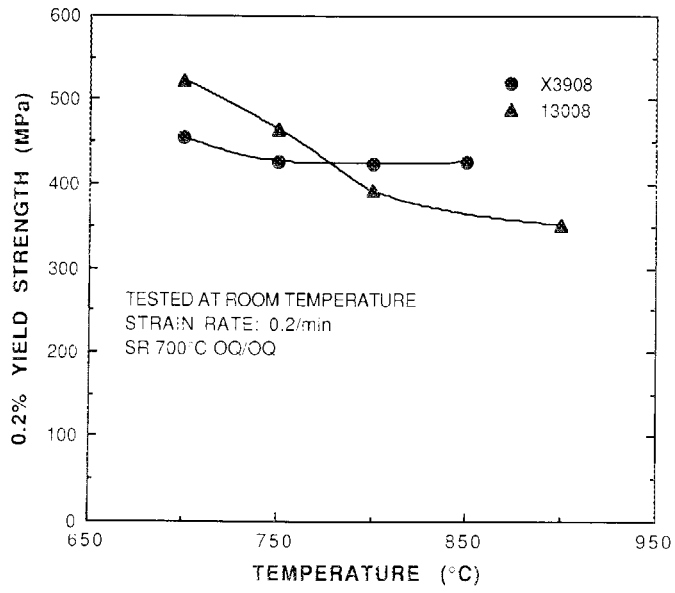

Fig. 31. Comparison of room-temperature yield strength of iron-aluminide alloy FAL [7-kg (15-lb) Heat 13008] melted at ORNL with 70-kg (150-lb) Heat X3908 melted at Combustion Engineering.

ORNL-DWG 90-2189

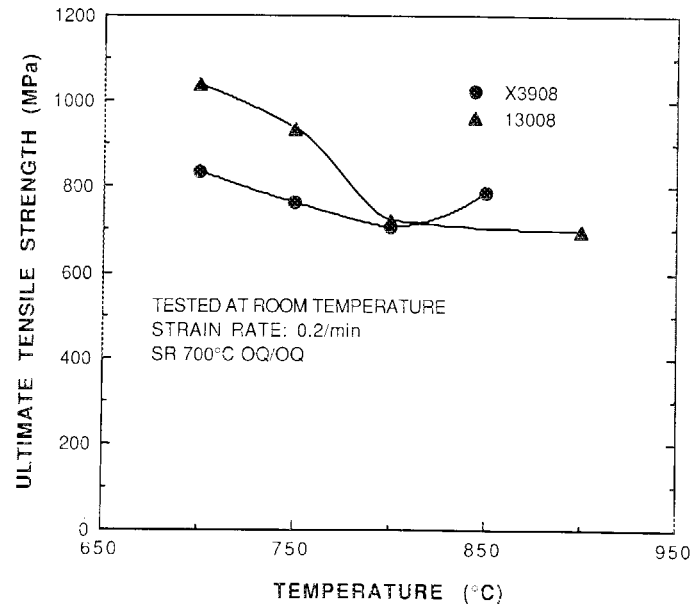

Fig. 32. Comparison of room-temperature ultimate tensile strength of iron-aluminide alloy FAL [7-kg (15-lb) Heat 13008] melted at ORNL with 70-kg (150-lb) Heat X3908 melted at Combustion Engineering.

ORNL-DWG 90-2190

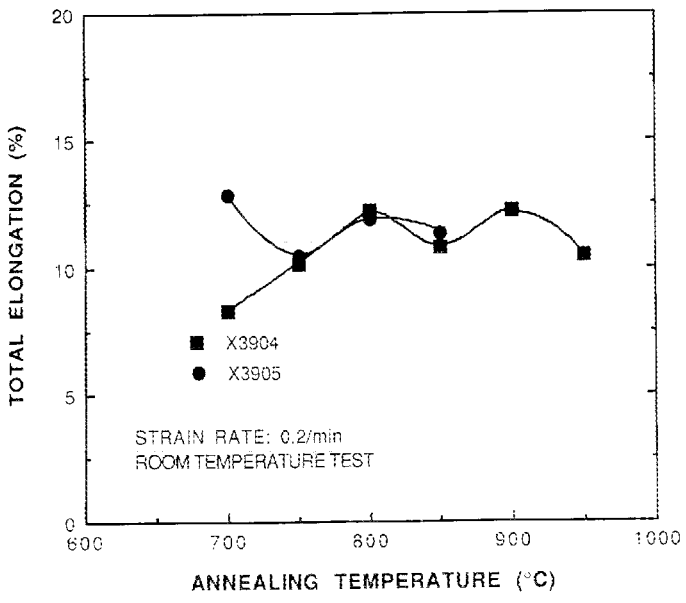

Fig. 33. Comparison of room-temperature total elongation as a function of annealing temperature for ingots X3904 and X3905 from air-induction-melted 70-kg (150-lb) heat of FA-129 at Combustion Engineering. All of the sheets were stress relieved at 700°C for 1 h followed by oil quenching prior to punching the specimens.

ORNL-DWG 90-2191

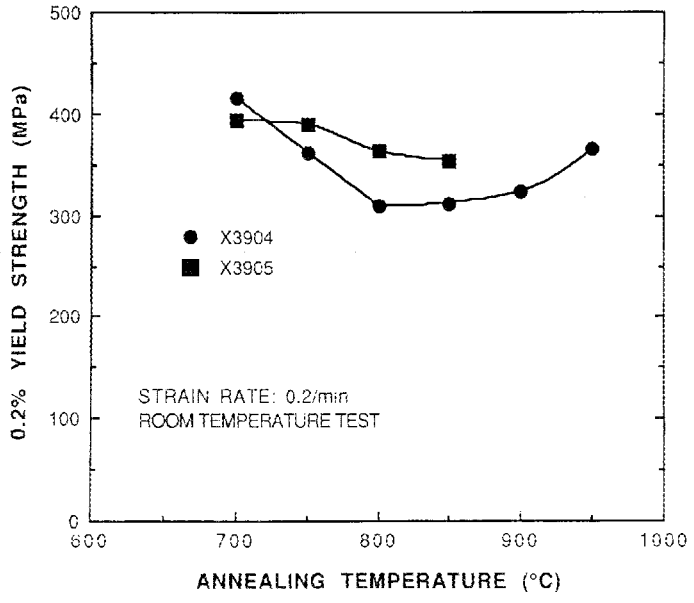

Fig. 34. Comparison of room-temperature yield strength (0.2% offset) as a function of annealing temperature for ingots X3904 and X3905 from air-induction-melted 70-kg (150-lb) heat of FA-129 at Combustion Engineering. All of the sheets were stress relieved at 700°C for 1 h followed by oil quenching prior to punching the specimens.

ORNL-DWG 90-2192

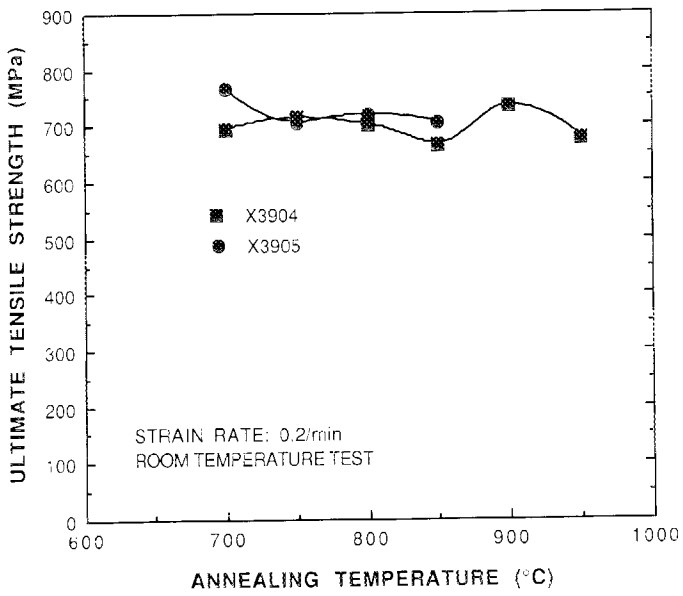

Fig. 35. Comparison of ultimate tensile strength as a function of annealing temperature for ingots X3904 and X3905 from air-induction-melted 70-kg (150-lb) heat of FA-129 at Combustion Engineering. All of the sheets were stress relieved at 700°C for 1 h followed by oil quenching prior to punching the specimens.

ORNL-DWG 90-2193

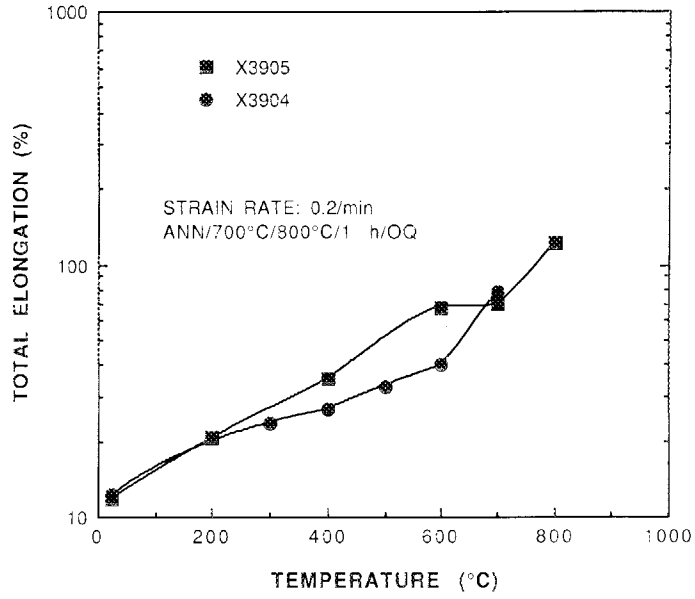

Fig. 36. Comparison of total elongation as a function of test temperature for ingots X3904 and X3905 from air-induction-melted 70-kg (150-lb) heat of FA-129 at Combustion Engineering.

ORNL-DWG 90-2194

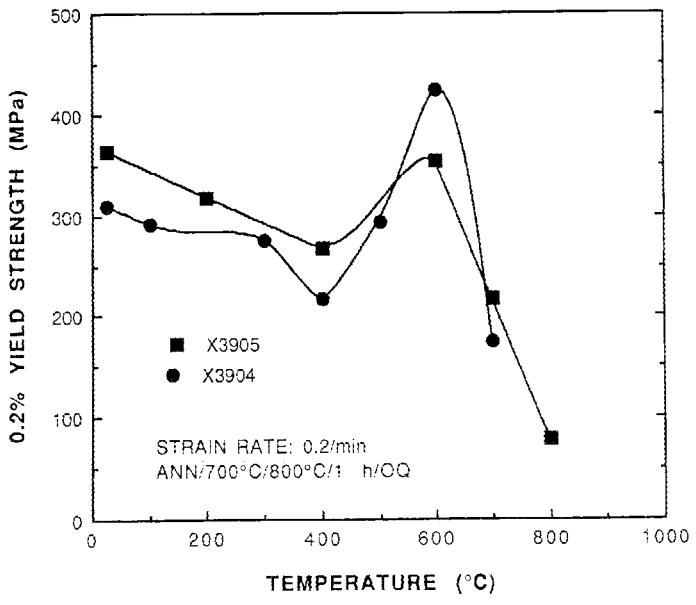

Fig. 37. Comparison of yield strength (0.2% offset) as a function of test temperature for ingots X3904 and X3905 from air-induction-melted 70-kg (150-lb) heat of FA-129 at Combustion Engineering.

ORNL-DWG 90-2195

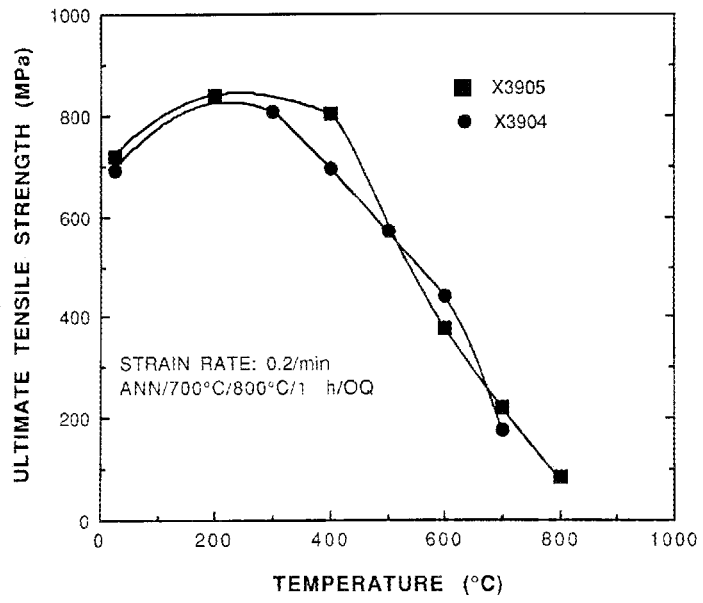

Fig. 38. Comparison of ultimate tensile strength as a function of test temperature for ingots X3904 and X3905 from air-induction-melted 70-kg (150-lb) heat of FA-129 at Combustion Engineering.

ORNL-DWG 90-2196

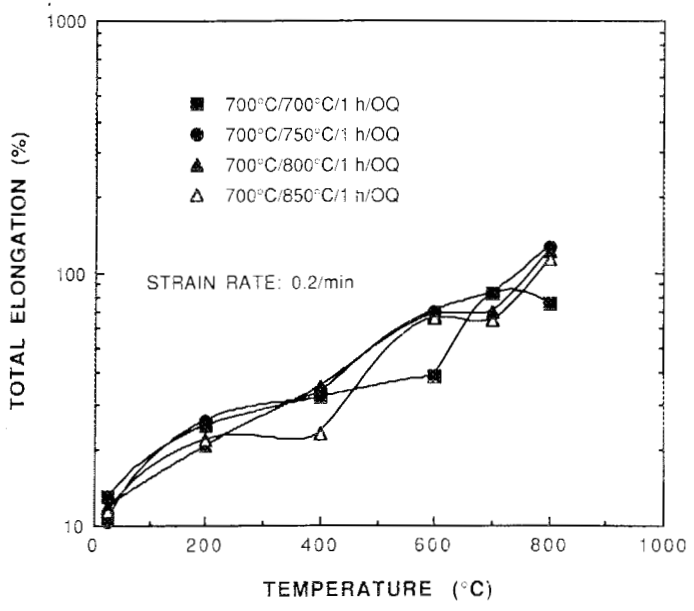

Fig. 39. Total elongation as a function of test temperature for ingot X3905 from air-induction-melted 70-kg (150-lb) heat of FA-129 at Combustion Engineering. Data are compared for four different annealing temperatures.

ORNL-DWG 90-2197

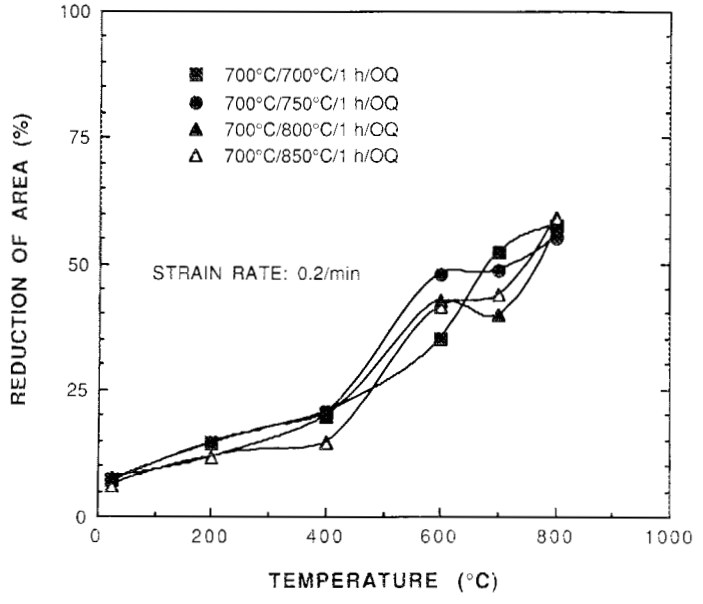

Fig. 40. Reduction of area as a function of test temperature for ingot X3905 from air-induction-melted 70-kg (150-lb) heat of FA-129 at Combustion Engineering. Data are compared for four different annealing temperatures.

ORNL-DWG 90-2198

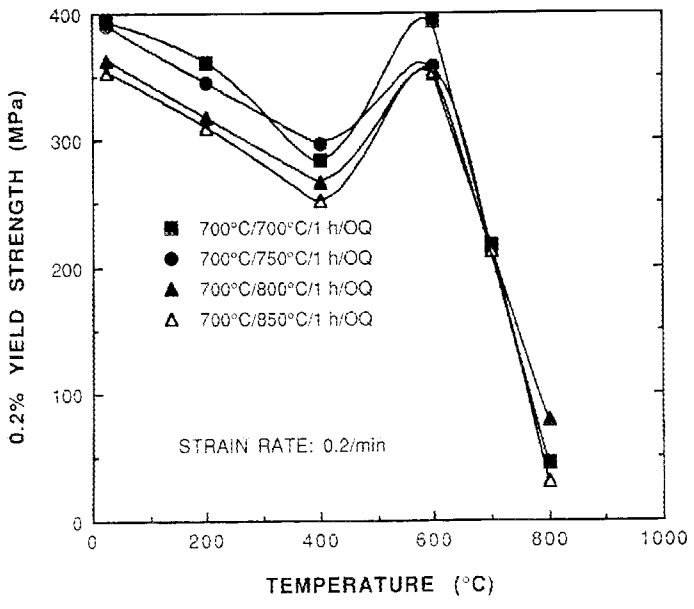

Fig. 41. Yield strength (0.2% offset) as a function of test temperature for ingot X3905 from air-induction-melted 70-kg (150-lb) heat of FA-129 at Combustion Engineering. Data are compared for four different annealing temperatures.

ORNL-DWG 90-2199

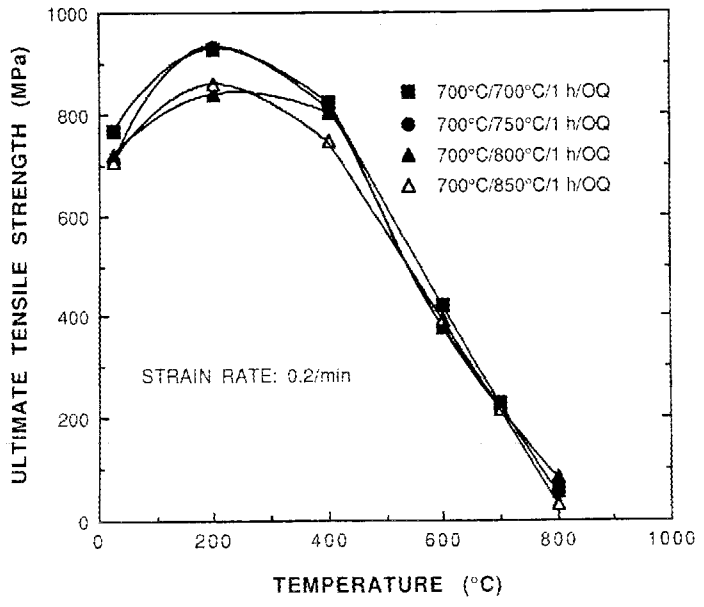

Fig. 42. Ultimate tensile strength as a function of test temperature for ingot X3905 from air-induction-melted 70-kg (150-lb) heat of FA-129 at Combustion Engineering. Data are compared for four different annealing temperatures.

and X3905 did not show a monotonic decrease from RT as was observed for FAL (Heat 13008) because the commercially melted ingots did not achieve their full ductility potential at RT (Fig. 13).

In addition to the air-induction-melted ingots, one vacuum-induction-melted heat (Heat 35 of FA-129) was also tested. The initial results on the vacuum-melted heat are compared with those of the air-melted heat data in Figs. 43-45. The most important property of interest, the RT ductility, is better for the vacuum-melted material than air-melted material for most of the annealing temperatures used. Ultimate tensile strength showed corresponding improvement. The yield strength of the vacuum-melted material is similar to the air-melted material. Additional testing of the vacuum-melted material is currently under way.

Alloy FA-123, a highly alloyed version of FA-129 (Table 3), is being developed for high-temperature service. This alloy was also melted in a 70-kg (150-lb) heat at Combustion Engineering. Only limited processing and testing of this alloy has been completed. The results of the study show that RT ductility values of 10% can be obtained for this alloy (Table 6). Note, however, that only one set of heat treatments was tried. Other treatments may result in even better ductility values.

7.2 CREEP PROPERTIES

A limited number of creep tests were conducted on alloys FAL (Heat 13008), FA-129 (Heat X3904), FAS (Heat 13345), FA-123 (Heat X3906), and an experimental version of FAL containing tungsten (FAL-W). On alloy FAS, the test temperature ranged from 450 to 700°C, and the test times ranged from 7 to 250 h (Table 7). Creep-rupture data on various iron aluminides are plotted and compared with the average curve for type 304 stainless steel in Fig. 46. The test temperature and rupture time were combined through the Larson-Miller parameter with a value of the constant of 20. Figure 46 shows (1) alloy FAS with 2% Cr has the lowest creep strength; (2) alloy FAL with 5% Cr has higher strength than the 2% Cr alloy FAS; (3) alloy FAL with tungsten has somewhat higher creep strength than FAL, reflecting the solid-solution strengthening caused by the addition of 1% W; (4) alloy FA129 (X3904), which contains 5% Cr, 1% Nb, and 0.05% C, is slightly stronger than FAL-W, probably because of strengthening from Nb and NbC; and (5) alloy FA-123, which contains 5% Cr plus Nb, Mo, C, and B, has the highest rupture strength, approaching that of type 304 stainless steel. The increased strength of FA-123 was probably caused by the solid-solution effects of Mo and Nb and the precipitation of NbC.

ORNL-DWG 90-2200

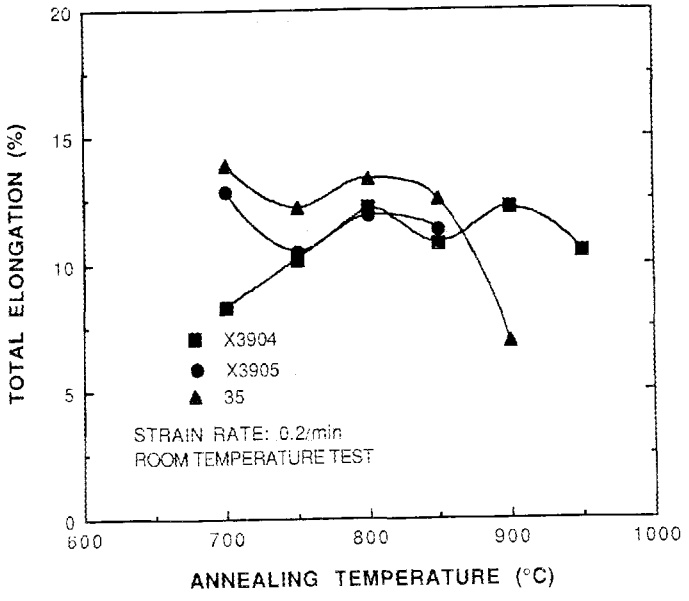

Fig. 43. Comparison of room-temperature total elongation of air-induction-melted ingots (X3904 and X3905) from Combustion Engineering with vacuum-induction ingot 35 melted at The Timken Company for alloy FA-129.

ORNL-DWG 90-2201

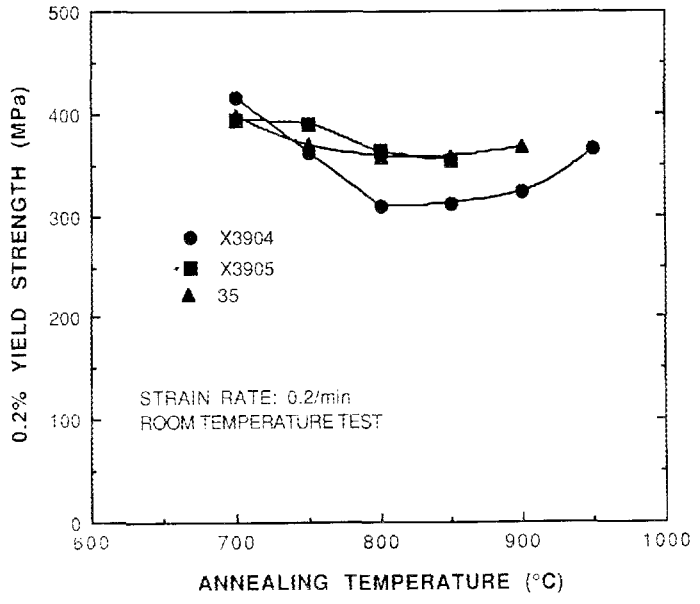

Fig. 44. Comparison of room-temperature yield strength (0.2% offset) of air-induction-melted ingots (X3904 and X3905) from Combustion Engineering with vacuum-induction ingot 35 melted at The Timken Company for alloy FA-129.

ORNL-DWG 90-2202

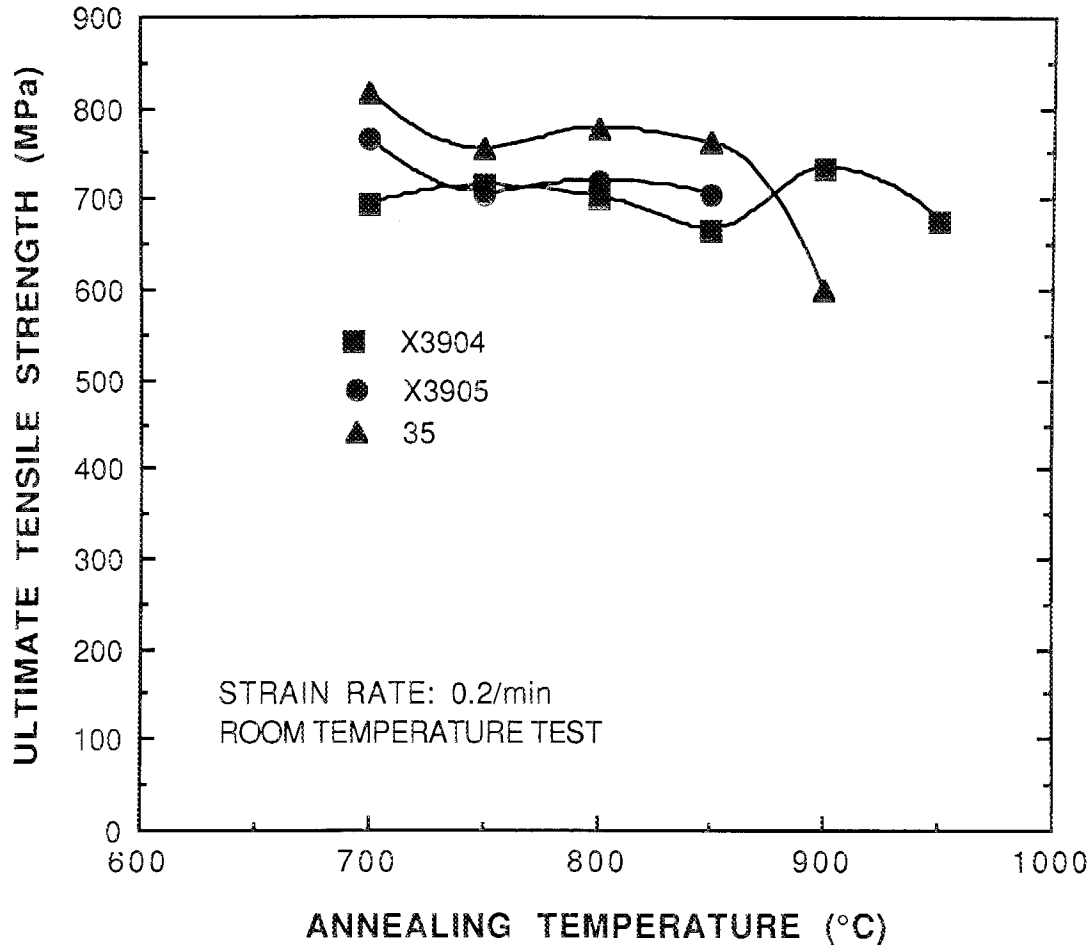

Fig. 45. Comparison of room-temperature ultimate tensile strength of air-induction-melted ingots (X3904 and X3905) from Combustion Engineering with vacuum-induction ingot 35 melted at The Timken Company for alloy FA-129.

Table 6. Tensile properties of iron aluminide {FA123 [70-kg (150-lb) heat, Heat X3906]} air-induction melted at Combustion Engineering and processed at ORNL[a]

Specimen number	Heat treatment						Test temperature (°C)	Strain rate (min^{-1})	Strength (MPa)		Ductility (%)	
	Sheet treatment			Specimen treatment					0.2% Yield	Tensile strength	Elongation	Reduction of area
	Temp. (°C)	Time (h)	Cooling medium[b]	Temp. (°C)	Time (h)	Cooling medium[b]						
1L	800	1	OQ	700	1	OQ	25	0.2	370	549	7.74	6.18
2L	800	1	OQ	700	1	OQ	25	0.2	c	c	6.14	c
3L	800	1	OQ	750	1	OQ	25	0.2	355	687	9.74	7.66
4L	800	1	OQ	750	1	OQ	25	0.2	338	713	11.50	7.71
5L	800	1	OQ	800	1	OQ	25	0.2	344	684	9.26	6.46
6L	800	1	OQ	800	1	OQ	25	0.2	347	671	9.24	5.22
7L	800	1	OQ	850	1	OQ	25	0.2	344	632	7.80	6.57
8L	800	1	OQ	850	1	OQ	25	0.2	313	625	7.94	3.92

[a]The 100-mm-diam (4-in.) ingot was extruded at 1000°C to a reduction ratio of 6:1. The sheet bar was hot rolled at 1000°C to 6 mm (0.25 in.), hot rolled at 850°C to 1.5-mm thickness (0.060-in.), and warm rolled at 650°C to finish at a 0.76-mm-thick (0.030-in.) sheet. The warm-rolled sheet was stress relieved prior to punching into tensile specimens, and the specimens were given the indicated treatment prior to testing.

[b]OQ = oil quench.

[c]Specimen broke in pinhole.

Table 7. Creep data for 7-kg (15-lb) air-induction-melted heat of alloy FAS (Heat 13345)

(All tests were conducted in air)

Test number	Specimen number	Heat treatment[a]	Test temperature (°C)	Stress (MPa)	Rupture time (h)	Total elongation (%)	Reduction of area (%)
26553	3L	700°C/700°C/1 h/OQ	450	379	191.9	18.62	26.79
26554	4L	700°C/700°C/1 h/OQ	500	310	30.4	27.46	21.38
26555	5L	700°C/700°C/1 h/OQ	525	276	12.5	25.51	37.94
26556	6L	700°C/700°C/1 h/OQ	550	241	7.1	43.10	34.30
26557	7L	700°C/700°C/1 h/OQ	600	103	31.9	68.41	52.24
26558	8L	700°C/700°C/1 h/OQ	650	34	251.5	121.83	75.63
26559	9L	700°C/700°C/1 h/OQ	700	21	207.6	113.57	78.32

[a]OQ = oil quench.

ORNL-DWG 90-2203

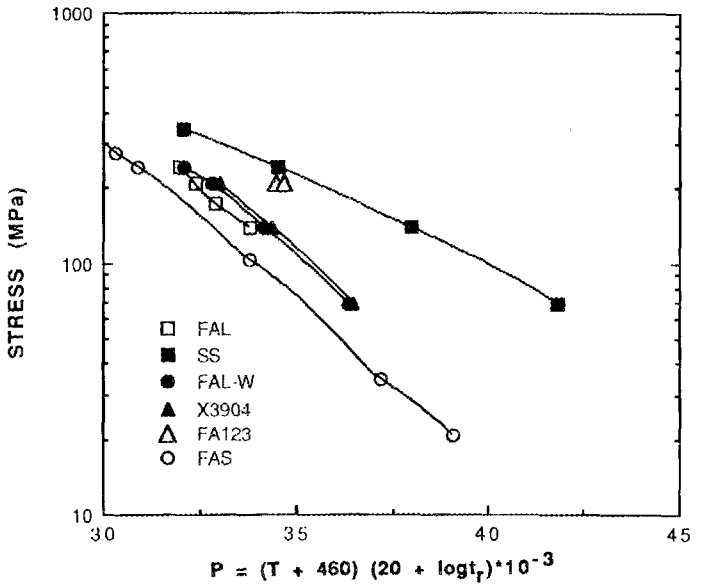

Fig. 46. Larson-Miller plot showing comparison of creep rupture strength of various iron aluminides to the average value curve for type 304 stainless steel.

Total creep elongation data for alloy FAS are plotted as a function of the Larson-Miller parameter (Fig. 47). These results showed that FAS was very ductile in creep and the creep elongation increased with increasing test temperature. Creep elongation tests conducted from 450 to 700°C varied from 20 to 120%. The creep reduction of area varied from 22 to 78% for the same temperature range. Data for other alloys are still being analyzed.

8. MICROSTRUCTURAL ANALYSIS

Microstructural examination in this study was limited to optical microscopy for general structure, scanning electron microscopy of fracture surfaces, and X-ray diffraction for structure determination.

8.1 OPTICAL MICROSTRUCTURE

The microstructure of a 76-mm-diam (3-in.) ingot from an air-induction-melted 7-kg (15-lb) heat of iron-aluminide alloy FAL (Heat 13259) is shown in Fig. 48. This heat was made using remelt stock typical of that used by commercial producers and was

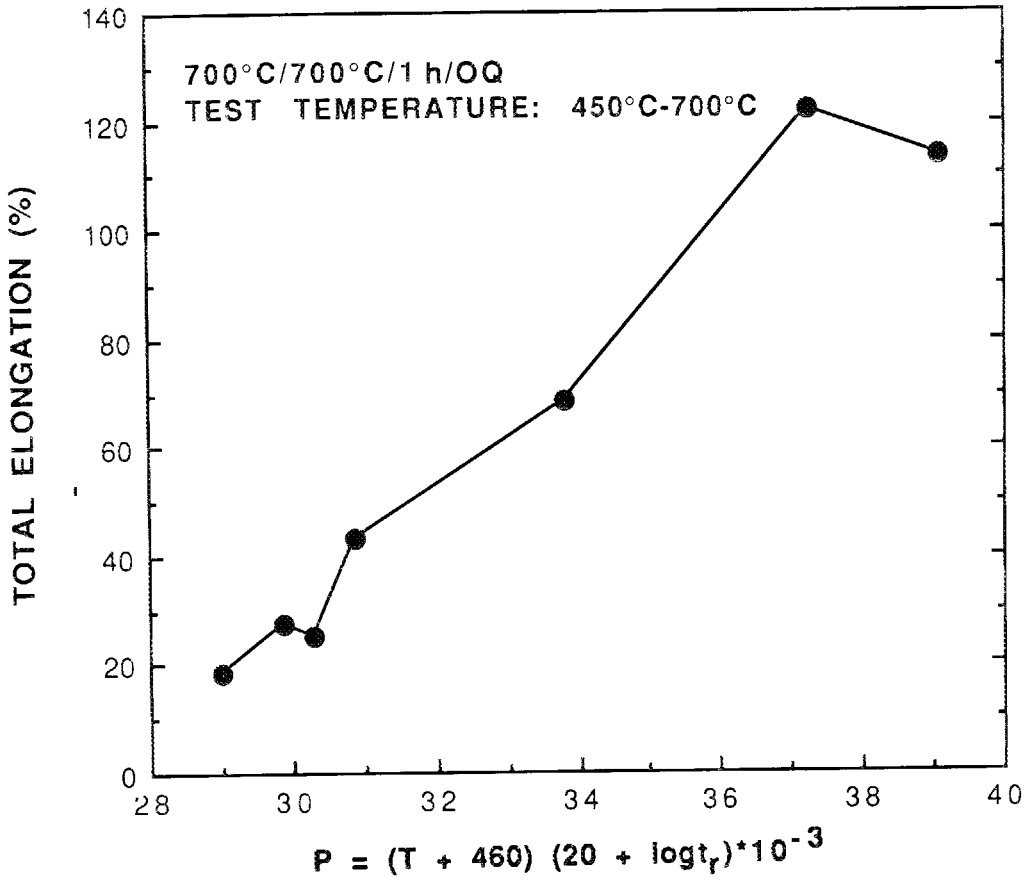

Fig. 47. Creep total elongation as a function of the Larson-Miller parameter for iron-aluminide alloy FAS (Heat 13345).

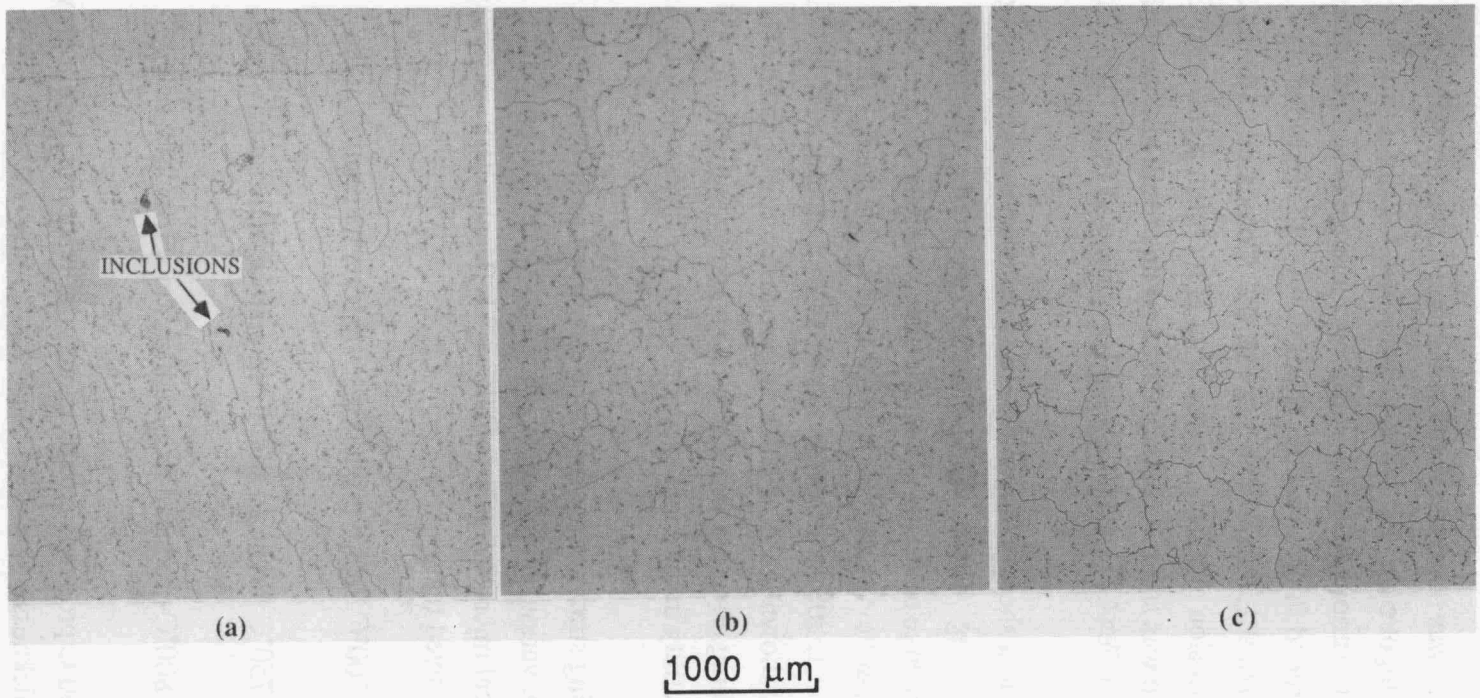

Fig. 48. Optical microstructure of a 76-mm-diam (3-in.) as-cast ingot of iron aluminide (FAL). The ingot was made using commercial melt stock for iron and aluminum. (*a*) Ingot edge, (*b*) one-half radius, and (*c*) center.

supplied by The Timken Company. The cast structure is very coarse and shows the typical variation of columnar grains near the ingot edge to equiaxed grains at one-half radius and ingot center location. No porosity was observed in the cast ingot; however, some inclusions were noticed near the ingot edge [Fig. 48(*a*)]. The 75-mm-diam (3-in.) air-melted ingots were hot extruded to various reduction ratios over a range of temperatures from 850 to 1100°C. The as-extruded microstructures of alloy FA-117, extruded at 1100°C to an area reduction ratio of 9:1, are presented in Fig. 49. Compared to the as-cast microstructure in Fig. 48, hot extrusion produces a significant grain refinement. However, we believe that the grain structure was still too coarse. Based on this result and strength data, the extrusion temperature for Fe_3Al-based alloys has been lowered from 1100°C to the range of 850 to 1000°C.

All material was processed to a sheet 0.76-mm (0.030-in.) thick prior to punching specimens for tensile and creep testing. The as-rolled sheet was too hard to allow the specimens to be punched without edge cracking. Thus, the sheets were stress relieved prior to punching. Various stress-relieving treatments were tried in this study. The microstructure of alloy FAL (Heat 13008) after a typical stress-relief treatment of 700°C for 1 h followed by oil quenching is shown in Fig. 50. The microstructure consisted of highly elongated grains in the rolling direction with essentially no recrystallization. This treatment produced sufficient ductility in the sheet to produce test specimens free of any edge cracks.

To minimize the die-punching strains at the specimen edges and to investigate the effect of percent recrystallization, various annealing temperatures were used on the specimens prior to testing. Optical microstructures of alloy FAL (Heat 13008) are shown in Figs. 51-53. These figures showed that

1. An annealing temperature of 700°C for 1 h produced some recrystallization at the specimen edge.
2. An annealing temperature of 750°C produced slightly more recrystallization at the specimen edge.
3. An annealing temperature of 800°C produced recrystallization across 80% of the specimen thickness.
4. An annealing treatment of 900°C produced complete recrystallization and grain growth across the entire specimen thickness.
5. The cooling medium after a stress-relief or annealing treatment did not have any significant effect on the microstructure for any of the annealing temperatures.

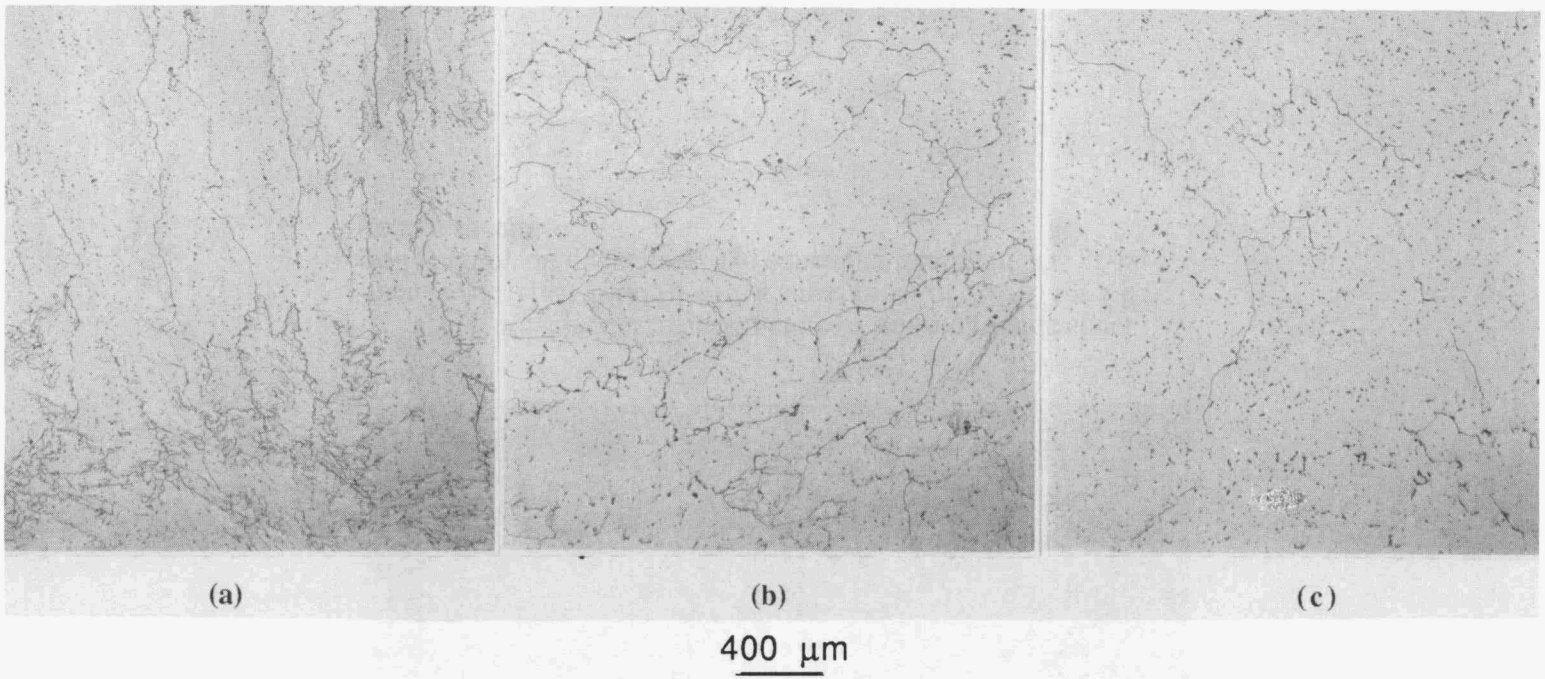

Fig. 49. Optical microstructure of as-extruded bar of iron aluminide [FA-117 (Heat 12864)]. The 76-mm-diam (3-in.) air-melted ingot was extruded at 1100°C to an area reduction ratio of 9:1. (*a*) Near edge, (*b*) one-half radius, and (*c*) bar center.

YP9713

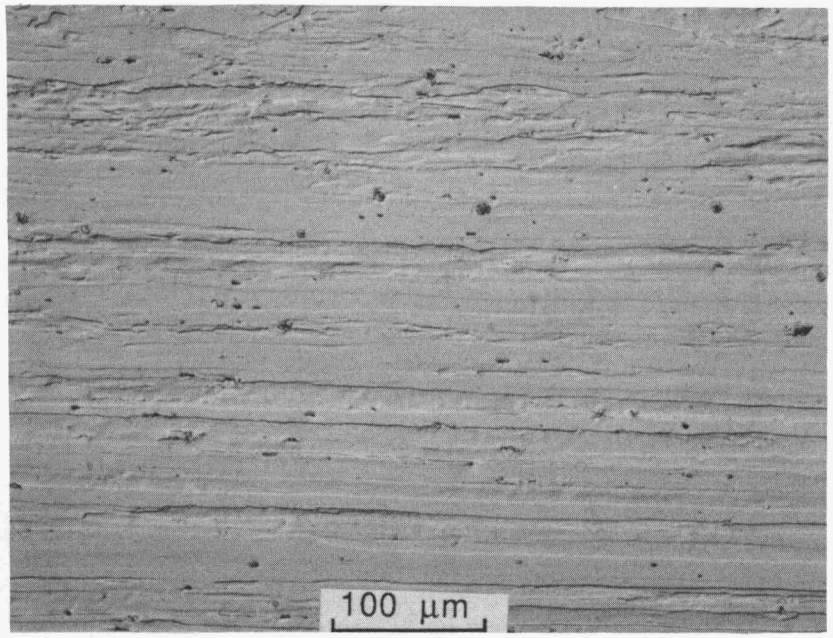

Fig. 50. Optical microstructure of iron-aluminide specimen [FAL (Heat 13008)] with a stress relief of 700°C for 1 h followed by oil quenching. No annealing treatment was given to this specimen.

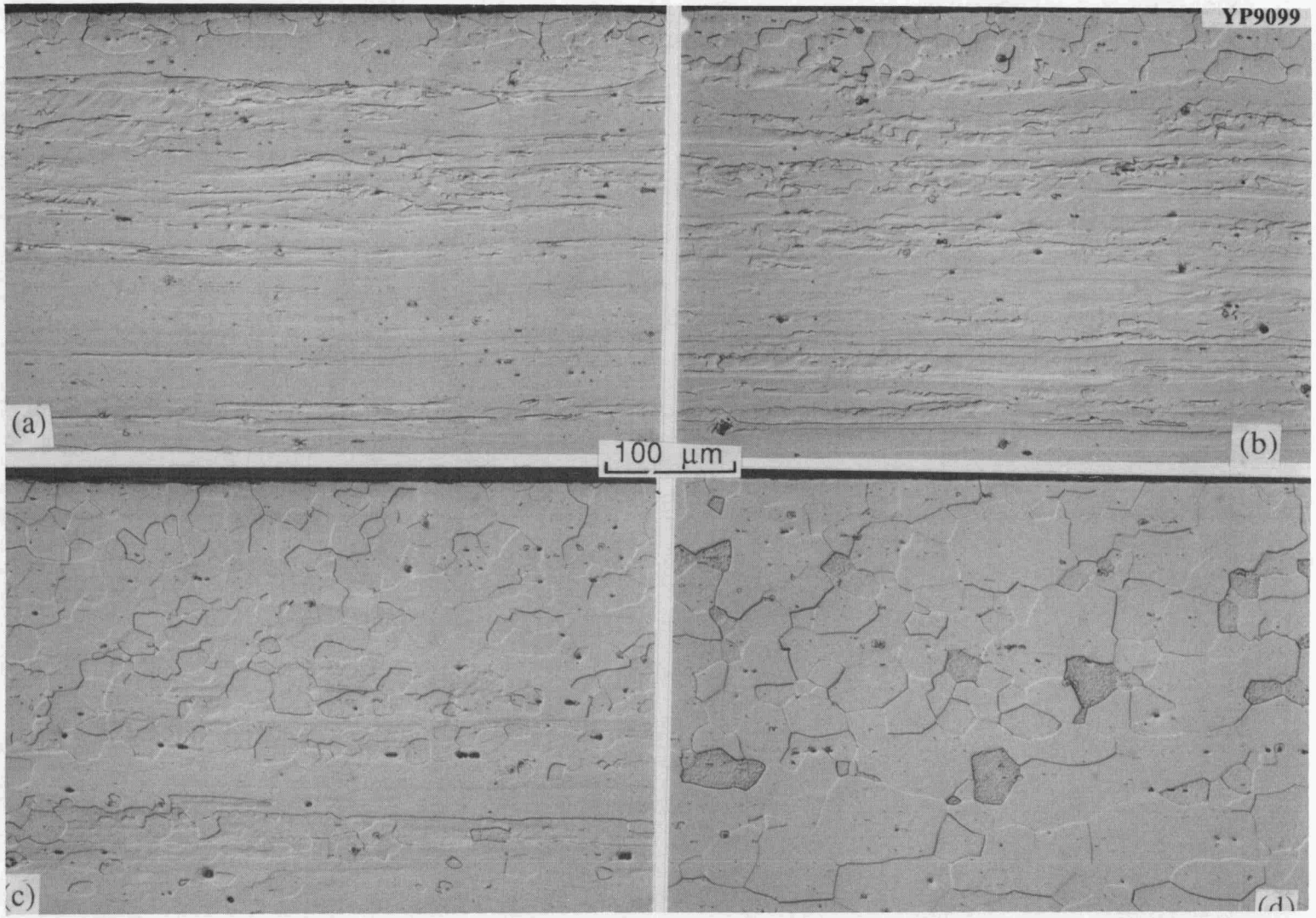

Fig. 51. Optical microstructure of iron-aluminide specimens [FAL (Heat 13008)] with a stress relief of 700°C for 1 h and subsequent annealing treatment for 1 h at (*a*) 700°C, (*b*) 750°C, (*c*) 800°C, and (*d*) 900°C. Both stress-relief and annealing treatments were followed by oil quenching.

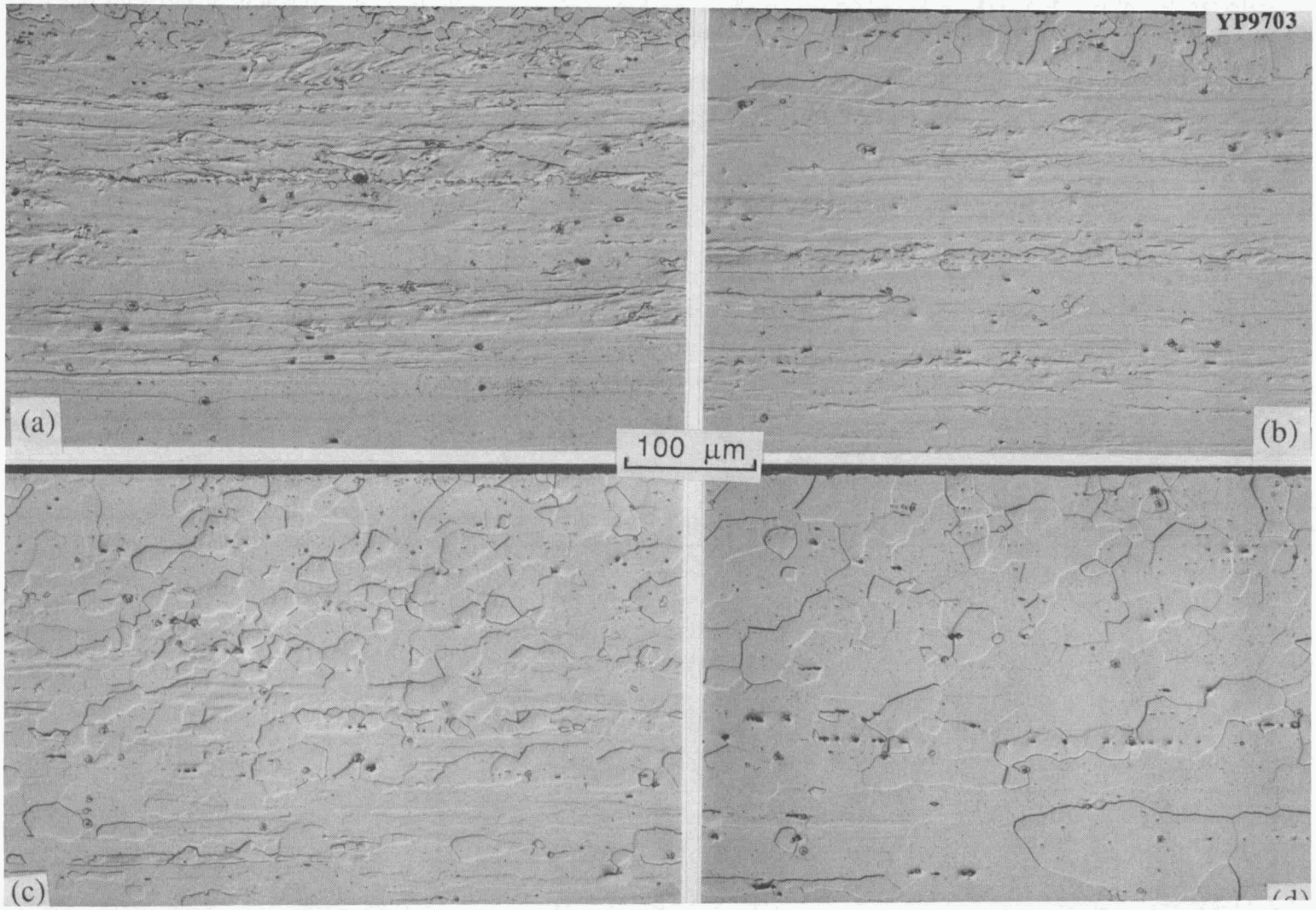

Fig. 52. Optical microstructure of iron-aluminide specimens [FAL (Heat 13008)] with a stress relief of 700°C for 1 h and a subsequent annealing treatment for 1 h at (*a*) 700°C, (*b*) 750°C, (*c*) 800°C, and (*d*) 850°C. The stress-relief treatment was followed by oil quenching, and the annealing treatment was followed by air cooling.

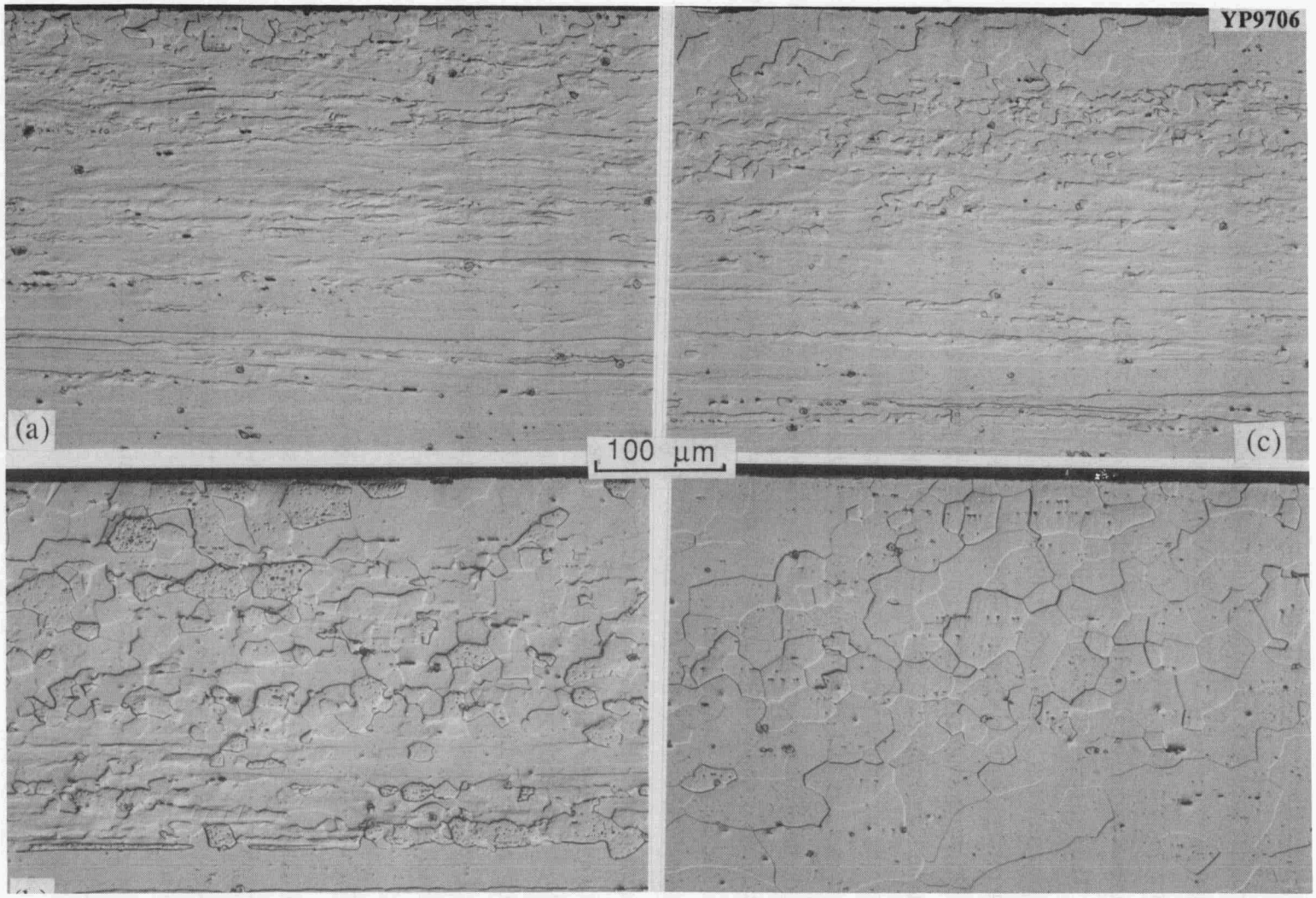

Fig. 53. Optical microstructure of iron-aluminide specimens [FAL (Heat 13008)] with a stress relief of 700°C for 1 h and a subsequent annealing treatment for 1 h at (*a*) 700°C (*b*) 750°C, (*c*) 800°C, and (*d*) 850°C. Both stress-relief and annealing treatments were followed by air cooling.

6. The specimens seemed to show the presence of inclusions, fine porosity, and precipitates that were are probably ZrB_2 in the FAL alloy.

The microstructures with minimum recrystallization (700 and 750°C) were associated with RT elongation values of 15 to 20%. The fully recrystallized structure produced ductility values of approximately 10%.

Microstructures of air-induction melted alloy FA 129 (ingot X3904) are shown in Fig. 54. The stress-relief treatment was 700°C for 1 h followed by oil quenching. The annealing treatments were 750, 800, 850, and 900°C for 1 h followed by oil quenching. The higher magnification optical micrographs of the set shown in Fig. 54 are presented in Fig. 55. Microstructures in Fig. 54 show that only partial recrystallization occurred after an annealing temperature of 750°C, whereas recrystallization was essentially complete at 800°C and higher temperatures. Surprisingly, the recrystallization temperature of FA-129 containing niobium and carbon was similar to that observed for FAL, which contained only small amounts of zirconium and boron. The higher magnification micrographs showed the presence of elongated porosity and a large density of precipitates. The precipitates and their size are more clearly shown in the scanning electron micrographs in Sect. 8.2.

A comparison of the microstructures for alloy FA-129 (ingot X3904) in the air-melted and vacuum-melted (Heat 35) conditions is shown in Fig. 56. Both samples received the same combination of stress-relief and annealing treatments of 1 h at 700°C, and both were followed by oil quenching. The figure shows that vacuum-melted material recrystallized much more at 700°C than air-melted material, and both materials showed a significant amount of precipitates. The air-melted material appeared to contain more porosity than the vacuum-melted material.

8.2 SCANNING ELECTRON MICROGRAPHS

The scanning electron micrographs* of the specimens from the air- and vacuum-melted materials of alloy FA-129 (X3905 and 35) are shown in Fig. 57. Both materials had undergone similar fabrication schedules and the same stress and annealing treatments and both showed large amounts of elongated precipitates [Figs. 57(*a*) and (*d*)]. More details about the particle shape and number density are available from Figs. 57(*b*), (*c*), (*e*),

*Work performed by Richard Wright at the Idaho National Engineering Laboratory.

YP9709

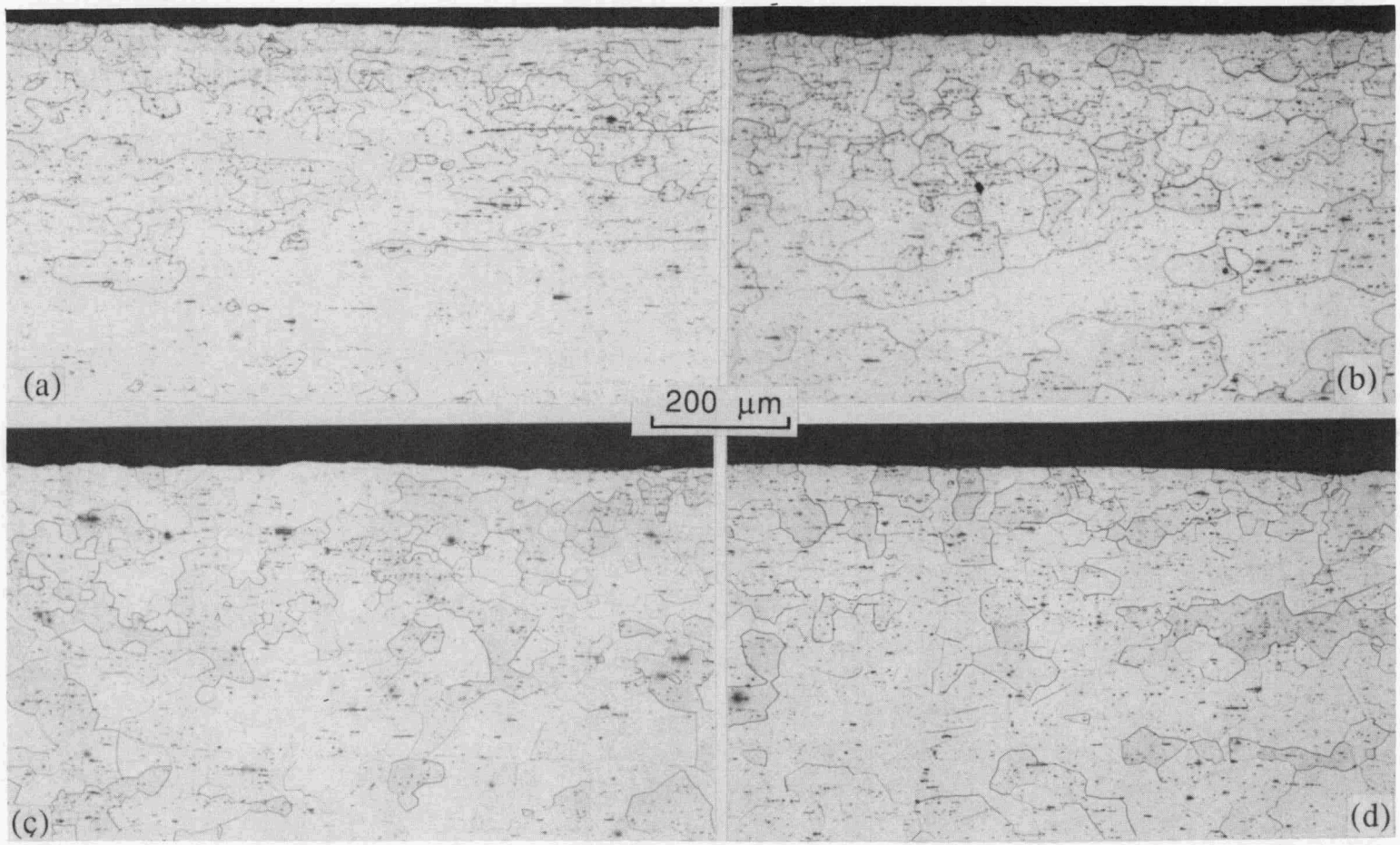

Fig. 54. Optical microstructure of iron aluminide (FA-129) for various annealing treatments of 1 h followed by oil quenching. Specimens were stress relieved for 1 h at 700°C followed by oil quenching, which preceded the annealing treatment. Heat X3904 was melted in air at Combustion Engineering. (*a*) 750°C, (*b*) 800°C, (*c*) 850°C, and (*d*) 900°C.

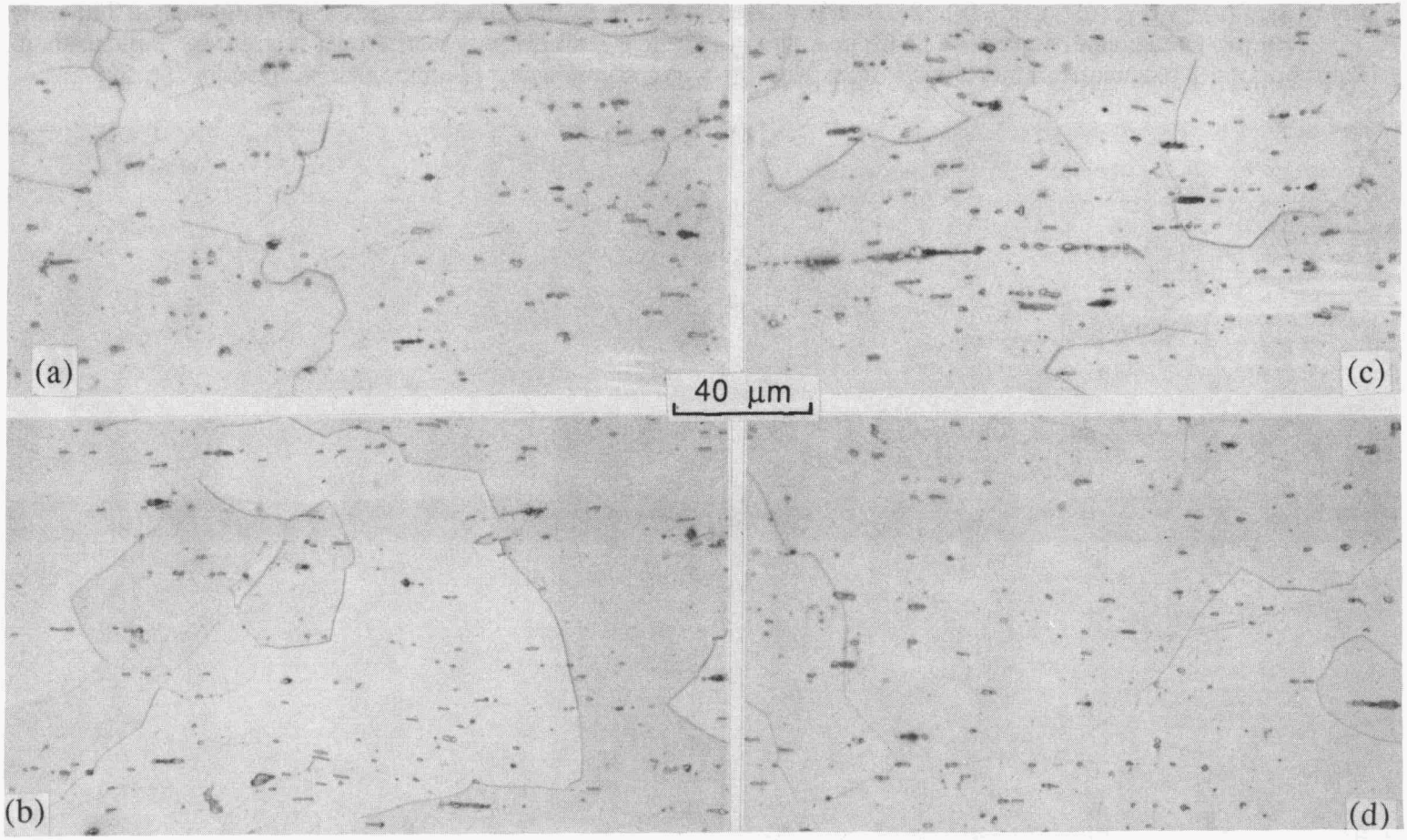

Fig. 55. Optical microstructure of iron aluminide (FA-129) for various annealing treatments of 1 h followed by oil quenching. Specimens were stress relieved for 1 h at 700°C followed by oil quenching, which preceded the annealing treatment. Heat X3904 was melted in air at Combustion Engineering. (*a*) 750°C, (*b*) 800°C, (*c*) 850°C, and (*d*) 900°C.

YP9701

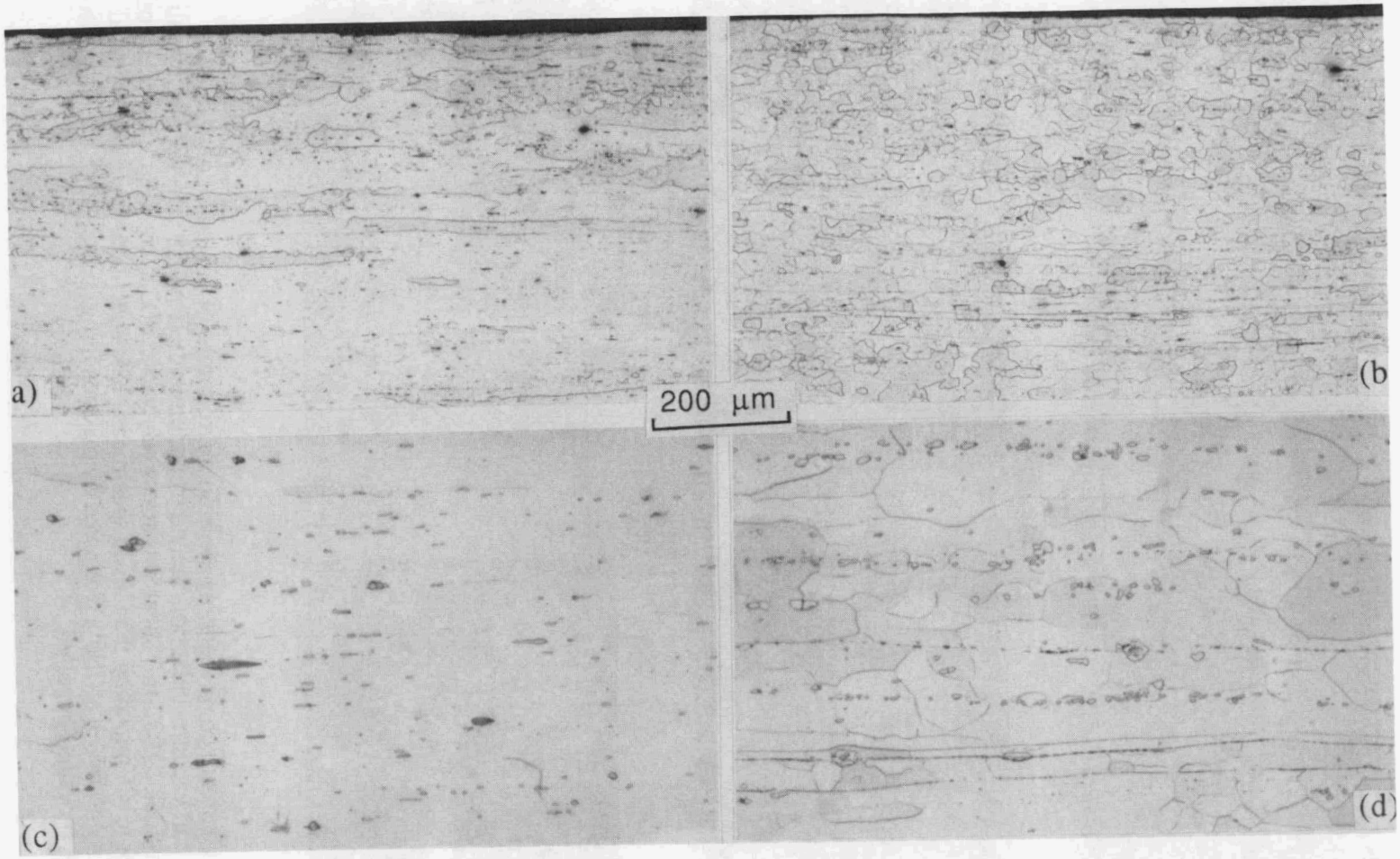

Fig. 56. Optical microstructure comparison of vacuum-melted and air-induction-melted iron aluminide (FA-129). Both sheets were 76-mm (0.030-in.) thick, stress relieved at 700°C for 1 h followed by oil quenching prior to die punching the tensile specimen. The specimens were given a final annealing treatment for 1 h at 700°C amd oil quenched. (*a*) through (*c*) Air-induction melted, and (*d*) through (*f*) vacuum melted.

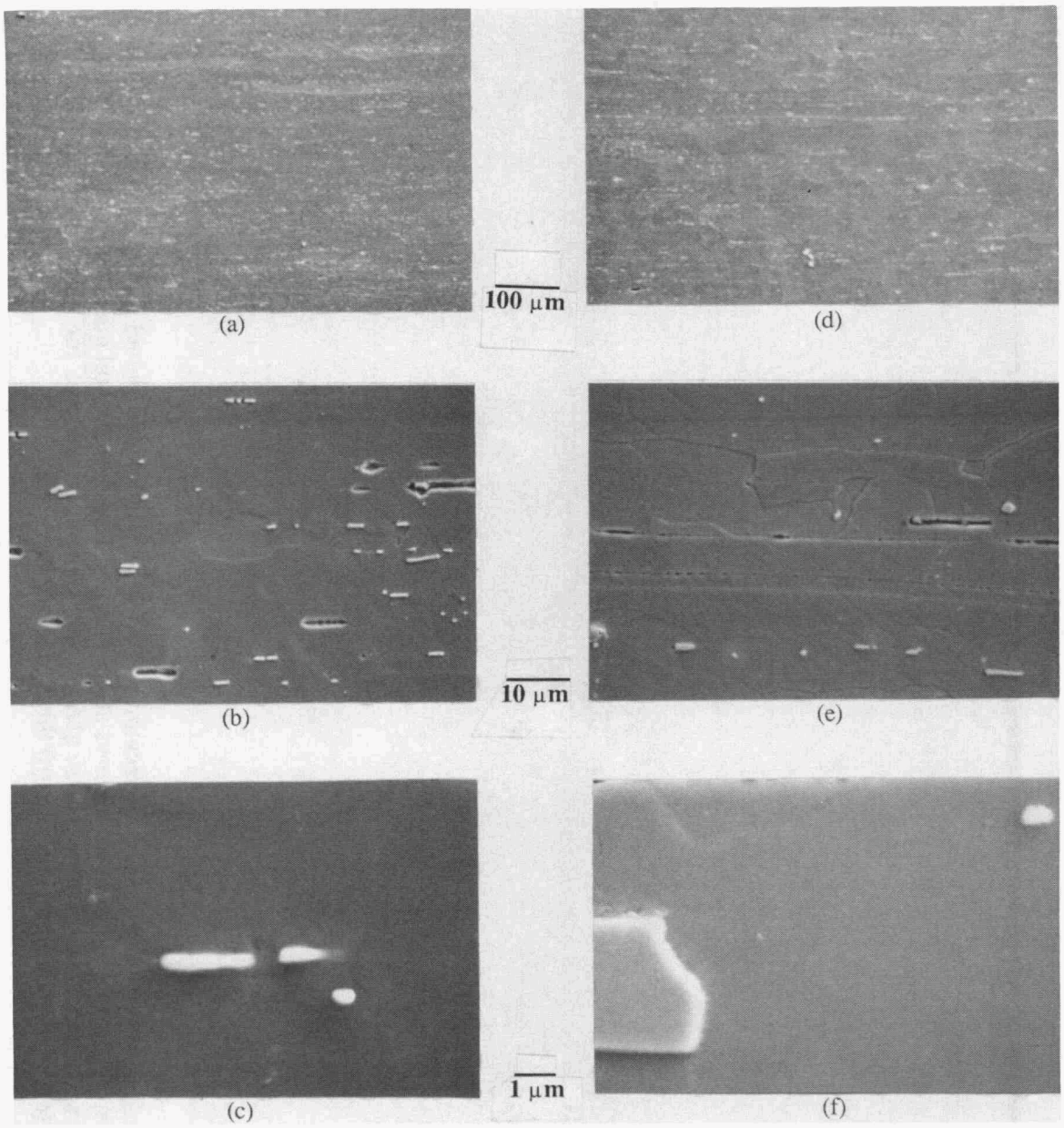

Fig. 57. Comparison of scanning electron micrographs of air-induction-melted ingot (X3904) and vacuum-induction-melted iron aluminide [FA-129 (Heat 35)]. In both cases a 76-mm-thick (0.030-in.) sheet was stress relieved at 700°C for 1 h followed by oil quenching prior to die punching the tensile specimens. The specimens were given a final annealing treatment for 1 h at 700°C followed by oil quenching. (*a*) through (*c*) Air melted, and (*d*) through (*f*) vacuum melted.

and (*f*). The energy dispersive X-ray (EDX) analysis (Fig. 58) of the precipitates showed them to be highly enriched in niobium. The EDX spectra were the same for both air- and vacuum-melted materials. The precipitates were assumed to be niobium carbide.

Fracture surfaces of the tensile specimens of alloy FAL (Heat 13008) with RT ductility values of 15.4 to 19.8% are presented in Figs. 59 and 60. These figures showed that the fracture was by cleavage with some ductile tearing. The fracture surfaces also showed long tears along the longitudinal boundaries. The reason for these tears is difficult to explain because additional testing is needed to determine the nature of the product on these surfaces.

8.3 X-RAY DIFFRACTION

Tensile specimens of alloy FAL (Heat 13008) with various heat treatments and ductility values were subjected to X-ray diffraction for phase identification. Table 8 shows the results, and in all cases the B2 structure, rather than the expected DO_3, was detected. In earlier studies at ORNL, the heat treatment consisted of air cooling from 850°C and performing a DO_3-ordering treatment at 500°C for 7 d. Figure 6 showed the ratio of total elongation observed for specimens with the B2 structure to that of, presumably, the DO_3 structure that was produced by 500°C treatment for 7 d. The ductility of the B2 structure material was always higher than the DO_3 structure. It was recognized that the heat treatments producing B2 and DO_3 structures also yielded significantly different microstructures and grain sizes. Additional work is needed to determine the role of microstructure, grain size, and crystal structure in improving the RT ductility of iron aluminide. This type of effort is currently under way at Idaho National Engineering Laboratory.

9. DISCUSSION

The most important finding of the investigation was that of RT ductility values of 15 to 20% can be achieved for Fe_3Al-based iron aluminides. These are the highest values ever reported for this class of materials tested in air (Table 1). From results of tests on many compositions, melting practices, processing steps, heat treatments, and test conditions used, several conditions for obtaining high ductility values are identified:

ORNL-DWG 90-2205

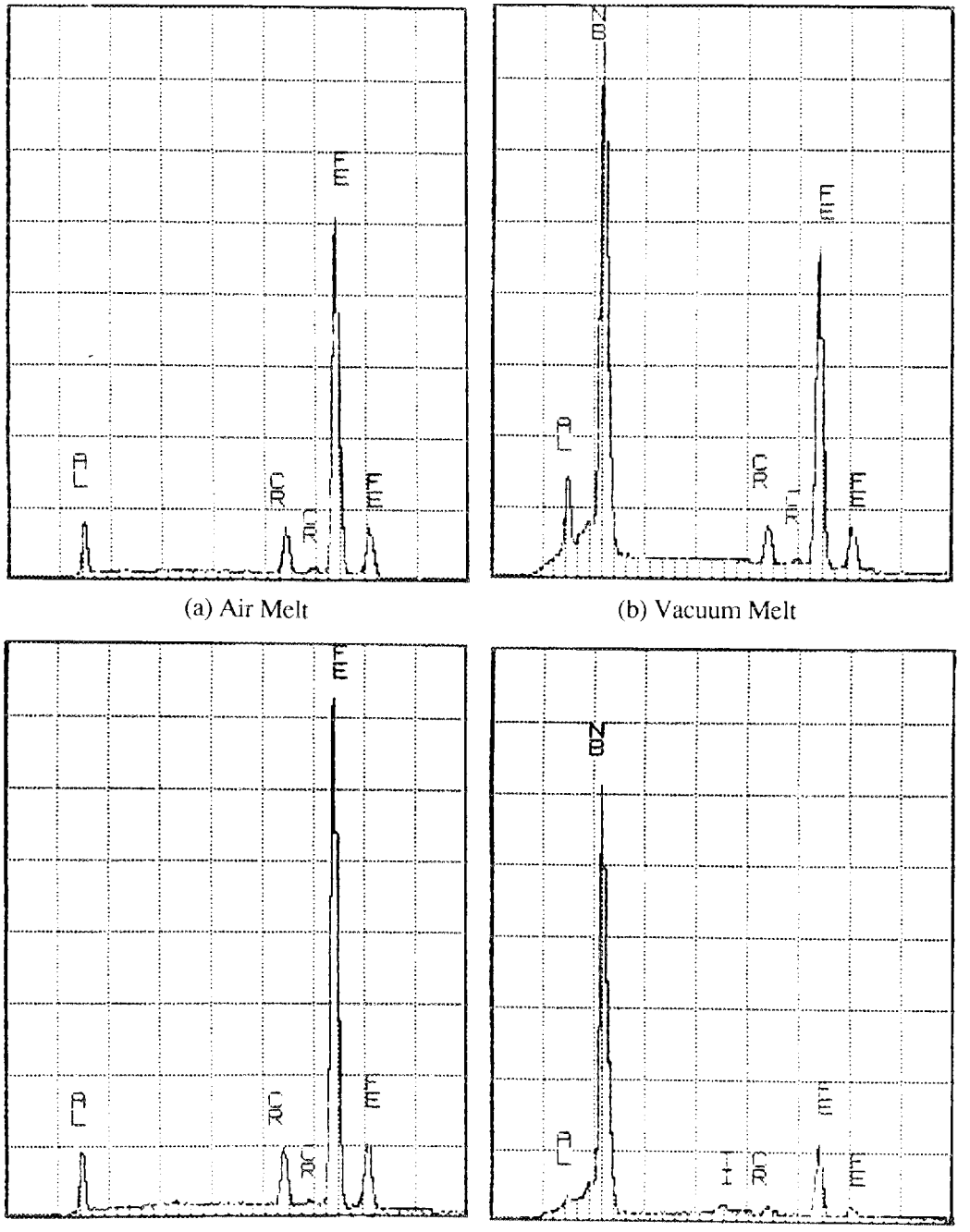

Fig. 58. Qualitative elemental analyses of matrices and precipitates in air-melted ingot material (X3904) and vacuum-melted material (Heat 35). (*a*) and (*c*) Matrices and (*b*) and (*d*) precipitates.

YP9711

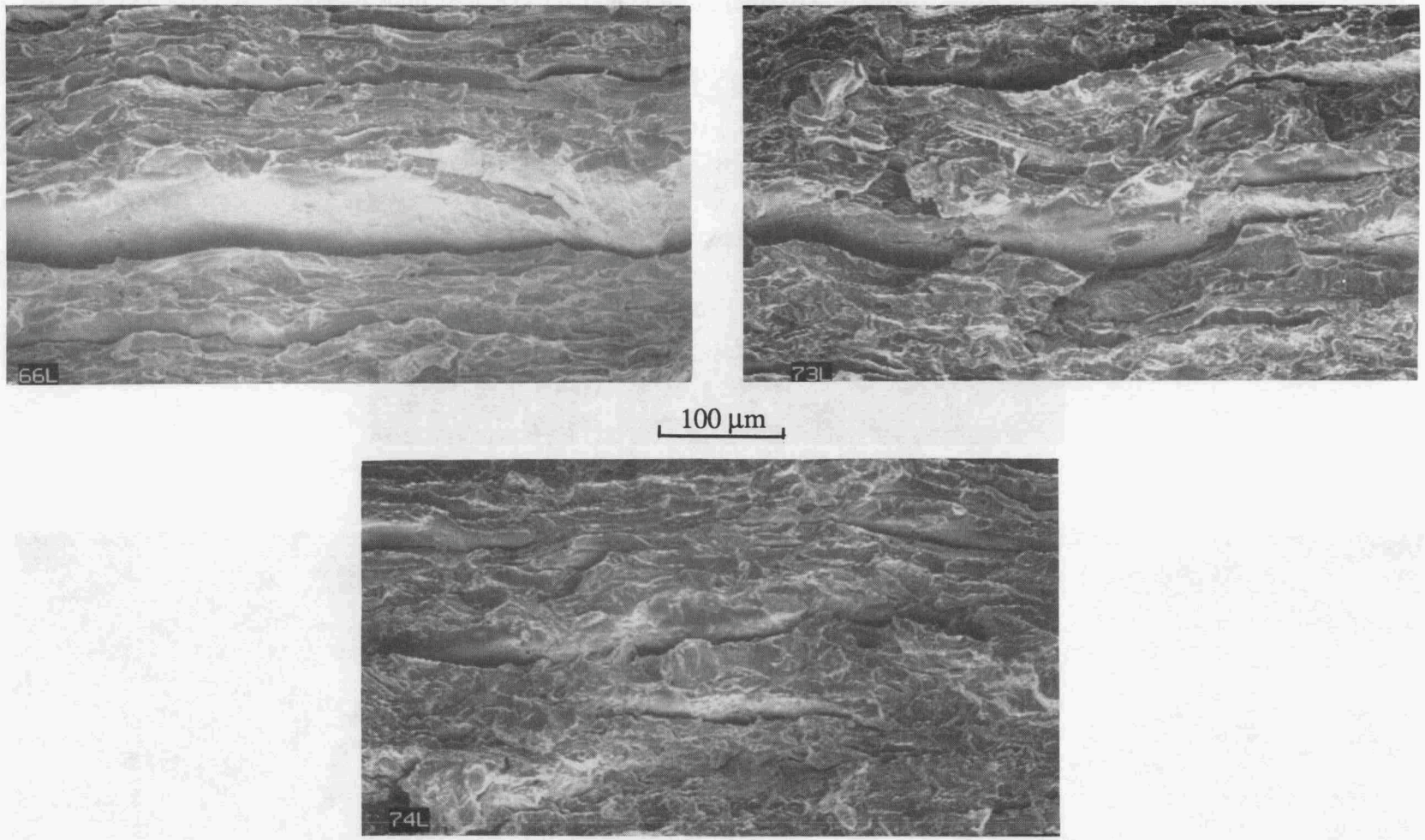

Fig. 59. Fracture surfaces of room-temperature tensile-tested specimens of iron-aluminide alloy [FAL (Heat 13008)]. (*a*) Stress relieved and annealed for 1 h at 700°C, and both were followed by air cooling; (*b*) stress relieved and annealed for 1 h at 750°C and 700°C, respectively, and both were followed by oil quenching; and (*c*) stress relieved and annealed for 1 h at 750°C, and both were followed by oil quenching. *Source*: INEL/EG&G.

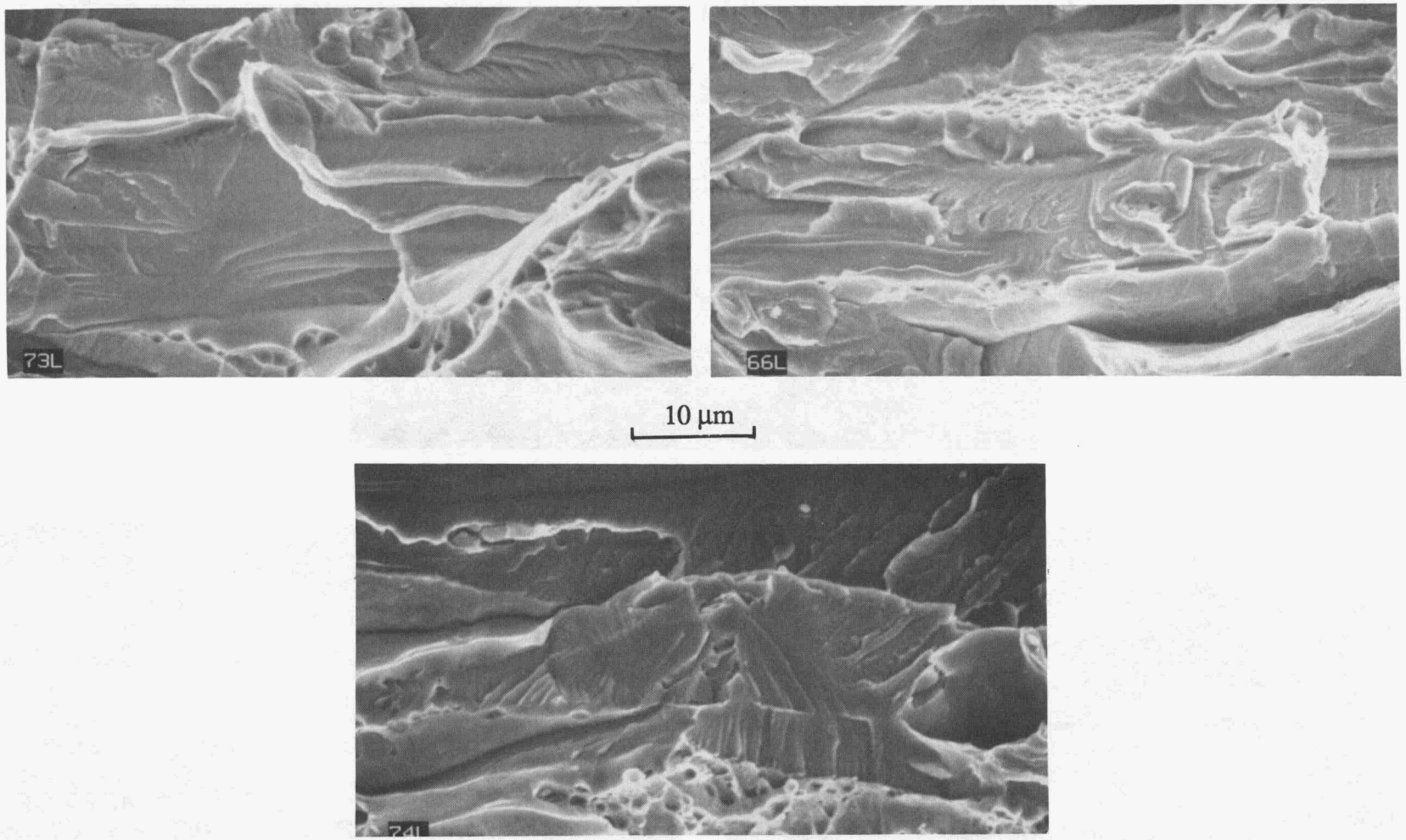

Fig. 60. Fracture surfaces at a higher magnification of room-temperature tensile-tested specimens of iron-aluminide alloy [FAL (Heat 13008)]. (*a*) Stress relieved and annealed for 1 h at 700°C, and both were followed by air cooling; (*b*) stress relieved and annealed for 1 h at 750°C and 700°C, respectively, and both were followed by oil quenching; and (*c*) stress relieved and annealed for 1 h at 750°C, and both were followed by oil quenching. *Source*: INEL/EG&G.

Table 8. X-ray diffraction results of high-ductility specimens of iron-aluminide (Heat 13008) FAL

Heat treatment (°C)	Ductility (%)	Structure[a]
700/AC/700/AC[b]	15.4	B2
750/OQ/700/OQ[c]	19.8	B2
750/OQ/750/OQ	17.1	B2

[a]No DO_3 peak was identified in these specimens.

[b]AC = air cool.

[c]OQ = oil quench.

1. The microstructure needs to be unrecrystallized or only slightly recrystallized.
2. Oil quenching is the best method for cooling the specimen after high-temperature treatment.
3. Higher test strain rates produce higher ductility.
4. Alloys "leaner" in alloying elements produce higher ductility.
5. Vacuum melting produces higher ductility material than air melting.
6. Laboratory (high-purity) melt stock produces higher ductility than the commercial (low-purity) melt stock.
7. A moisture-free environment produces higher ductility (Table 9).

The fact that the ductility of iron aluminides decreased with decreasing strain rate and decreasing temperature above room temperature[6,7] suggested the possibility for hydrogen embrittlement for these alloys. Hydrogen embrittlement requires (1) a source of the embrittling hydrogen, (2) the absence of a kinetic barrier-to-hydrogen absorption, (3) reasonable diffusion kinetics for absorption and interaction with the deformation process, and (4) susceptible material and/or microstructure.

While hydrogen adsorption and absorption may occur when the iron aluminide is exposed to water vapor, hydrogen interaction with deformation requires appropriate hydrogen diffusion kinetics and a susceptible alloy. Some instances of indirect evidences for hydrogen diffusion and interaction with the deformation process are:

Table 9. Effect of environments on tensile properties of iron-aluminide alloy (FAL)[a,b]

Test environment (gas pressure)	Elongation (%)	Yield strength (MPa)	Ultimate strength (MPa)
Air	9.4	296	654
O_2[c]	23.8	304	957
Ar + H_2[c]	14.6	315	785
H_2O vapor	8.1	296	630

[a]All were tested at room temperature, 0.2/min.

[b]This alloy contained 0.04 wt % B, as compared to 0.01 wt % B in standard FAL alloy.

[c]0.0667 MPa (500 torr).

1. Introducing an oil film on the specimen surface puts a barrier between the aluminum atoms and the moisture and leads to high RT ductilities (Table 10). For some specimens, if the oil is removed, the ductility values are reduced to half, suggesting hydrogen generation and diffusion into the specimen.

2. Testing in 0.0667-MPa (500-torr) dry oxygen produced twice the ductility than in air containing water vapor (Table 9). The same material tested in water vapor produced lower ductility than that observed in laboratory air. Tensile testing in 0.0667-MPa (500-torr) molecular hydrogen in an argon environment produced higher ductilities than in air, suggesting that molecular hydrogen is not as detrimental as atomic hydrogen produced by the reaction with moisture during testing (Table 9). The lower ductilities in molecular hydrogen compared to oxygen may have been caused by moisture in the argon cover gas.

3. The unrecrystallized microstructure, which contained extremely few transverse grain boundaries, produced the highest ductility values. This suggested that the hydrogen produced at the metal surface was not able to diffuse into the specimen in the absence of these grain boundaries. When the microstructure was recrystallized, the large number of grain boundaries provided a path for easy diffusion of hydrogen and reduced the observed ductility.

Table 10. Effect of quenching and heat treatment on mechanical properties of an experimental iron-aluminide alloy (FA-124)

Heat treatment (°C)	Cooling treatment	Test conditions[a]	Yield strength (MPa)	Ultimate strength (MPa)	Elongation (%)
1 h/850 + 5 d/500/air	Air/air	Air	256	564	7.6
1 h/750/air	Oil[b]	Air	367	724	13.2
1 h/750/air	Oil[c]	Air	342	509	4.5
1 h/750 + 4 d/500/air	Oil[c]/air	Air	269	512	6.2

[a]Strain rate is 0.2 in./in./min.

[b]Not cleaned.

[c]Cleaned.

Hydrogen is not only of concern for RT properties; it can also have an undesirable effect during melting and casting. Both iron and aluminum melt stock, if left open in a laboratory environment, can adsorb water vapor, and this can result in some hydrogen dissolving in the metal by the reactions described previously. During air melting, additional hydrogen is produced from reactions of both the aluminum and iron melt stocks with moisture. This hydrogen dissolves in the molten metal, and when cast into molds, it tends to escape during solidification. The gas content can be sufficiently large to produce a bulge in the ingot hot-top instead of the conventional shrinkage. Initial 230-kg (500-lb) air-induction-melted heats at Combustion Engineering showed bulging and large gas-related porosity in the ingot. However, when moisture in the melt stock was baked out and small-size [70-kg (150-lb)] heats were melted, the gas-related porosity was minimized. A 230-kg (500-lb) heat, when melted at The Timken Company and cast into a 250-mm (10-in.) mold, produced material that was similar in appearance to that of Swiss cheese. The ORNL-melted 7-kg (15-lb) air-induction heats did not have any gas-related porosity or bulging of the hot-top. It is believed that the ORNL heats are better because the melt stock was kept in desiccators prior to melting.

Vacuum-induction-melted heats using the same melt stock that produced the Swiss-cheese type structure were free of any gas porosity. Vacuum melting helps in two ways: (1) it eliminates most moisture in the system and prevents the hydrogen-producing reaction with aluminum and iron, and (2) it helps to pump out any hydrogen that might have been dissolved in the melt stock.

Based on the above results and those of Liu, McKamey, and Lee,[6] it appears that iron-aluminide alloys are susceptible to hydrogen embrittlement through a chemical reaction of aluminum and iron with moisture in air. The results in this report have presented some means for reducing the effect and improving the ductility. Whereas a highly elongated grain structure can improve ductility, this microstructural approach is limited to sheet and plate applications; it cannot be used for castings and forgings or after high-temperature aging. Oil quenching provides additional improvement in ductility and may be useful in some cases. The ideal method of addressing the environmental problem is to add alloying elements that will permit quick surface passivation. Such alloy additions are currently under investigation.

In addition to melt practice, impurities such as silicon and manganese tend to reduce the ductility of Fe_3Al-based iron aluminides. Table 11 shows the data on a 500-g (1-lb) drop casting of alloy FA-129 to which 0.20 wt % Mn and 0.40 wt % Si were intentionally added. The presence of these impurities permitted only a maximum ductility of 9% as compared to 15 to 17% observed for some alloys without these impurities. Another example of impurity effect is shown in Table 12. Data in this table are for alloy FAL that was melted using the commercial melt stock, which was supplied by The Timken Company. This melt-stock analysis should have resulted in residual amounts of Mn, Si, and Mg. (Magnesium comes from impurities in the aluminum.) Once again, the best RT ductility for this alloy was 12% as opposed to 20%, which was observed for the same alloy using pure melt stock at ORNL. The impurity content of these heats also required higher forging and rolling temperatures.

The air-induction-melted ingot (X3908 of FAL) resulted in maximum RT elongation values of 12%. Detailed chemical analysis of this ingot showed that it contained 0.2 wt % Mn and 0.50 wt % Si. Based on the results in Table 11 for 0.20 wt % Mn and 0.40 wt % Si addition, it is believed that the lower ductility values observed for ingot X3908 were caused by its high manganese and silicon contents.

Table 11. Tensile properties of iron aluminide {FA-129MnSi [500 g (1 lb), Heat 13232]} arc melted at ORNL and drop cast into a 25 × 12 × 125 mm (1 × 1/2 × 5 in.) water-cooled copper mold[a]

Specimen number	Heat treatment						Test temperature (°C)	Strain rate (min^{-1})	Strength (MPa)		Ductility (%)	
	Sheet treatment			Specimen treatment					0.2% Yield	Tensile strength	Elongation	Reduction of area
	Temp. (°C)	Time (h)	Cooling medium[b]	Temp. (°C)	Time (h)	Cooling medium[b]						
1L	700	1	OQ	700	1	OQ	25	0.2	500	737	7.66	5.83
2L	700	1	OQ	700	1	OQ	25	0.2	467	725	7.44	7.72
3L	700	1	OQ	750	1	OQ	25	0.2	414	718	9.06	8.04
4L	700	1	OQ	750	1	OQ	25	0.2	425	596	4.66	4.71
5L	700	1	OQ	800	1	OQ	25	0.2	371	594	6.62	5.84
6L	700	1	OQ	800	1	OQ	25	0.2	367	655	8.44	6.52
7L	700	1	OQ	850	1	OQ	25	0.2	375	672	8.70	4.90
8L	700	1	OQ	850	1	OQ	25	0.2	380	660	8.90	6.69

[a]Manganese and silicon were intentionally added to the FA-129 composition to simulate the residual elements from scrap. The ingot was hot forged at 1000°C from 12- to 6-mm (1/2- to 0.25-in.) thickness followed by hot rolling at 850°C to 1.25-mm (0.060-in.) thickness. This sheet was warm rolled at 650°C to 0.76-mm (0.030-in.) thickness. The sheet was stress relieved prior to punching into tensile specimens, and the specimens were given various treatments prior to testing.

[b]OQ = oil quench.

Table 12. Tensile properties of iron aluminide [FAL (Heat 13259)] air-induction melted at ORNL from commercial melting stock provided by The Timken Company[a]

Specimen number	Stress-relief treatment			Annealing treatment			Strength (MPa)		Ductility (%)	
	Temperature (°C)	Time (h)	Cooling[b]	Temperature (°C)	Time (h)	Cooling[b]	0.2% Yield	Ultimate tensile	Total elongation	Reduction of area
1L	700	1	OQ				452	452	1.20	1.67
2L	700	1	OQ				499	499	1.44	1.65
3L[c]	700	1	OQ	700	1	OQ	475	609	7.52	5.06
4L	700	1	OQ	700	1	OQ	346	691	10.30	6.56
7L	700	1	OQ	750	1	OQ	257	669	9.86	6.09
8L	700	1	OQ	750	1	OQ	368	614	7.58	5.68
11L	700	1	OQ	800	1	OQ	357	674	9.68	5.30
12L	700	1	OQ	800	1	OQ	369	674	9.46	6.47
15L	700	1	OQ	850	1	OQ	362	607	8.02	5.97
16L	700	1	OQ	850	1	OQ	356	660	10.02	5.02
5L	750	1	OQ	700	1	OQ	315	573	7.36	9.78
6L	750	1	OQ	700	1	OQ	351	710	11.14	7.92
9L	750	1	OQ	750	1	OQ	356	669	10.74	7.46
10L	750	1	OQ	750	1	OQ	310	675	11.02	9.35
13L	750	1	OQ	800	1	OQ	373	704	10.98	7.36
14L	750	1	OQ	800	1	OQ	361	697	10.58	7.80
17L	750	1	OQ	850	1	OQ	312	718	11.94	5.52
18L	750	1	OQ	850	1	OQ	357	661	9.86	6.81

[a]The heat was cast into a 76-mm-diam (3-in.) graphite mold and homogenized for 16 h at 1000°C to 25-mm-thick (1-in.) slab. The slab was hot rolled at 900°C to 2.5-mm (0.100-in.) thickness followed by warm-roll finishing at 700°C to 0.76-mm (0.030-in.) thickness. The specimens were punched following a stress-relieving treatment, and the specimens were tested at room temperature and 0.2/min after various heat treatments.

[b]OQ = oil quench.

[c]Specimen was preloaded.

10. APPLICATIONS

Iron aluminides can replace carbon steels for some applications and, in other instances, stainless steels. The advantages of iron aluminides include (1) oxidation resistance as good or better than all steels (carbon, low alloy, and stainless); (2) sulfidation resistance better than all steels; (3) resistance to stress corrosion cracking comparable to carbon and low-alloy steels; (4) good corrosion resistance in molten nitrates as compared to all steels; (5) resistance to atmospheric corrosion (rusting) at RT in a humid environment which helps eliminate special handling procedures during shop fabrication; (6) RT tensile strength superior to carbon and stainless steels; (7) high-temperature strength superior to carbon, low-alloy steels, and stainless steels up to 600°C; (8) creep strength better than carbon and low-alloy steels up to 600°C; and (9) lower cost than many advanced metallic materials.

Specific applications will depend on the performance required of iron aluminides compared to the currently used materials. Sample materials of iron aluminides are being tested for several of the potential applications which include (1) hot-gas filters, (2) automotive exhaust systems, and (3) sulfur-containing environments.

11. FUTURE WORK

1. We are striving to develop compositions that will be free from, or minimize, environmental effects on mechanical properties.

2. The effect of melting practice such as vacuum induction, vacuum arc remelting, and electroslag remelting on mechanical properties will be determined.

3. Alloy compositions with minimum environmental effects will be scaled up and tested for tensile and creep properties.

12. SUMMARY AND CONCLUSIONS

Iron aluminides based on Fe_3Al are ordered intermetallic alloys that offer good oxidation resistance, excellent sulfidation resistance, and relatively low material cost. These materials also conserve strategic elements such as chromium and have a lower density than stainless steels. However, limited ductility at ambient temperature and a sharp drop in strength above 500°C have been major deterrents to their acceptance for structural applications. This report presents the most recent improvements in RT ductility of these aluminides, effects of composition on ductility, effects of test temperature and strain rate on

tensile properties, scaleup and fabrication of selected compositions, mechanical properties of scaled-up heats, environmental effects, potential applications, and future plans. The following statements summarize the present work:

1. Iron aluminides based on Fe-28 at. % Al have been ductilized to RT tensile elongations of 15 to 20% for the first time.
2. Ductility improvements have been achieved through thermomechanical processing and heat-treatment control. This method of ductility improvement has been demonstrated for a range of compositions.
3. Melting, casting, and processing of 7-kg (15-lb) heats at ORNL and 70-kg (150-lb) heats at a commercial vendor were described. Considering the information available, vacuum melting is recommended for these materials. Other refining processes such as electroslag remelting are also desirable.
4. The Fe_3Al-based iron aluminides are easily hot worked by forging or extruding at temperatures in the range of 850 to 1100°C. Rolling is usually recommended at 800°C with the final 50% reduction at 650°C. Based on the data presented, these alloys should be readily hot workable. Some care will be required in processing at RT because of limited ductility at this temperature.
5. Tensile and creep properties of 7- and 70-kg (15- and 150-lb) heats were presented. The RT tensile elongation and related ultimate tensile strength values were most different between ORNL and commercially melted material. Lower values for commercially melted material were explained in terms of impurity effects, especially manganese and silicon. Creep properties of the alloys that are the most ductile at RT are significantly lower than those observed for type 304 stainless steel. At least one composition suggests that creep properties equal to type 304 stainless steel may be possible.
6. Data presented in this report suggest that the Fe_3Al-based compositions tested so far are sensitive to environmental effects. The environment of concern is water vapor, which reacts with aluminum and iron to form hydrogen at the metal surface. The hydrogen produced is adsorbed and absorbed in the specimen during testing and results in low RT ductilities. The use of highly elongated grains with essentially no transverse boundaries is one way of reducing the hydrogen diffusion and thereby increasing the ductility. An oil treatment provides additional improvement in ductility by providing a barrier for interaction of the metal surface with moisture. However, alloy modifications, which can provide rapid passivation of the surface at RT and thus

prevent hydrogen from diffusing into the specimen, are the best solution to minimizing the environmental effects. Work is currently under way on such alloy modifications.

13. REFERENCES

1. C. G. McKamey and C. T. Liu, "Development of Iron Aluminides for Gasification Systems," pp. 207-17 in *Proceedings of the Instrumentation, Components, and Materials Contractors Meeting*, DOE/METC-86/6069, U.S. Department of Energy, September 1986.

2. C. G. McKamey et al., *Evaluation of Mechanical and Metallurgical Properties of Fe_3Al-Based Aluminides*, ORNL/TM-10125, September 1986.

3. C. G. McKamey et al., *Development of Iron Aluminides for Coal Conversion Systems*, ORNL/TM-10793, July 1988.

4. J. H. DeVan, H. S. Hsu, and M. Howell, *Sulfidation/Oxidation Properties of Iron-Based Alloys Containing Niobium and Aluminum*, ORNL/TM-11176, May 1989.

5. R. E. Hook, D. W. Johnson, and J. P. Erfort, "A Review of Some of the Key Work on the Mechanical Properties of Fe-Al Alloys," report of the paper presented at ASM Materials Week, Orlando, Fla., Oct. 7, 1986.

6. C. T. Liu, E. H. Lee, and C. G. McKamey, "An Environmental Effect as the Major Cause for Room Temperature Embrittlement in FeAl," *Scr. Metall.* **25**, 875-880 (1989).

7. R. E. Ricker and D. J. Duquette, *Metall. Trans.* **19A**, 1775 (1988).

14. ACKNOWLEDGMENTS

The authors thank J. D. Vought for preparation of the experimental alloys; J. D. Vought and G. E. Angel for air-induction melting of 7-kg (15-lb) heats; K. S. Blakely and C. W. Holland, Jr., for forging and rolling; C. E. Dunn for the billet preparation; and C. T. Liu and P. F. Tortorelli for reviewing the manuscript. The authors also acknowledge Richard Wright of EG&G Idaho for helping with X-ray analysis and fracture surface photomicrographs of several specimens. The authors offer special thanks to M. L. Atchley for typing the draft and M. R. Upton for preparing the final manuscript.

INTERNAL DISTRIBUTION

1-2. Central Research Library
3. Document Reference Section
4-5. Laboratory Reference Section
6. Laboratory Records, ORNL RC
7. ORNL Patent Section
8-10. M&C Records Office
11. D. J. Alexander
12. G. E. Angel
13-19. R. H. Baldwin
20. T. M. Besmann
21. C. R. Boston
22. R. A. Bradley
23. D. N. Braski
24. C. R. Brinkman
25. V. R. Bullington
26. P. T. Carlson
27. R. H. Cooper
28. J. I. Federer
29. C. W. Francis
30. E. P. George
31. F. M. Haggag
32. J. A. Horton
33-37. C. R. Howell
38. C. R. Hubbard
39. R. R. Judkins
40. M. A. Karnitz
41. J. R. Keiser
42. K. C. Liu
43. P. J. Maziasz
44. D. J. McGuire
45-49. C. G. McKamey
50. R. K. Nanstad
51. R. W. Reed
52. P. L. Rittenhouse
53. R. D. Roop
54. A. C. Schaffhauser
55. J. H. Schneibel
56. L. G. Shrader
57-61. V. K. Sikka
62. G. M. Slaughter
63. J. O. Stiegler
64. R. L. Swain
65. R. W. Swindeman
66. V. J. Tennery
67. P. F. Tortorelli
68. D. F. Wilson
69. J. R. Weir
70. T. Zacharia
71. A. D. Brailsford (Consultant)
72. H. D. Brody (Consultant)
73. D. P. Pope (Consultant)
74. M. L. Savitz (Consultant)
75. E. R. Thompson (Consultant)
76. J. B. Wachtman (Consultant)

EXTERNAL DISTRIBUTION

77-78. AIR FORCE WRIGHT AERONAUTICAL LABORATORIES, Metals and Ceramics Division, Wright-Patterson Air Force Base, OH 45433
D. M. Dimiduk
W. R. Kerr

79. ALUMINUM COMPANY OF AMERICA LABORATORIES, Alcoa Technical Center, Route 780, Seventh Street Road, Alcoa Center, PA 15269
G. MacZura

80. AMERICAN WELDING SOCIETY, 550 LeJeune Road, Miami, FL 33126
H. G. Ziegenfuss

81. AMETEK SPECIALTY METAL PRODUCTS DIVISION, Route 519, P.O. Box 427, Eighty Four, PA 15330
J. H. Reinshagen

82. ARGONNE NATIONAL LABORATORY, Materials Science and Technology Division, 9700 S. Cass Ave., Argonne, IL 60439
K. Natesan

83-84. BABCOCK & WILCOX COMPANY, 20 S. Van Buren Ave., Barberton, OH 44203
M. Gold
J. E. Mack

85. CARNEGIE-MELLON UNIVERSITY, Department of Metallurgical Engineering and Materials Science, Pittsburgh, PA 15213
T. B. Massalski

86. CASE WESTERN RESERVE UNIVERSITY, Department of Metallurgical and Materials Science, 10900 Euclid Avenue, Cleveland, OH 44106
K. Vedula

87. COMBUSTION ENGINEERING, INC., 911 W. Main Street, Chattanooga, TN 37401
D. A. Canonico

88-89. CORNELL UNIVERSITY, Ithaca, NY 14850
Che-Yu Li
S. L. Sass

90. CYTEMP POWDER PRODUCTS, 600 Mayer Street, Bridgeville, PA 15017
L. W. Lherbien

91-92. EG&G IDAHO, INC., Idaho National Engineering Laboratory, P.O. Box 1625, Idaho Falls, ID 83415
J. E. Flinn
R. N. Wright

93-96. ELECTRIC POWER RESEARCH INSTITUTE, 3412 Hillview Avenue, P.O. Box 10412, Palo Alto, CA 94303
W. T. Bakker
D. J. Frey
R. I. Jaffee
J. Stringer

97. EXXON RESEARCH AND ENGINEERING COMPANY, Clinton Township, Route 2, East, Annandale, NJ 08801
M. L. Gorbaty

98. FOSTER WHEELER DEVELOPMENT CORPORATION,
12 Peach Tree Hill Road, Livingston, NJ 07939
J. L. Bough

99-100. GARRETT TURBINE ENGINE COMPANY, Advanced Materials,
Materials Engineering, 111 South 34 Street, P.O. Box 5217,
Phoenix, AZ 85010
G. S. Hoppin
B. Keiser

101. GENERAL ATOMICS, P.O. Box 81608, San Diego, CA 92318
D. I. Roberts

102-104. GENERAL ELECTRIC COMPANY, Bldg. 81, Room E102,
Schenectady, NY 12345
K. M. Chang
S. C. Huang
A. I. Taub

105. GENERAL ELECTRIC COMPANY, Corporate Research and Development,
P.O. Box 8, Schenectady, NY 12301
R. L. Fleischer

106. GENERAL ELECTRIC COMPANY, Quartz and Chemicals Department,
24400 Highland Road, Richmond Heights, OH 44413
G. W. Weber

107. GENERAL MOTORS RESEARCH, Metallurgical Department,
Warren, MI 48090-9055
S. Schron

108. GEORGIA INSTITUTE OF TECHNOLOGY, School of Materials Engineering,
Bunger-Henry Bldg., Atlanta, GA 30332
S. Antolovich

109. HAYNES INTERNATIONAL, Technology Dept., 1020 W. Park Avenue,
Kokomo, IN 46901
A. Asphahani

110. INSTITUTE OF DEFENSE ANALYSES, 1801 Beauregard Street, Alexandria,
VA 22311
T. F Kearns

111. LEHIGH UNIVERSITY, Materials Research Center, Bethlehem, PA 18015
Y. T. Chou

112-113. LOCKHEED CORPORATION, Palo Alto Laboratories, 3251 Hanover Street, Palo Alto, CA 94303
E. C. Burke
R. A. Perkins

114-116. LOS ALAMOS NATIONAL LABORATORY, Los Alamos, NM 87545
S. P. Chen
P. J. Hay
R. S. Skaggs

117. THE MATERIALS PROPERTIES COUNCIL, INC., 345 E. Forty-Seventh Street, New York, NY 10017
M. Prager

118-119. MICHIGAN TECHNOLOGICAL UNIVERSITY, Department of Metallurgical Engineering, Houghton, MI 49931
D. Mikkola
C. L. White

120. MONSANTO COMPANY, P.O. Box 1311, Texas City, TX 77590
P. S. Gupton

121. NAVAL SURFACE WEAPONS CENTER, Code R32, White Oak, Silver Spring, MD 20910
H. M. DeJarnette

122. NAVAL SURFACE WEAPONS CENTER, Surface Weapons Materials Technology Program, Dahlgren, VA 22448
W. T. Messick

123. NORTH CAROLINA STATE UNIVERSITY, Materials Engineering Dept., Raleigh, NC 27650
C. C. Koch

124. OAK RIDGE ASSOCIATED UNIVERSITIES LIBRARY, Oak Ridge, TN 37831
MERT Division

125. RENSSELAER POLYTECHNIC INSTITUTE, Materials Engineering Department, Troy, NY 12181
N. S. Stoloff

126. SORELL CONSULTING SERVICES, 49 Brookside Terrace, North Caldwell, NJ 07006
G. Sorell

127. THE TIMKEN COMPANY, 1835 Dueber Avenue, SW, Canton, OH 44706
P. W. Lee

128. UNITED TECHNOLOGIES, Pratt and Whitney, Engineering Division, North, 400 Main St., East Hartford, CT 06108
D. N. Duhl

129. UNIVERSAL CYCLOPS SPECIALTY STEEL DIVISION, 650 Washington Road, Pittsburgh, PA 15228
H. L. Black

130. UNIVERSAL ENERGY SYSTEMS, INC., 4401 Dayton-Xenia Road, Dayton, OH 45432
M. G. Mendiratta

131. UNIVERSITY OF MASSACHUSETTS, Department of Polymer Science, Room 701, GRC, Amherst, MA 01003
R. S. Porter

132. UNIVERSITY OF TENNESSEE, Materials Science and Engineering Department, Knoxville, TN 37996
C. R. Brooks

133. VANDERBILT UNIVERSITY, Station B, P.O. Box 1621, Nashville, TN 37235
J. J. Wert

134. VIRGINIA POLYTECHNIC INSTITUTE AND STATE UNIVERSITY, Blacksburg, VA 24016
D. A. Farkas

135-137. DOE, ENERGY SYSTEMS RESEARCH AND DEVELOPMENT, Office of Conservation and Renewable Energy, Forrestal Building, Independence Avenue, Washington, DC 20585
J. J. Brogan
J. J. Eberhardt
S. M. Wolf

138-143. DOE, MORGANTOWN ENERGY TECHNOLOGY CENTER, P.O. Box 880, Morgantown, WV 26505
R. A. Bajura
R. C. Bedick
J. W. Byam, Jr.
R. J. Dellefield
J. M. Hobday
J. S. Wilson

144-145. DOE, OAK RIDGE OPERATIONS, P.O. Box 2001, Oak Ridge, TN 37831-8600
Assistant Manager for Energy Research and Development
E. E. Hoffman

146-148. DOE, OFFICE OF FOSSIL ENERGY, Washington, DC 20545

D. J. Beecy, FE-14
J. P. Carr, FE-14
R. T. King, FE-14

149. DOE, OFFICE OF VEHICLE AND ENGINE R&D, Route Symbol CE-131, Forrestal Building, Washington, DC 20585

R. B. Schulz

150-159. DOE, OFFICE OF SCIENTIFIC AND TECHNICAL INFORMATION, Office of Information Services, P.O. Box 62, Oak Ridge, TN 37831

For distribution by microfiche as shown in DOE/OSTI-4500, Distribution Categories UC-103 (Fluidized Bed Combustion), UC-109 [Coal Gasification (Surface and Underground)], and UC-114 (Coal-Based Materials and Components)